RESEARCH, DEVELOPMENT AND VERIFICATION OF AN OPERATIONAL AND INTERACTIVE SYSTEM TO FORECAST HEAVY RAINFALL

(PROGRAIN)

LL Dyson • J van Heerden

WRC Report No. 1333/1/06

Water Research Commission

RESEARCH, DEVELOPMENT AND VERIFICATION OF AN OPERATIONAL AND INTERACTIVE SYSTEM TO FORECAST HEAVY RAINFALL

(PROGRAIN)

LL Dyson • J van Heerden

Report to the Water Research Commission
by
Department of Geography, Geoinformatics and Meteorology
University of Pretoria

WRC Report No 1333/1/06
ISBN No 1-77005-401-4

January 2006

Disclaimer

This report emanates from a project financed by the Water Research Commission (WRC) and is approved for publication. Approval does not signify that the contents necessarily reflect the views and policies of the WRC or the members of the project steering committee, nor does mention of trade names or commercial products constitute endorsement or recommendation for use.

Printed by Silowa Printers 012 804 1164

EXECUTIVE SUMMARY

Abstract

The PROGRAIN project deals with the development of heavy rainfall identification systems over South Africa. An ingredients based approached is used and a heavy rainfall identification system combines atmospheric criteria, which must all co-exist to identify areas of heavy rainfall. In this research two heavy rainfall identification systems were developed and implemented operationally at the South African Weather Service on the Eta model. First the Tropical Heavy Rainfall Identification System (THERIS) identifies heavy rainfall from continental tropical weather systems. The second is the Coastal Zone Heavy Rainfall Identification System. Three different versions of the Coastal Zone Heavy Rainfall Identification System were implemented along the South West Coast, the South Coast and the East Coast. Statistical results reveal that the system works very well along the South West Coast but the results are not as favourable along the South and East Coasts. All the products developed in the PROGRAIN project have been disseminated to the forecasting offices of the SAWS and are available on the web site of the SAWS. Additional forecasting products were also developed for the regional stations in South Africa.

Introduction

Widespread heavy rainfall is extremely difficult to predict despite the phenomenal improvements in numerical weather prediction (NWP). It is important to accurately predict the geographical extent of widespread and heavy rainfall timeously as the accompanying flooding causes loss of life and severe damage to the infrastructure. NWP models are very good in simulating atmospheric flow fields and are unsurpassed in predicting the development and movement of weather systems known to be potential heavy rainfall producers. Unfortunately the rainfall fields generated by these models are nowhere as good as the circulation fields they produce and this had led to a lack of confidence in the rainfall prognoses. Furthermore the area where heavy rainfall will concentrate cannot yet be predicted reliably.

This report details the research that has led to the development and implementation of operational heavy rainfall prediction systems that operate on the prognostic fields generated by NWP models. An ingredients based approach is followed and a heavy rainfall identification system identifies atmospheric criteria, which must co-exist to pin point heavy rainfall. In this research emphasis was placed on continental tropical weather systems as well as weather systems causing heavy rainfall along the coastal plains of South Africa.

Aims of the PROGRAIN Project

The main aim of this project was to develop a system to predict heavy rainfall but in an operational weather forecasting environment.

During the course of the project the following steps and/or supporting research to achieve this aim were completed:

- Methods to isolate heavy rainfall developing in continental tropical and extra-tropical as well as in coastal zone baroclinic weather systems
- Inclusion of topographic effects in the operational coastal zone heavy rainfall forecast system
- A method to modify Numerical Weather Prediction Model rainfall prognoses by incorporating satellite derived rainfall
- On site training of SAWS staff in the use of the operational heavy rainfall forecasting systems

The second aim of the project was the development of a statistical validation system for the rainfall fields produced by the research and operational heavy rainfall systems.

Major Results and Achievements

A system exists which can delineate areas where heavy rainfall can be expected with a considerable degree of accuracy. All the components of these systems are based on well-proven meteorological dynamics but depend on the accuracy of the data fields generated by the analyses or prognoses of the Eta model. All the heavy rainfall identification systems were developed for the operational meteorologist and delineate areas of possible heavy rainfall. The systems use the prognostic fields of the Eta model and are available for use anywhere over the Eta domain by disseminating the products through the web site of the SAWS.

Two heavy rainfall identification systems are now available to the South African forecasters.

The first is the Tropical Heavy Rainfall Identification System (THERIS) which was adapted to run on the Eta model.

Secondly, Coastal Zone Heavy Rainfall Identification Systems were developed for three coastal areas of South Africa: the South West Coast, the South Coast and the East Coast. A thorough investigation into the prognostic fields of the Eta model revealed that the atmospheric flow fields are simulated very well over the South West Coast but the model does not fare as well over the South and East Coasts. However, by identifying the appropriate variables in the Eta model prognosis, heavy rainfall identification systems were developed for all three areas. The criteria used to isolate heavy rainfall are season and area dependent.

A variable, not directly available from the Eta model output, referred to as the topographical upward motion, was developed. The topographical upward motion simulates the upward motion forced by the surface wind blowing against the topography. This 'new' variable forms an important part of the coastal heavy rainfall identification systems. In addition the research revealed that in order to identify heavy rainfall along the coast the lower levels of the atmosphere (below 800hPa) are very important. The forecasters are encouraged to investigate variables at the 1000-800hPa pressure levels and to be conscious of critical values of vertical motion associated with heavy rainfall.

All heavy rainfall identification systems are available on the SAWS web site for use in the forecasting offices in South Africa. In addition to the heavy rainfall forecast products, extra forecasting products were developed for use at the regional offices in South Africa. This was done in consultation with the weather forecasters, which ensured their active participation in the project. Ms Liesl Dyson visited all the regional offices to introduce the operational forecasters to the heavy rainfall products.

All heavy rainfall systems were verified for the period between September 1999 and March 2002. The Eta model precipitation forecast was also validated for the same period. The heavy rainfall systems all have some skill in predicting heavy rainfall. The best results were achieved over the South West coast in winter but THERIS also faired well in identifying heavy rainfall days over the interior in summer.

The project has made a significant contribution to the understanding of the way that the Eta model handles atmospheric flow fields along the coast and identified the variables associated with heavy rainfall. In doing so the major objectives of the project have been met.

A data archive was created. This consists of the prognostic fields of the SAWS Eta model as well as daily rainfall for a three-year period. These date are available for use by permission of the SAWS.

Recommendations

The systems developed are powerful and provide tools to the meteorologist, not available before. In order for the heavy rainfall identification systems to be fully used the support of the weather forecasters as well as of their managers is required. The Internet provides a powerful tool for the dissemination of NWP products and this should be explored further and additional products developed.

The current operational NWP models at the SAWS do not predict convective rainfall adequately. Research is required to optimise the output of the available NWP models to predict convective precipitation better. Research during the PROGRAIN project had also indicated that heavy rainfall prediction is region dependant. It is proposed that a project be funded to regionalise the prediction system and at the same time to target specific areas such as: the Umgeni river catchment; the Vaal river catchment; the Breede river catchment as well as smaller regions with large urban settlements such as Gauteng Province. If this work is funded it will be important to involve Water and Disaster Mitigation managers right from the start.

A student project associated with PROGRAIN explored the interactive modification of the model's rainfall prognoses using satellite data. Results were very promising and it is important to develop this, using the full available range of remote-sensing products for rainfall estimation in an operational rainfall prognoses modification scheme. This can then become part of the greater operational rainfall forecast system.

During the course of the PROGRAIN excellent rapport was established with Managers and Forecasters of the SAWS. All possible steps should be taken to continue this and to extend this to Water Managers.

Unfortunately the preparation of a proper quantitative precipitation forecast proved impossible. It is recommended that the SAWS upgrade their models to small resolution regional models.

Conclusions

This project was very cost effective and delivered an important tool for forecasting heavy rain. It provided the opportunity for capacity building as well as the training of forecasters both local and abroad. Several research papers were published or are in the process of publication. Several previously disadvantaged students participated and benefited from this project.

The support of the Water Research Commission made the research possible. The SAWS provided data, guidance and allowed some of their staff to participate in the project.

ACKNOWLEDGEMENTS

The project team would like to thank the Water Research Commission, especially Dr G C Green, who provided the support, which made this project possible.

The project steering committee gave invaluable guidance and support. The following persons all served on the steering committee:

Dr GC Green (Chairman)	Mr DB du Plessis (DWAF)	Mr S Sinclair (UKZN)	Mr E Poolman (SAWS)	Mr P Visser (SAWS)
Ms E De Coning	Mr S Steyn (UFS)	Prof GGS Pegram (UKZN)	Prof S Walker (UFS)	Mrs CM Smit (Secretary)

The University of Pretoria (UP) provided most of the infrastructure, which made the project run smoothly. The support and encouragement of Prof K S O Beavon (Head: Department of Geography, Geoinformatics and Meteorology, UP) is gratefully acknowledged.

The successful completion of this project and the operational implementation on the SAWS web site was greatly facilitated by Mr. Louis van Hemert (SAWS). He provided software and advice and was always available for consultation.

The weather forecasters and managers of the SAWS are thanked for their continued support, advice and honesty. The success of this project can only be measured by their participation. As always the advice and criticism of Evert Scholtz, is acknowledged.

The project leaders would like to express heart felt appreciation to Ms Helen Kenyon for many years of loyal service. We wish her and her family well in future endeavours.

The project team herby acknowledge, with sincere thanks, the contribution and support of the following people

Prof B Hewitson (UCT)	Ms HG Marx (SAWS)	Ms G Swart (SAWS)	Ms C De Villiers (SAWS)	Ms K Marias (SAWS)
Ms J Nel (UP)	Dr W Tennant (SAWS)	Ms A Demertzis (SAWS)	Dr H Brooks (NSSL)	

The project leaders appreciate the contribution of all the students who participated in this project. We will, with expectation, follow their careers as meteorologists.

The Project Team consisted of:

Prof J van Heerden (UP)	Ms LL Dyson (UP)	Ms H Kenyon (UP)	Ms L Clark (SAWS)	Mr L Masimini (UP/SAWS)
Mr A Moatshe (UP/SAWS)	Mr L Fernandes (UP/SAWS)	Ms L Burger (UP/SAWS)	Mr M Roux (UP/SAWS)	Ms M Martin (UP/SAWS)

TABLE OF CONTENTS

KEY WORDS AND DEFINITIONS

Atlantic Ocean High (AOH): High pressure system which originates over the Atlantic Ocean and which forms part of the sub-tropical high pressure belt. Moves from east to west near South Africa in association with extra tropical cyclones.

Adiabatic: Refers to a process in which a parcel of air is moved vertically in the atmosphere without any energy or mass transfer into or out of the parcel.

Advection: Transported by the atmospheric winds. Generally in the horizontal plane

Ageostrophic: Atmospheric flow across to the isobars (or contours)

Anti-cyclonic: Anti-clockwise rotation of the wind (in the Southern Hemisphere)

BARCOZ : A coastal zone heavy rainfall identification system for baroclinic weather s systems

BARLUT: A coastal zone heavy rainfall identification system with the unit wind vector

Baroclinic: Weather systems which possess vertical wind shear. An atmosphere where the density depends on pressure and temperature.

CAPE: Convective available potential energy. An indicator of the instability of the atmosphere and used to forecast convective cloud.

Components of the horizontal wind: The horizontal air motion is divided into two components: first, an east-west component (along latitude lines) referred to as the 'x' component, denoted by 'u', sign positive eastwards; second, a north-south component (along meridians) referred to as the 'y' component, denoted by 'v', sign positive northward.

Continental circulation: Refers to atmospheric circulation over the continents.

Contours: Iso-lines of atmospheric geopotential on a constant pressure level. Generally used to delineate (define, isolate) pressure systems in the upper air.

Convective, convection: Upward motion in the atmosphere forced by unequal heating of the surface.

Convergence: Normally the convergence of the horizontal wind or the convergence of the wind along a constant pressure surface. Computed as the divergence but in this case $D < 0$.

Cut-off low (COL): Low pressure system in upper troposphere isolated from the mid-latitude westerlies, north of 40 S, which is cold cored and has a closed circulation from the upper troposphere to the surface.

Cyclogenesis: The process of development (intensification) and eventual decay of a mid-latitude low-pressure system with associated cold and warm fronts.

Cyclonic circulation: Clockwise rotation of the wind around a low pressure system (Southern Hemisphere).

Divergence: Normally referred to as the divergence of the horizontal wind or along a constant pressure surface. Outflow or air from a point by the divergent component of the wind. $D = \nabla_p \bullet \mathbf{V} > \mathbf{0}$.

Equivalent potential temperature: The temperature that a parcel of air will attain if the parcel is first moved upward till all the water vapour has been condensed and removed from the parcel and then brought down to the 1000 hPa level while heating at the dry adiabatic lapse rate. The entire process takes place under adiabatic conditions.

Eta model: A limited area numerical weather prediction model referred as the Eta model.

FAR : The false alarm ratio.

FORFLOOD: Short Term Weather Forecasting Techniques for Heavy Rainfall. WRC Project No 1011/1/02

Geopotential: The geopotential energy per unit mass at a pressure level z metre above sea level.

Geopotential height: Expressed as geopotential metre (gpm). Defined as the geopotential ($\Phi = \int gdz$) divided by constant gravitational acceleration (g=9.8 ms^2). Used commonly when discussing the synoptic circulation patterns on pressure levels.

Geostrophic wind: Approximation of the horizontal wind on the synoptic scale, assuming that the flow remains frictionless and constant in a straight line. The flow is tangent to the isobars (contours) and the only two forces acting are the pressure gradient force and the Coriolis force which are equal and opposing. $\mathbf{V}_g = \mathbf{k} \times (f^{-1}\rho^{-1})\nabla p$ or $\mathbf{V}_g = \mathbf{k} \times (f^{-1})\nabla\Phi$ in pressure coordinates.

Heat low: A shallow continental low pressure system which develops because of intense heating of the surface by solar radiation. It is principally a daytime and summer feature.

High-pressure: Area of above average atmospheric pressure

Inter-Tropical Convergence Zone (ITCZ): Zones over the tropical regions where lower troposheric winds converge.

Isobar: Line of equal pressure. Generally refers to lines to delineate pressure systems and gradients along the earth's surface.

Isohyet: As above but refers to equal rainfall depth measured in millimetres.

Lapse rate: Rate at which the atmospheric temperature decreases with height. Expressed in Kelvin per metre (or 100 K/ 1000 metre).

Maritime systems: Refers to weather systems prevailing or originating over the ocean.

Meridional flow: Atmospheric winds parallel nearly parallel to the earth's meridians (north/south flow).

Mesoscale: Weather systems with horizontal length scale of the order of 100 km.

Mid-latitude westerly circulation: Southern hemisphere mid-latitude belt dominated by westerly winds

MITS: Model for the identification of tropical weather systems.

Mixing ratio: Mass of water vapour per unit mass of dry air.

MM5 model: A limited area numerical weather prediction model referred as the MM5 model.

NCEP data: National Centre for Environmental Processes computer generated meteorological data fields.

Numerical models: Computer models of the atmospheric flow fields based on the equations of motion and incorporating atmospheric physics and thermodynamics.

NWP: Numerical weather prediction.

Omega (ω): Vertical motion in the pressure coordinate system ($\omega = \frac{dp}{dt}$).

PCGRADS: Personal Computer Graphics and Display System.

POD: The probability of detection.

PROGRAIN: Research, Development and Verification of an Operational and Interactive System to Forecast Heavy Rainfall

Precipitable Water: Maximum depth of rain produced if all the water vapour in a vertical column of air condenses and precipitates out.

Pressure gradient force: Measured across the isobars (contours). Normally expressed as force per unit mass. PGF = $\rho^{-1}\nabla p$ (ρ, density, p, surface pressure).

QPF: A quantitative precipitation forecast.

Quasi-geostrophic theory: Dynamical analysis of the atmospheric flow fields, on the synoptic scale, by assuming that the horizontal wind can be approximated by the geostrophic approximation and that vertical accelerations are small.

Relative humidity: Degree of saturation by water vapour of the air. Defined as ratio of the observed vapour pressure divided by the saturation vapour pressure at the same temperature.

Relative vorticity (ζ): Vertical component of the vorticity. $\zeta=\mathbf{k}\bullet\nabla\times\mathbf{V}$. Normally computed on a pressure surface and is a measure of the rotation of the wind at a point.

Ridging Atlantic Ocean High (AOH): High pressure system located over the southern Atlantic Ocean extending (moving) eastward and normally south of South Africa.

Saturated adiabatic lapse rate (SALR): As the DALR but for a parcel of air saturated with water vapour. The SALR ≈ 0.6 K/100m near the earth's surface.

Saturation: Refers to the state when an equal number of water molecules evaporate from an open water body into the atmosphere as the number returning to the water body from the atmosphere. This number of molecules in the air during this state is the maximum the air can contain at the current temperature. This number increases as the temperature of the air increases.

SEC: Divergence of the gradient vector of the southeastern vapour flux component. $SEC = \overline{\nabla} \bullet \overline{\nabla}(qV_{SE})$

Scale (large, small, synoptic): Refers to the horizontal scale of the atmospheric motion.

Specific Humidity (q): Mass of water vapour per unit mass of moist air.

Synoptic scale: Refers to motions with horizontal scale of the order of 1000 km and a time scale of days.

THERIS: Tropical heavy rainfall identification system.

Total Static Energy (TSE): Total thermodynamic and geopotential energy of the air.

Tropical cyclones: Also referred to as Hurricanes or Typhoons. Very intense tropical low-pressure systems accompanied by destructive wind and rain.

Tropical temperate trough (TTT): A low pressure zone (trough) extending southwards from tropical low to mid-latitude low pressure system.

Tropopause: Boundary between the troposphere and the stratosphere and located where the temperature decrease with height (in the troposphere) is reversed or terminates.

Vapour flux:	Product of the specific humidity (q) and the wind velocity **V**. Components of the vapour flux referred to are the meridional vapour flux component (qv) and the southeast wind component of the vapour flux (qv_{SE}).
Vapour pressure:	Partial pressure exerted by the water molecules contained in the air.
Vorticity:	Three dimensional vector quantity describing the rotation of a fluid at a point. $\varpi = \nabla \times \mathbf{V}$.
Water vapour:	Water molecules (H_2O) (gaseous state of water) in the mixture of atmospheric gases.

CHAPTER 1
INTRODUCTION

1.1 Introduction

Heavy rainfall and floods occur frequently over southern Africa and lead to large financial losses, damage to infrastructure and tragically loss of life. Viljoen, cited in Alexander and van Heerden (1991), lists 184 noteworthy flood events during the years from 1911 to 1988. Close to 30% of these flood events occurred over KwaZulu-Natal and 42% over the four northern provinces and the central interior of South Africa. Poolman, cited in Dyson et al (2002) showed how most heavy rainfall days occurred over the eastern and northeastern parts of South Africa during summer months. A recent example of extreme rainfall over Southern Africa is the devastating flood over the Limpopo Province of South Africa during February 2000. This floodwater devastated large parts of the Limpopo Province and adjacent regions of Mozambique (Dyson and van Heerden, 2001). The famous Kwazulu-Natal floods of September 1987 resulted in the death of more than 300 people and damage to the infrastructure in excess of one billion Rand (Triegaardt et al 1988). Flood related water resource management becomes extremely difficult, if not impossible, without prior warning of heavy rains. Better advance warning on the spatial and temporal distribution of heavy rainfall can be of vital importance to the survival of communities living on flood plains and can go a long way to minimise damage to infrastructure.

In spite of the tremendous advances that have been made with Numerical Weather Prediction (NWP) during the last decade, weather forecasters and water managers are at present still unable to provide accurate heavy rainfall forecasts. Pinpointing the exact area where the heavy rainfall will concentrate is very difficult. During the heavy rainfall events of February 2000 the precipitation forecast generated by the South African Weather Service (SAWS) Limited Area Model (LAM) Eta, underestimated the rainfall totals by close to 50% (Dyson and Van Heerden 2001). De Coning et al. (1998) described the heavy rainfall event during February 1996 over central South Africa. The precipitation forecast of the SAWS Eta model captured the spatial distribution well but predicted rainfall amounts that were considerably less that the actual rainfall.

NWP models are very good in simulating atmospheric flow fields and are unsurpassed in predicting the development and movement of weather systems known to be potential heavy rainfall producers. Unfortunately the rainfall fields generated by these models are nowhere as good as the circulation fields they produce and this had led to a lack of confidence in the rainfall prognoses. Furthermore the area where heavy rainfall will concentrate cannot yet be predicted reliably.

This report details the research that had led to the development and implementation of operational heavy rainfall prediction systems that operate on the prognostic fields generated by the SAWS Eta model.

1.2 Earlier Research: The FORFLOOD Project.

The FORFLOOD Project (Short term Weather Forecasting Techniques, 6-48 hours ahead, dedicated to flood management systems, WRC Report No 1011/1/02) set out, amongst other things, to develop a computer-based quantitative precipitation forecast system for South Africa. The aims also included research on past heavy rainfall events, evaluation of their predictability and the classification of associated systems according to their dynamical characteristics. This project researched systems with the potential to isolate heavy rainfall from tropical and coastal zone baroclinic weather systems. Much of the research reported here is based on the achievements of the FORFLOOD Project that had identified weather systems producing heavy rainfall.

1.2.1 Tropical Weather Systems.

Tropical weather systems over southern Africa generally occur during summer months and over the northern regions of the country (Van Heerden and Taljaard, contributing to Karoly and Vincent ,1998). A very basic definition of tropical weather systems requires that the vertical wind field must have very little wind shear (Holton, 1992). However, the FORFLOOD project developed a Model for the Identification of Tropical Weather Systems (MITS), which describes the atmospheric criteria of a continental tropical weather system. Research on the heavy rainfall produced by tropical weather systems resulted in the development of the system referred to as THERIS (tropical heavy rainfall identification system). THERIS isolates heavy rainfall forced by tropical weather systems. THERIS is novel, unique and was designed with the operational meteorologist in mind. The case studies, using THERIS, showed that this system performed well on NCEP data.

1.2.2 Baroclinic Weather Systems.

Baroclinic weather systems can be defined as having significant vertical wind shear (Holton, 1992). Over South Africa they occur right through the year and are linked to the mid-latitude westerly circulation systems. Research on heavy rainfall events during the FORFLOOD project resulted in the development of BARCOZ (baroclinic coastal zone heavy rainfall system). BARCOZ, operating on NCEP data, showed some potential to isolate the areas where heavy rainfall is possible along the southern and eastern coastal zone of South Africa.

1.3 Flood producing weather systems over South Africa

Weather systems causing heavy rainfall over southern Africa are: tropical cyclones, the cut-off low (COL), the ridging Atlantic Ocean high (AOH) behind the cold front and the tropical temperate trough (TTT) (Alexander and van Heerden, 1991, Taljaard, 1985, Triegaardt el al, 1991).

Tropical cyclones making landfall in southern Africa are rare events. However when this does happen, extreme rainfall and flooding result (Poolman and Terblanche, 1984 and Dyson and van Heerden, 2001).

Many flood events over South Africa have been caused by cut-off low (COL) pressure systems (Taljaard, 1985). When a COL occurs in winter, wide spread and heavy snowfall can occur. This happened during July 1996 (Strydom and Nel, 1996).

Crimp et al. (1997) and Harrison (1983,1986) provided a thorough explanation of the importance of the tropical-temperate trough (TTT) in producing rainfall over South Africa. They estimated that approximately 39% of the mean annual rainfall can be attributed to the TTT.

In this research emphasis was placed on continental tropical weather systems as well as weather systems causing heavy rainfall along the coastal plains of South Africa.

The Western Cape Province as well as the coastal zone stretching eastward to KwaZulu-Natal often receive heavy rainfall during the passage of intense mid-latitude weather systems associated with potent cold fronts followed by a strong ridge of the AOH. Over the Cape Peninsula and surrounds, heavy rainfall generally occurs in the northwesterly flow ahead of the cold front. The southern and southeastern coastal areas usually experience heavy rainfall after the passage of the cold front when an intense ridge of the AOH cause a strong southerly to southwesterly on-shore flow (Alexander and van Heerden, 1991 and van Heerden and Hurry, 1987). The heavy rainfall associated with these weather systems may or may not be accompanied by upper tropospheric weather systems such as an upper air trough or COL. In this research focus is placed on heavy rainfall caused by surface forcing along the coast of South Africa. It is accepted that the escarpment, which rises to approximately 1500 m within 200 – 300 km from the coast, plays a significant role in the production of the heavy rainfall along the coast (De Villiers, 1992, Dyson and van Heerden, 2001, Tennant and van Heerden, 1994 and Triegaardt et al., 1988). Triegaardt et al. (1988) showed that the heavy rainfall over the Kwazulu-Natal is predominantly due to a strong surface on-shore flow.

Continental tropical weather systems occur infrequently over South Africa and are most common during late summer (January to March) (Dyson, 2000 and Van Heerden and Taljaard contributing to Karoly and Vincent ,1998). Two well-known heavy rainfall events caused by continental tropical weather systems occurred in February 1988 (Triegaardt et al., 1991) and February 2000 (Dyson and van Heerden, 2001)

1.4 Aims of the research

The main aim of the Research, Development and Verification of an Operational and Interactive System to Forecast Heavy Rainfall (PROGRAIN) project was to develop a system to predict heavy rainfall but in an operational weather forecasting environment.

During the course of the project the following studies and/or supporting research to achieve this aim were undertaken:

- Methods to isolate heavy rainfall developing in continental tropical and extra-tropical as well as in coastal zone baroclinic weather systems
- Inclusion of topographic effects in the operational coastal zone heavy rainfall forecast system
- A method to modify Numerical Weather Prediction Model rainfall prognoses by incorporating satellite derived rainfall
- On site training of SAWS staff in the use of the operational heavy rainfall forecast systems

The second aim of the project was the development of a statistical validation system for the rainfall fields produced by the research and operational heavy rainfall systems.

To achieve these aims, research was subdivided into the following steps, detailed per chapter in the report.

Chapter 2 details the data fields and prognostic model fields on which most of the research was performed. This chapter also provides detail on the NWP models that were available to the project.

Chapter 3 deals in considerable detail with the long search to find a reliable coastal zone heavy rainfall prediction scheme. This chapter provides detail on the configuration and requirements of the operational systems that were accepted for regions of the coastal zone.

The heavy rainfall identification systems were developed to run on the SAWS Eta model. Chapter 4 details the criteria of the operational THERIS and coastal zone heavy rainfall identification systems.

Chapter 5 deals with the statistical evaluation of the research and operational systems described in Chapters 3 and 4.

A method to combine the output of the precipitation forecast of a NWP model and observed rainfall fields is detailed in Chapter 6 while Chapter 7 details the operational implementation of the systems at the SAWS. The conclusions and recommendations are dealt with in Chapter 8 and Chapter 9 reports on capacity building. Chapter 9 includes several case studies conducted by students contributing to the PROGRAIN project.

CHAPTER 2
DATA

This chapter describes the different data sets used in this report. The numerical weather prediction (NWP) models are described briefly as well as the observational rainfall data. An extensive data archive was produced, the details of which are given in Section 2.3.

2.1 Numerical Weather Prediction Data.

2.1.1 NCEP Data

All the heavy rainfall identification systems were originally developed on the data available from the National Centre for Environmental Prediction (NCEP). These data are considered to provide realistic atmospheric flow fields on the synoptic scale. NCEP data are freely available and may be downloaded from www.cdc.noaa.gov in a format ready for use in display and analysis programs such as Grid Analysis and Display System (GrADS). The NCEP data are available in 17 vertical levels and the horizontal resolution is 2.5°. The horizontal and vertical resolution of the NCEP data are suitable to research weather systems on the synoptic scale. Small or mesoscale features will not be adequately resolved by this data set.

The NCEP data provide a so-called perfect prognosis or analysis field, which is unfortunately not available in an operational environment. It was required to test and further develop the heavy rainfall identification systems on the prognostic fields of a numerical weather prediction model (NWP). In this research the MM5 and Eta models were utilized.

2.1.2 MM5 Model

The prognostic fields from Fifth-Generation National Centre for Atmospheric Research (NCAR)/Penn State Mesoscale Model also referred to as the MM5 model, were used in this report. The MM5 model data were made available from two sources. Prof Bruce C. Hewitson, (Climate Systems Analysis Group (CSAG), University of Cape Town) provided three model runs for past heavy rainfall events. Two runs were performed for September 1968 and another for August 2002. The details of these runs are provided in Chapter 3. The South African Weather Service provided two model runs, for the 18th and 19th of March 2003, that were used in Chapter 6 to demonstrate how measured rainfall and the rainfall prognosis from NWP models may be combined to provide an improved Quantitative Precipitation Forecast (QPF).

The model is available freely for research purposes from NCAR/Penn State MM5 web page (http://www.mmm.ucar.edu/mm5). Full model details are also available from this website.

The MM5 model is a limited area model of atmospheric systems, over regions ranging from thousands to hundreds of kilometres. Initial conditions and forcing for lateral boundaries come from external sources: global models and observations (Michalakes, 1997). NCEP data were used for the initial and boundary conditions in the CSAG model runs while in the SAWS model runs Eta data were used.

The model is a primitive momentum equation model, using the full terms of the vertical momentum equation, also referred to as non-hydrostatic. However, it should be noted that the runs conducted by the SAWS were done in hydrostatic mode. Surface pressure as well as the thermodynamic prognostic equations are incorporated. The co-ordinate system is the (x,y,σ) system also referred to as the sigma co-ordinate system.

Model physics, numerical schemes and temporal finite differencing schemes are all adequately described in the MM5 model specifications available at the website. However it should be noted that because the hydrostatic approximation is not made, solutions of the model equations include sound waves. Therefore some of the equation terms have to be calculated on a shorter time step. Certain processes are treated implicitly for numerical stability.

Details of the horizontal and vertical resolution of the MM5 runs are provided in the relevant chapters.

2.1.3 Eta model data

The SAWS currently runs the Eta model operationally and it was therefore imperative to develop and test the heavy rainfall identification systems on the prognostic fields of this model.

The prognostic fields of the SAWS Eta model are available in a horizontal resolution of 50km and vertical resolution of 50hPa. The current Eta model domain covers Southern Africa and surrounding oceans from approximately 9° S to 48° S and 13° W to 53° E. The model is run twice daily, with initial conditions at 12 UTC and 00 UTC. Both grid scale (Zhao and Carr, 1997) and convective precipitation (Betts and Miller, 1986; Janjic', 1994) are produced. Sub-grid scale convection processes play a major role in the ability of the model to accurately forecast rainfall. In the SAWS Eta model, the Betts-Miller convective parameterisation scheme is used in which moisture or upward vertical motion is not required explicitly to compute precipitation (Betts 1986; Betts and Miller 1986). A comprehensive description of the Eta model is provided by Mesinger et al. (1988). Janjic' (1984, 1990) describes the parameterizations of atmospheric processes employed in the Eta model.

One of the major differences between the MM5 and Eta model is the vertical co-ordinate. The MM5 model uses the sigma co-ordinate system while the Eta model uses the step-mountain or eta vertical co-ordinate (Mesinger, 1984). The step-mountain co-ordinate is constructed as discrete steps, with tops located at model interfaces. The Eta and MM5 model will therefore deal with locations with steep or complex topography differently. In South Africa this is especially relevant for the escarpment where the plateau in most areas rises steeply over the first 200-300 km inland from the coast. Chapter 3 describes some of the challenges in developing an objective heavy rainfall scheme in areas of steep topography.

2.1.4 Comparing Eta prognosis and NCEP data.

The heavy rainfall identification systems were initially developed utilizing NCEP data. The operational version of these systems is available on the prognostic fields of the SAWS Eta model. The horizontal resolution of these two data sets are quite different and this has a significant influence on setting critical values for variables such as wind divergence, moisture flux convergence and vertical velocity. NCEP data have a horizontal resolution of approximately 250km while the Eta data have a horizontal resolution of close to 50km.

Figure 2.1 depicts the 1000hPa height field expressed in geopotential metres (gpm) as well as winds from the (a) Eta model and (b) NCEP data on the 19th of July 2001 at 18UTC. Comparing the winds depicted in figure 2.1 (a) and (b) allows some understanding of the difference in the model resolution. The wind speed and direction at the locations where the grid points of the two data sets co-inside are very similar but the winds from the Eta model are generally 5 knots stronger than the NCEP winds. The geopotential height fields from the different data sets compare well except that the Eta model has a better-defined trough just off the South African west coast. Accepting that the NCEP field may be considered a perfect prognosis it is quite clear that the 18-hr prognosis of the Eta model simulated the 1000hPa atmospheric conditions satisfactorily.

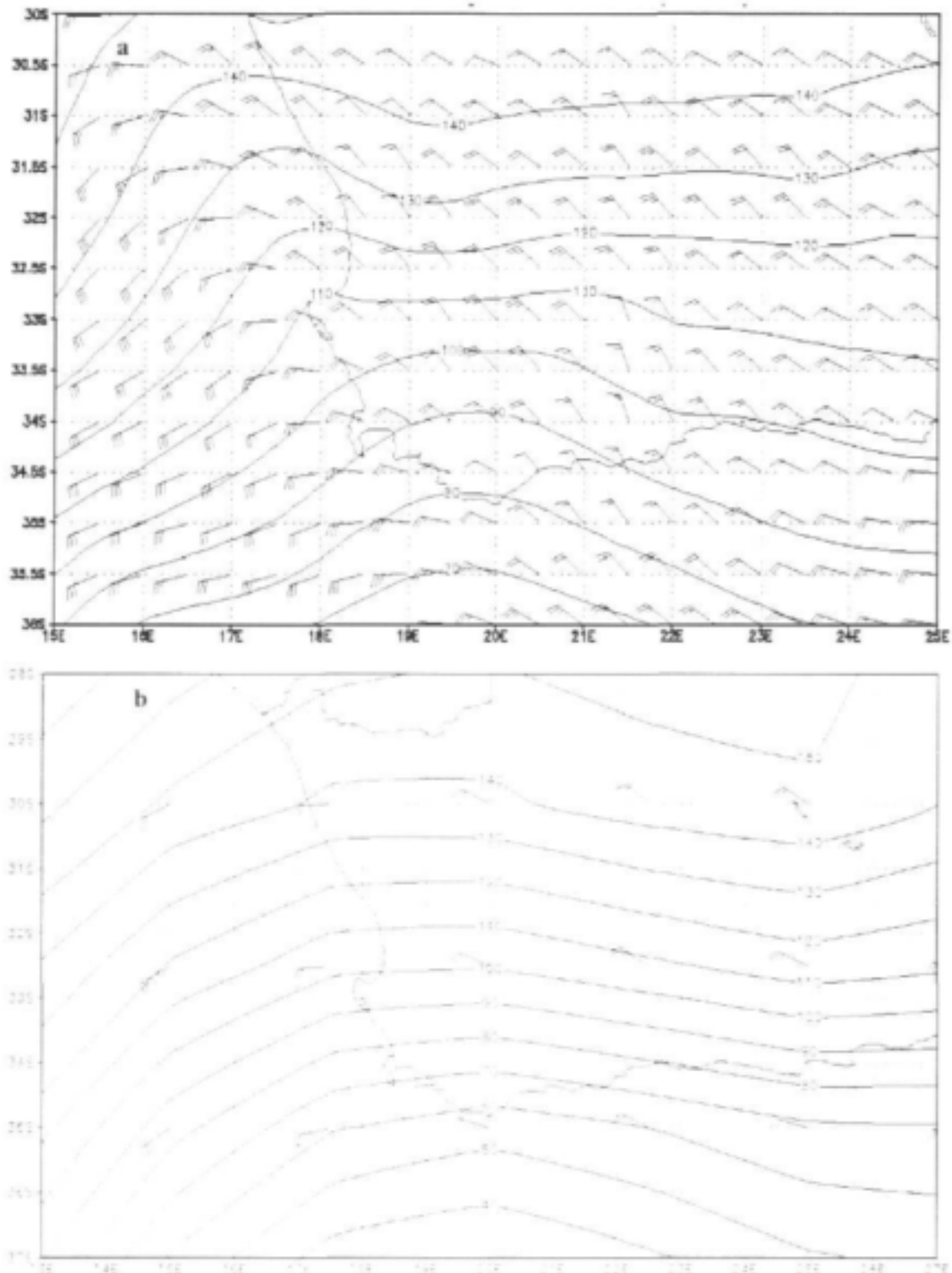

Figure 2.1: The 1000hPa geopotential height field in gpm and winds (knots) from the (a) Eta model and (b) NCEP data on the 19th of July 2001 at 18UTC.

Figure 2.1 also reveals that the horizontal wind speed is of the order of 10 ms^{-1} and this is in good agreement with the scale value set by Holton (1992). Spatial derivatives are approximated using centred differences. This means that changes in the parameters between grid points are divided by 100 km in the case of the Eta model and by 500km for NCEP data. Accepting that the magnitude of the horizontal wind components are generally of the order of 10 ms^{-1} it then follows that the scale values assigned to divergence and omega are of the scale depicted in table 2.1. The scale value computed for the horizontal divergence is an order of magnitude smaller than the scale value for each of the two terms because they are generally of opposite sign.

Table 2.1 Scale values for horizontal wind divergence in the Eta and NCEP data.

		NCEP (500km)	Eta (100km)
Divergence (s^{-1})	$\overline{\nabla} \bullet \overline{V}_H = \frac{\partial u}{\partial x} + \frac{\partial v}{\partial y}$	$\frac{10}{5*10^5} = 10^{-5} \Rightarrow 10^{-6}$	$\frac{10}{10^5} = 10^{-4} \Rightarrow 10^{-5}$
Omega (Pa s^{-1})	$\overline{\nabla} \bullet \overline{V}_H + \frac{\partial \omega}{\partial p} = 0$	10^{-1}	1

This table, where $\overline{\nabla} = \frac{\partial}{\partial x}\bar{i} + \frac{\partial}{\partial y}\bar{j}$ and the horizontal wind $\overline{V}_H = u\bar{i} + v\bar{j}$, shows that the magnitude of the horizontal wind divergence computed at the Eta model grid scale is an order of magnitude larger than for computations at the scale of the NCEP data. Vertically integrating the continuity equation from the surface to a mid-tropospheric level, and accepting that the horizontal divergence can be kept constant and at a scale value of magnitude depicted by table 2.1, results in scale values for omega as in table 2.1. Note that the magnitude of omega is an order of magnitude larger in the Eta model than in the NCEP data.

Figure. 2.2 shows that the magnitude of the horizontal wind divergence at the 1000hPa level computed from the Eta model prognoses is close to an order of magnitude larger than for NCEP data. This figure also reveals that the areas of convergence (negative) and divergence (positive) are quite different in the two data sets. The area of divergence (Fig. 2.2a) over the north-western interior is absent in the NCEP data (Fig. 2.2b).

Figure 2.3 shows the significant difference in omega between the two data sets. This figure depicts a vertical profile of omega values at 32.5°S and 17.5°E. The minimum value of omega (maximum upward motion) is an order of magnitude larger in the Eta model than in the NCEP data. These differences in the computation of derivatives arise predominantly because of the difference in model resolution. Variables such as mixing ratio, temperature and even precipitable water are very similar in the different data sets but behave as described here whenever spatial differentiation in the different horizontal resolutions apply.

The different scale values valid for derivatives such as the divergence and vertical motion required a re-evaluation of all the critical values set for model derivatives previously used to isolate areas of probable heavy rainfall.

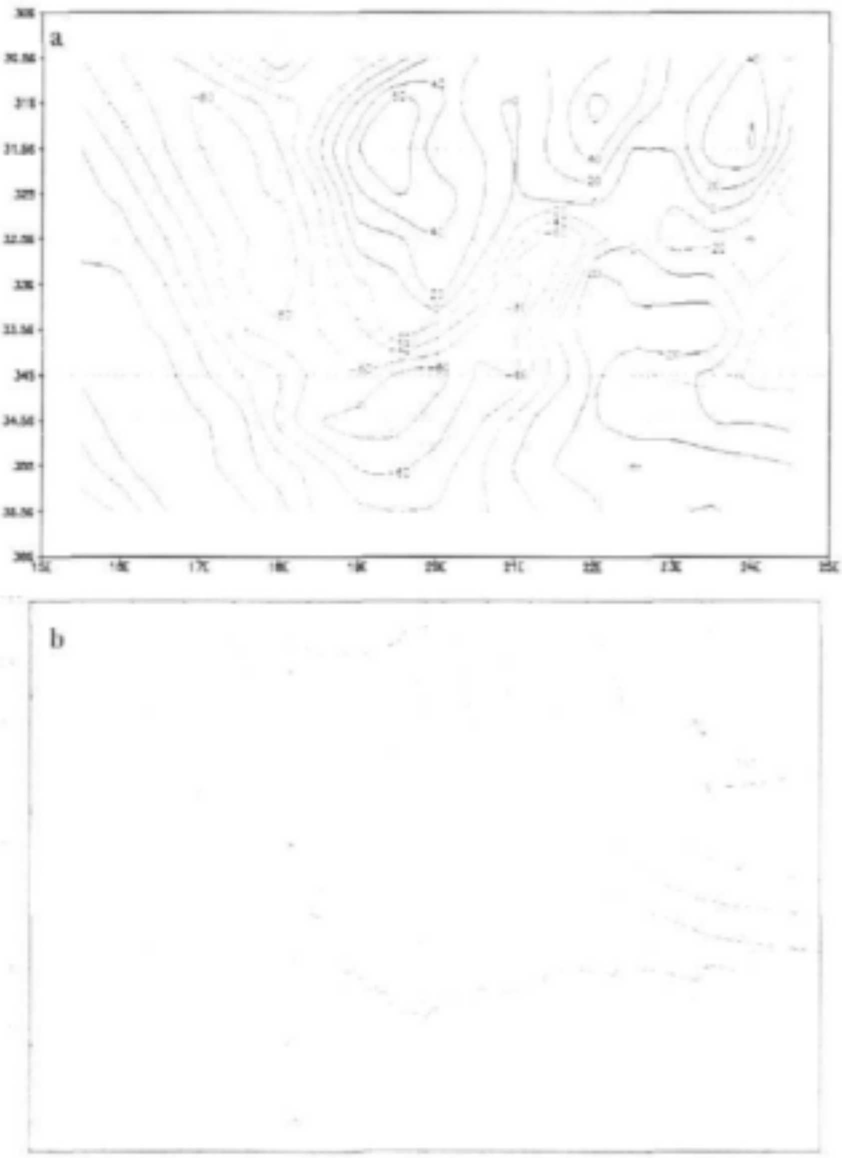

Figure 2.2: As for Fig 2.1 (a) and (b) but for horizontal wind divergence (s^{-1}). Divergence values multiplied by 10^{5}.

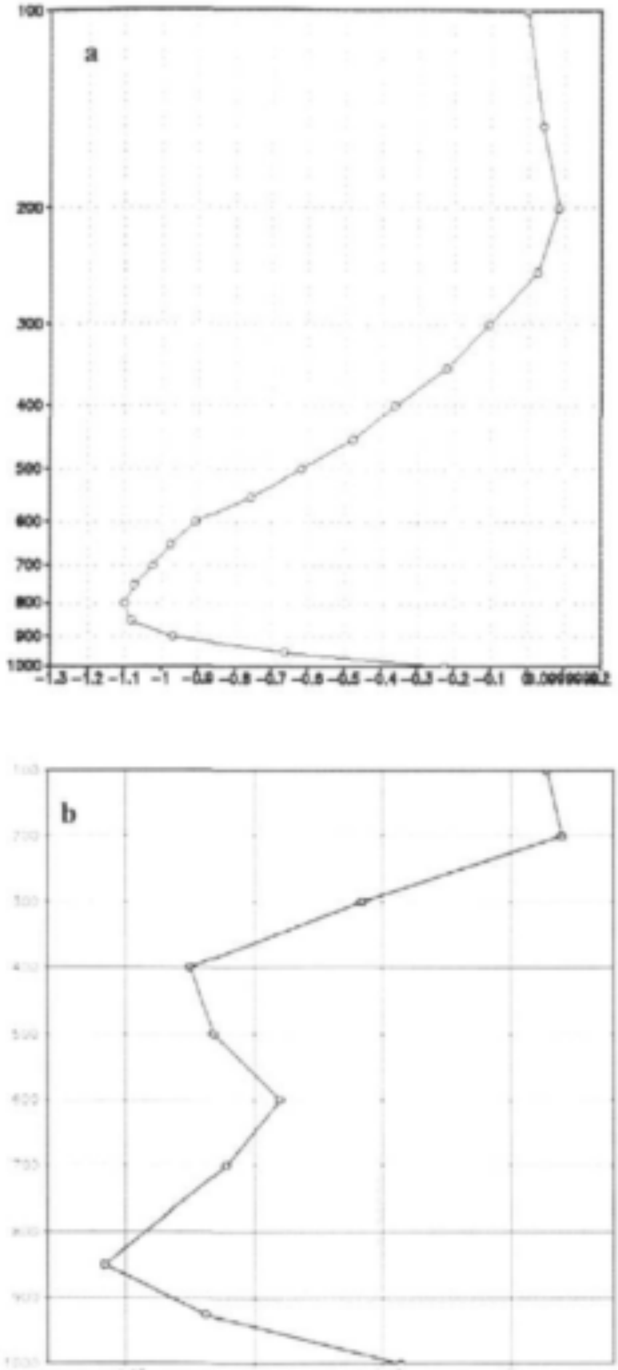

Figure 2.3: Vertical profile of omega (Pa s^{-1}) at 32.5°S 17.5°E from the (a) Eta model and (b) NCEP data on the 19th of July 2001 at 1800UTC.

2.2 Rainfall data

Rainfall data used in this report were obtained from the SAWS. Daily gauge data were obtained for the period September 1999 to March 2002. During this period approximately

1500 SAWS stations recorded rainfall over South Africa. The data are available in 24-hr periods and are observed daily at 0600 UTC. The rainfall data were used to develop and validate the heavy rainfall identification systems.

Satellite rainfall data were obtained from the SAWS, Bethlehem for March 2003. These rainfall fields are available as part of the SIMAR project (Pegram, 2004). The satellite rainfall was used rather than the integrated SIMAR rainfall field, as it was available in 1-hrly intervals. It was also preferred above the RADAR rainfall field as it provided a geographical coverage over the entire Southern Africa. The satellite rainfall was compared with the rainfall prognosis of the MM5 model in order to demonstrate how satellite rainfall and the rainfall prognosis from NWP models may be combined to provide an improved Quantitative Precipitation Forecast (QPF).

2.3 Data archive

Daily NCEP, Eta and rainfall data were obtained for the period September 1999 to March 2002. This is in total 943 days. The first and most challenging task was to convert all these disparate data fields into a common format to facilitate inter-comparison.

The daily NCEP data were downloaded from www.cdc.noaa.gov. The data are available in the so-called netcdf format and may be displayed in GRADS without complication. The following variables were obtained on the 1000, 925, 850, 700, 600, 500, 400, 300, 250 and 200 pressure levels: height of the pressure level in geopotential metres (gpm) (referred to as geopotential height), temperature (K), meriodonial and zonal wind components (ms^{-1}), vertical motion (Pas^{-1}), and relative humidity. The data are available in 6-hr intervals and all heavy rainfall identification systems were calculated for a 24-hr period which coinsides with the 24-hr period the SAWS uses for daily rainfall i.e. 0600 UTC on day one to 0600 UTC on day two.

Figure 2.4b depicts the geographical position of the NCEP grid points over South Africa. A NCEP grid point represents a geographical area of 2.5 by 2.5 degrees with the grid point in the centre of the area. Utilizing the daily SAWS rain gauge data an average rainfall value was calculated for the geographical area represented by each NCEP grid point. The grid points outside the borders of South Africa or where no rainfall stations were operational were denoted by a value of –77. In addition to the average rainfall, the maximum rainfall at any station in the area was noted. The number of rainfall stations and the percentage of rainfall stations, which recorded more than 0 mm of rainfall was also calculated for each grid point on a daily basis. Appropriate FORTRAN programs were developed to write these values into grid format to be able to display and manipulate them in GRADS. The final product enables the user to simply type in a date and the NCEP data as well the rainfall data become available for use in GRADS.

The same procedure was followed with the Eta data. The geographical positions of the Eta grid points over Southern Africa are depicted in figure 2.4a. An average rainfall value, the maximum rainfall, the number of rainfall stations as well as the percentage of rainfall stations reporting more than 0 mm of rainfall was calculated for each Eta grid point. These data were also written into GRADS format for easy comparison with the Eta data.

The SAWS archives the Eta model data on a daily basis. The model is run twice a day with initial times at 0000 UTC and 1200 UTC. These data are stored in grid format and are written out every 3-hrs from the 0-hr to the 48-hr prognosis. Every prognostic output field for the appropriate hour is stored in a separate file, each approximately 3MB in size. To store the entire data set for a single Eta model run requires close to 45MB. This data set (in grid format) is not easily accessible and in order to use the data it had to be transformed into a format, which is accessible in a display system such as GRADS. The decision was taken to use only data from the 0000 UTC run and only up to the 30-hr prognosis. The 30-hr prognosis of the 0000 UTC model run is valid for 0600 UTC on the following day and this ensured that the model data were available for the same period that the SAWS uses for daily rainfall. It was also decided to ingest into GRADS format only those Eta model variables, which are relevant for the forecasting of heavy rainfall. They are:

- Horizontal winds (ms^{-1}) on 19 pressure levels
- Air temperature (K) for 19 pressure levels
- Specific humidity (kg/kg) for 19 pressure levels
- The geopotential heights (gpm) for 19 pressure levels
- Vertical motion (Pas^{-1}) for 19 pressure levels
- Height of the freezing level (m)
- Total precipitation (mm)
- Sea level pressure (Pa)
- Water temperature (K)
- Surface temperature (K)
- The 2m air temperature (K)
- The 2m dew point temperature (K)
- 10m horizontal winds (ms^{-1})

Data are available from 1000 to 100 hPa and in 50hPa intervals. Unfortunately the Eta model was archived on only 764 days of the possible 943 days. Of these 427 were in summer (October to March) and 337 in winter (April to September).

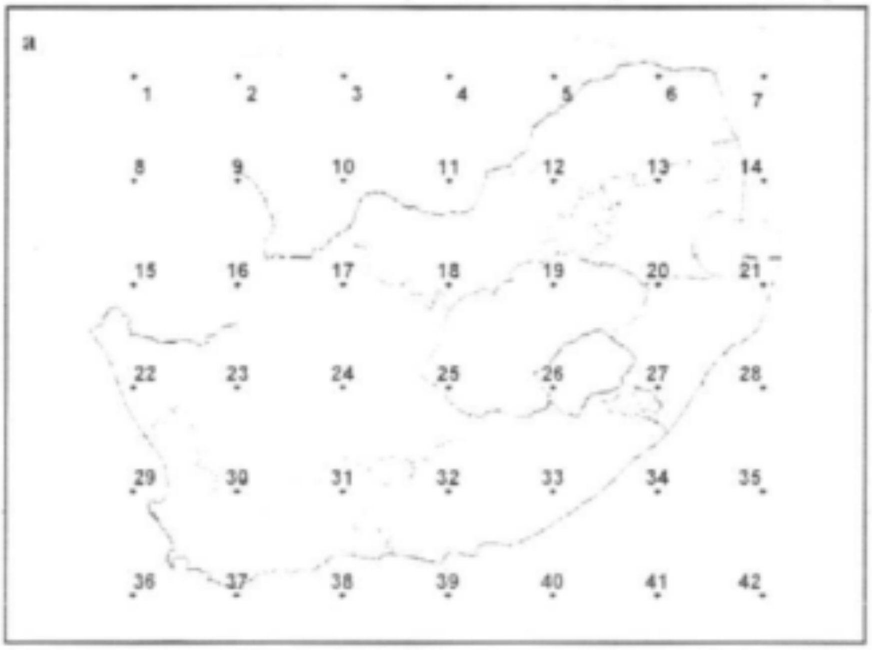

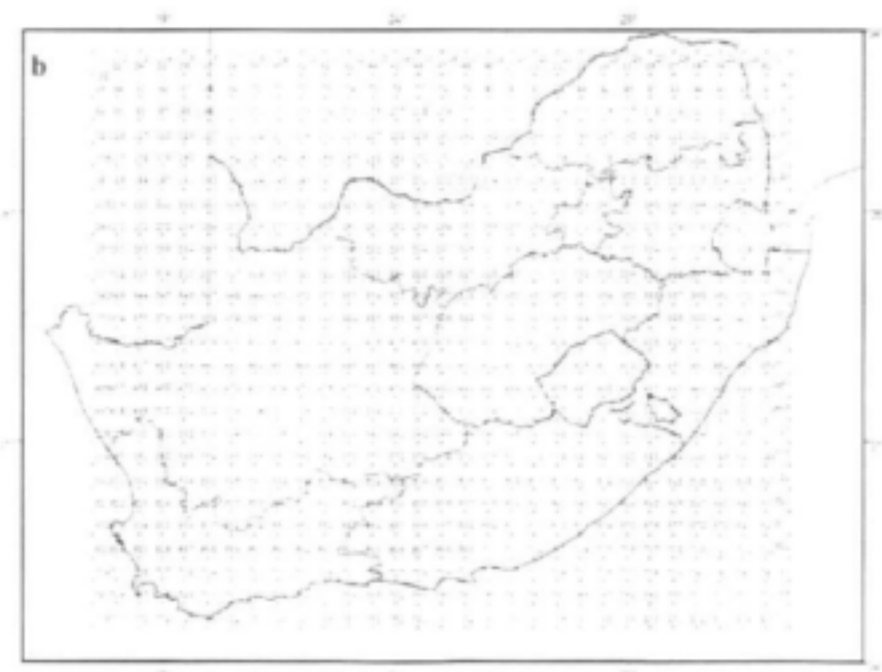

Figure 2.4: The (a) NCEP and (b) Eta grid points maps over Southern Africa.

CHAPTER 3

HEAVY RAINFALL ALONG THE COAST OF SOUTH AFRICA – PRELIMINARY MODEL INVESTIGATIONS

(Including a contribution by Mr. Luthando Masimini)

3.1 Introduction

Baroclinic weather systems producing heavy rainfall over the coastal zone are truly significant features of the South African rain regime. Taljaard (1985), Triegaardt (1988), Preston-White and Tyson (1993) as well as Harrison (1983) described the baroclinic weather systems over South Africa, most of which produce widespread heavy precipitation over the coastal zone. Several significant circulation features common to baroclinic weather systems producing heavy rain are recognized:

- *Large values of relative vorticity advection in the 200-300 hPa layer occurring above surface convergence.*
- *Upward motion occurring through most of the lower and middle troposphere.*
- *Sustained in-phase lower tropospheric temperature advection. This means lower tropospheric cold air advection below the upper trough and warm moist air advection below and upstream of the upper ridge.*
- *Significant convergence of water vapour in the lower layers of the atmosphere.*

In developing the coastal zone heavy rainfall forecast systems, emphasis is placed on heavy rainfall that occurs along the coast of South Africa and is caused predominantly by surface forcing. The synoptic scale weather system responsible for this type of rainfall is usually an extra tropical cyclone, which is followed by the movement south of the country by an Atlantic Ocean high (AOH). This may or may not be accompanied by an upper air trough or even a cut-off low (COL). This research focuses on the lower levels of the atmosphere and endeavours to predict the forced rising of moisture laden air along the escarpment of South Africa.

This chapter briefly describes the original versions of the baroclinic coastal zone heavy rainfall system (BARCOZ) developed by Dyson et al (2002). The challenges in applying BARCOZ to the prognostic fields of a NWP model are detailed. The most challenging aspect in developing an objective rainfall identification system is to identify the appropriate moisture variable. In the operational versions of BARCOZ the preferred moisture variables are precipitable water and moisture flux convergence. However, several other moisture variables were investigated during the course of the research in order to obtain optimal results. These moisture variables as well as well as other atmospheric criteria used to research heavy rainfall along the coast of South Africa will briefly be detailed.

3.2 Coastal heavy rainfall utilizing NCEP data

The availability of NCEP data and analysis systems such as the GRADS package allowed the re-examination of several noteworthy rainfall events. GRADS allows the computation and display of circulation features. This powerful tool was not available to earlier researchers. The most important events re-analysed were:

- *The September 1968 Port Elizabeth flood (Hayward and van den Berg, 1968).*
- *The Laingsburg flood (Estie 1981).*
- *The September 1987 Natal flood (Triegaardt. et al., 1988).*

The strong flow of moist maritime air from the south-east over the coastal regions was noted by the authors cited as well as by several other researchers, notably De Villiers (1992), Taljaard (1985) and Tennant and Van Heerden (1994). All concurred that this strong flux of moisture laden maritime air is one of the primary forcing mechanisms for heavy coastal zone rainfall. Strong gradients of moisture flux along the S/N and SE/NW azimuth lines were observed near to areas of heavy rainfall. This observation led to the computation of the gradient of the water vapour flux by the south-east component of the near surface winds $\overline{\nabla}(qV_{SE})$. This vector was observed to converge near areas with heavy rain. The computation of its divergence defined the parameter **SEC**:

Divergence of the gradient vector, of the water vapour flux, by the SE wind component $(\overline{\nabla} \bullet \overline{\nabla}(qV_{SE}))$

SEC has units of **kgkg^{-1} m^{-1} s^{-1}**. The units differ from the conventional divergence of the water vapour flux $(\overline{\nabla} \bullet (q\overline{V}))$ **(kgkg^{-1}s^{-1})** because the gradient of the flux component was used and not the flux vector. GRADS analysis of the NCEP data sets of historic heavy rainfall events led to the experimental determination of the following criteria to be met for heavy coastal zone rainfall (BARCOZ):

- Omega (ω) < -0.2 Pa s^{-1} at both the 700 and 600 hPa levels.
- SEC< -50 *10^{-13} kgkg^{-1}m^{-1}s^{-1}.

A GRADS script was designed to isolate areas where these two conditions were met and became known as the baroclinic coastal zone (BARCOZ) heavy rainfall system. Dyson et al (2002) developed BARCOZ for the WRC Project: FORFLOOD. In this report the further development and implementation of BARCOZ and some of its successors on the prognostic fields of a NWP model are described. Chapter 5 details the verification of the original BARCOZ developed on the NCEP data as well as the operational versions available on the prognostic fields of the Eta model.

3.3 A Novel Approach to Moisture Flux Convergence

(Contribution by Mr Luthando Masimini)

The application of BARCOZ on NCEP re-analysis data showed that the system could identify heavy rain areas fairly well and it was also noted that BARCOZ handled summer rainfall better than winter (heavy) rainfall. Details of this are given in Chapter 5. Dyson et al. (2002) suggested that the topography of South Africa and inadequate handling of water vapour could explain some BARCOZ failures.

The success of the parameter SEC in locating heavy rainfall along the southeast and east coast is due to the fact the system advecting water vapour onshore is an intensifying high pressure over the South Atlantic Ocean. A strong south-easterly onshore flow forces water vapour up and over the escarpment resulting in abundant orographic rainfall. This moisture uplift may further enhance cloud development in favourable prevailing weather systems.

The synoptic scale analysis of the moisture flux (qV) indicates that the contribution of the individual variable is such that $q \sim 10^{-2}$ $kgkg^{-1}$ and $V \sim 10ms^{-1}$. The magnitude of V will therefore dominate the value of moisture flux. To reduce the dominance of the wind component in the computation of moisture flux or SEC the wind vector was replaced by its dimensionless unit vector:

$$\overline{\psi} = \frac{\overline{V}}{|\overline{V}|}$$

The unit moisture flux can then be expressed by $q\overline{\psi}$. This new moisture flux variable can now be used to calculate the unit moisture flux convergence or to calculate a modified version of SEC.

a. *Unit moisture flux in a modified version of SEC*

A version of SEC was developed using the unit moisture flux. The new threshold value for SEC was determined experimentally. The modified version of BARCOZ applied the following conditions:

- Modified SEC < $-8*10^{-13}$ $kgkg^{-1}ms^{-1}$
- $\omega < -0.2 Pas^{-1}$ at both the 600 and 700hPa levels

In the figures 3.1(a) and (b) the SEC values differ by more than an order of magnitude along the south coast between the original and modified BARCOZ. But in figure 3.1(c) and (d) the magnitude of the SEC values along the south coast do not differ significantly but the area of maximum convergence off the southeast coast is shifted westward.

Modified BARCOZ fields were generated and compared with the original (old) BARCOZ fields and verified against the observed rainfall. Figure 3.2 displays these fields as well as the observed rainfall for the 25th January 1981. The two BARCOZ results are similar, but in the modified BARCOZ the area over the interior of the Eastern Cape Province is excluded. This reflects the shift of the convergence area to the west where most of the rainfall occurred. In figure 3.3 for the 1st September 1968 the new BARCOZ now includes an area over the Eastern Cape Province. The corresponding modified SEC field in figure 3.1 also moved the area of maximum convergence to this area.

The modified SEC fields limited the surface moisture convergence to the coastal areas and led to a marked improvement in BARCOZ performance.

b. Unit moisture flux convergence

As will be detailed in section 3.4.2 it was decided not to use SEC in future development and the unit moisture flux was therefore used to calculate the unit moisture flux convergence $\overline{\nabla} \bullet q\overline{\psi}$. The second version of BARCOZ, referred to as BARLUT, applies the following criteria

- Unit moisture flux < $-50*10^{-8}$ s^{-1}
- $\omega < -0.2 Pas^{-1}$ at both the 600 and 700hPa levels

The details of the performance of BARLUT are provided in Chapter 5.

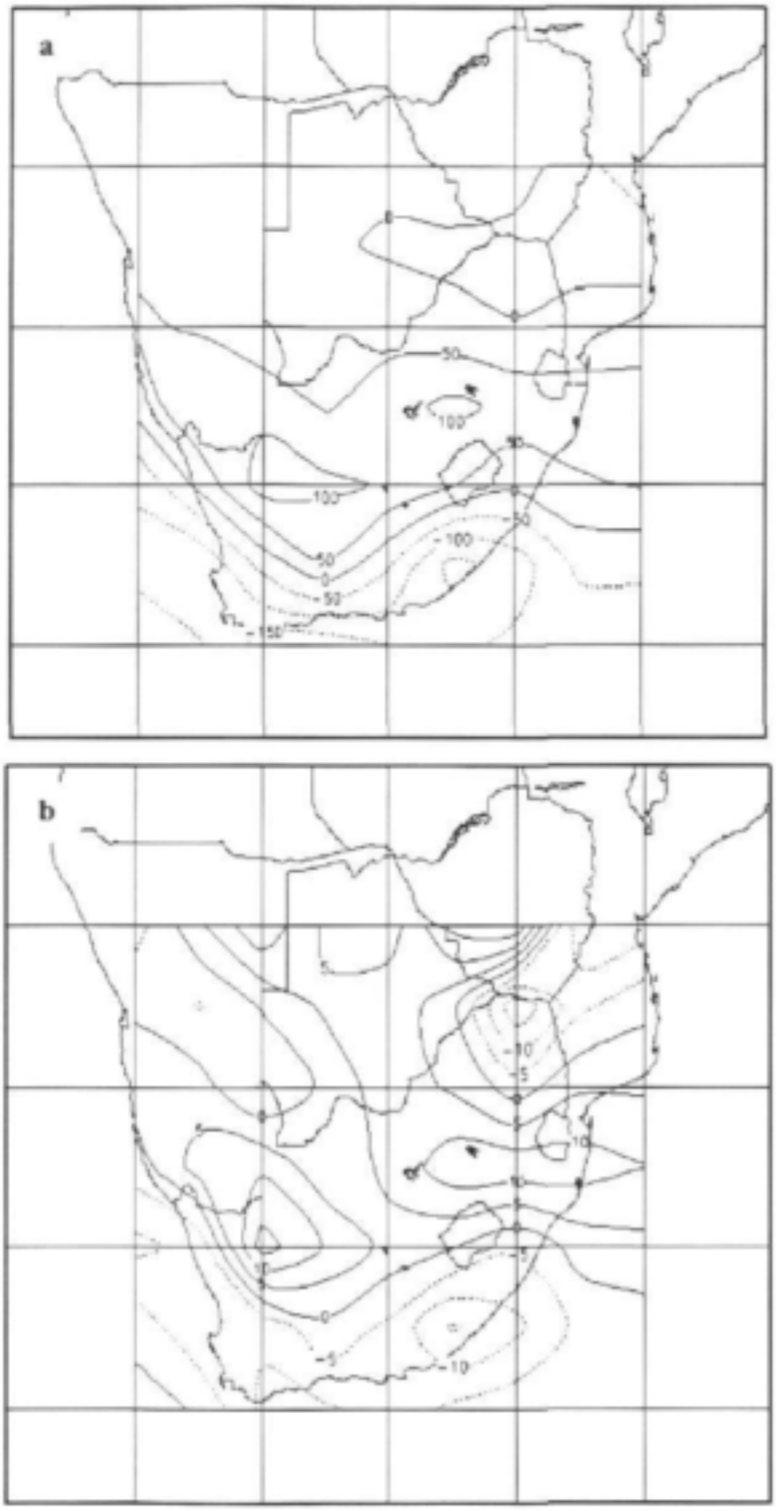

Figure 3.1a&b Old SEC field (a) and modified SEC field (b) on the 25[th] of January 1984. (Laingsburg flood). Positive values are convergence and negative values divergence.

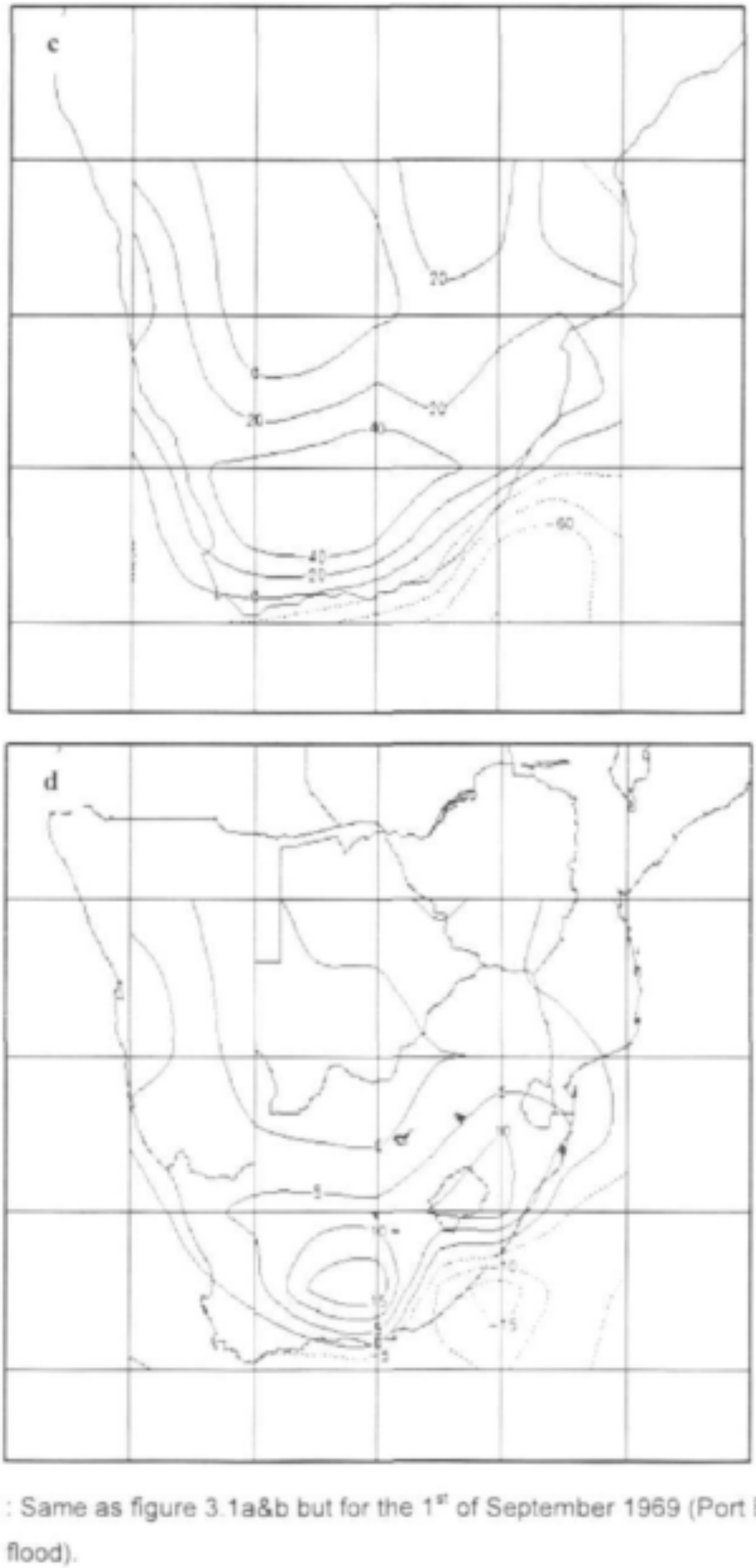

Figure 3.1c&d : Same as figure 3.1a&b but for the 1st of September 1969 (Port Elizabeth flood).

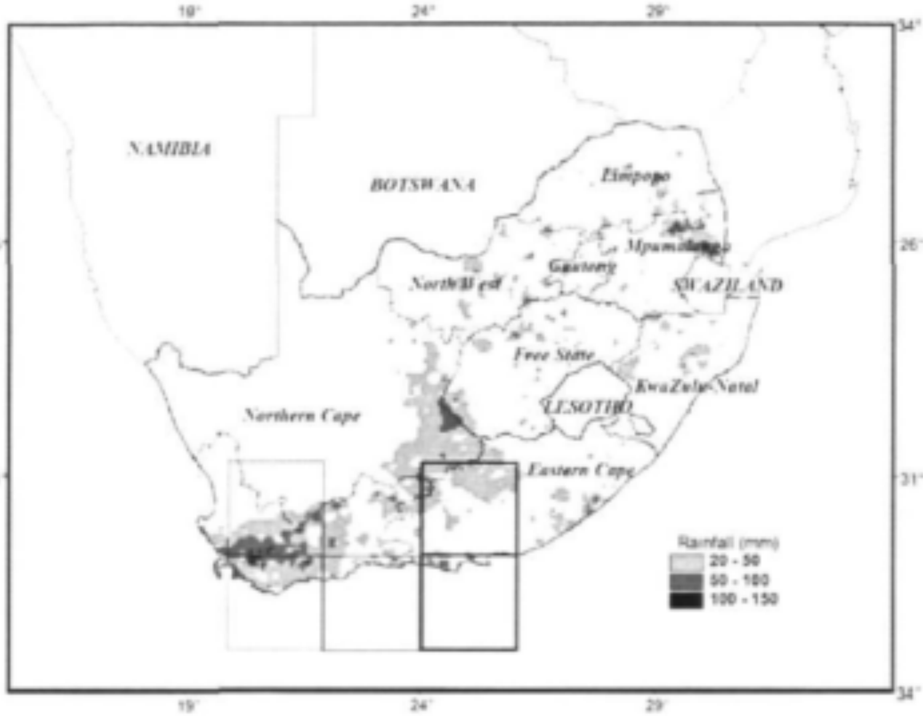

Figure 3.2: Observed rainfall (mm) on the 25th of January 1981. BARCOZ forecast indicated by rectangles. The two bold rectangles were excluded in the modified BARCOZ forecast.

3.4 BARCOZ on the prognostic fields of Numerical Weather Prediction models.

Chapter 2 details the NWP models providing prognostic fields on which further BARCOZ development and testing took place. It was recognized from the outset that in order for BARCOZ and THERIS to have any use they had to isolate areas of heavy rain reliably using the NWP prognoses. It was also accepted that the rainfall predicted by these models was often misleading and generally considered as the model's weakest product. This belief in no way detracts from the excellent prognoses of atmospheric flow fields produced by current NWP models but rather reflects the inability of the cloud and precipitation schemes built into these models to take into consideration factors such as moisture flux convergence, vertical profile of wind divergence, vertical motion and conditions of atmospheric instability amongst others.

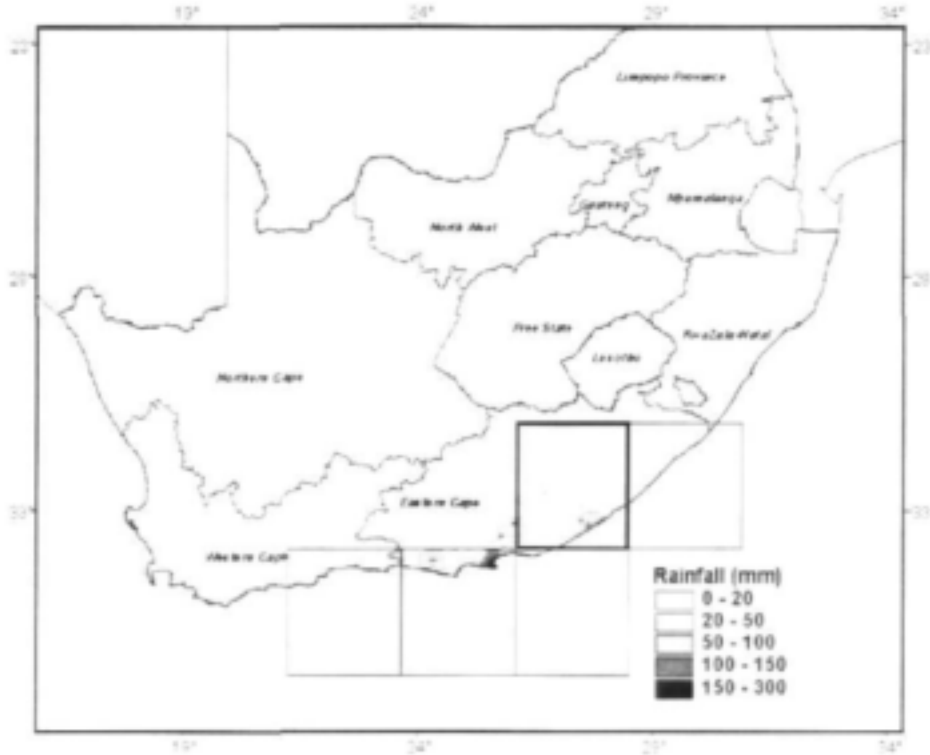

Figure 3.3: Observed rainfall (mm) on the 1st of September 1968. BARCOZ forecast indicated by thin rectangles. The bold rectangle was included in the modified BARCOZ forecast.

BARCOZ on the other hand does not concern itself with cloud and precipitation schemes but rather identifies regions where some form of significant lower level water vapour convergence and vertical motion coincide. BARCOZ recognises the fact that near surface sources of water vapour produce the rain and that in all heavy rainfall events the depth of rainfall far exceeds the mass of water vapour integrated through the depth of the tropopause at that point. The minimum horizontal scale that can be detected is one model grid box of approximately 2500 km^2.

3.4.1 BARCOZ and MM5 model output

Three different MM5 model runs provided prognostic fields on which BARCOZ was tested. The first run was on data starting at 0000 UTC on 30 August 1968, referred to as 1968 RUN1. The model was run with a vertical resolution of 20 levels and a time step of 120 seconds. Output is available every 6 hours. The second model run referred to as 1968 RUN2, started on the same date but the vertical levels were increased to 40. Output of RUN2 is available every 3 hours. Both these model runs cover the period when the so-called Port Elizabeth flood took place and were terminated at 0000 UTC on 3 September 1968. This event is well documented in Dyson et al (2002) and Hayward and van den Berg (1968). The second run (1968 RUN2) was executed in order to determine the cause of anomalous perturbations in the MM5 model prognostic fields.

The third model run started at 0000 UTC on 13 August 2002 and ended at 0000 UTC on 17 August 2002 and is referred to as the 2002 RUN. During this event very heavy rainfall occurred in the East-London region.

The MM5 model produces prognostic fields on 19 pressure levels from 1000 to 100 hPa. The first level refers to land and sea surface data. The following prognostic variables were used by BARCOZ versions: model surface geopotential height; and, at the 19 pressure levels, geopotential height (GPM), temperature (°K), horizontal wind (U and V (ms^{-1})), vertical wind (W (ms^{-1})) and mixing ratio (Q kg/kg).

a. 1968 RUN1

On 1 September 1968 more than 400 mm rain fell over Port Elizabeth. Heavy rain persisted and spread eastwards to the East London region by 3 September 1968. Figure 3.3 depicts the rainfall along the Eastern Cape Province coastal regions on 1 September 1968.

The MM5 model succeeded in predicting the development and movement of the cut-off low (COL) fairly accurately. However the model output contains serious and spurious anomalies in the geopotential height and wind fields. Anomalous short wavelength perturbations are modelled over the eastern escarpment and east coastal regions. No such perturbation was observed in the hand analysis performed by Van den Berg and Hayward (1968) and it also does not appear in the NCEP analysis (Dyson et al, 2002) (not shown). Figure 3.4 shows this perturbation for 1 September 1968 at 1800UTC at 500 hPa. These perturbations also appear at all levels to 200 hPa.

These anomalous short wavelength upper air perturbations had large values and gradients of relative vorticity and vertical motion. Figure 3.5 depicts the vertical motion field on 1 September 1968 at 1800 UTC. Extreme values of upward motion greater than 25 cm s^{-1} are evident. Following Holton (1992) the perturbations should move downstream rapidly. The prognostic fields fail to do this. Furthermore these large vertical ascents are far removed from the area where the heavy rain occurred. All of the BARCOZ versions require lower tropospheric vertical motion and convergence of water vapour. The unrealistic vertical motion field resulted in erroneous BARCOZ analysis.

Considerable smoothing of the MM5 prognostic fields using the GRADS 9 point filter reduced the amplitudes of the perturbations but failed to remove them. It was suggested (B. Hewitson, personal communication) that running the model at higher vertical resolution may improve matters.

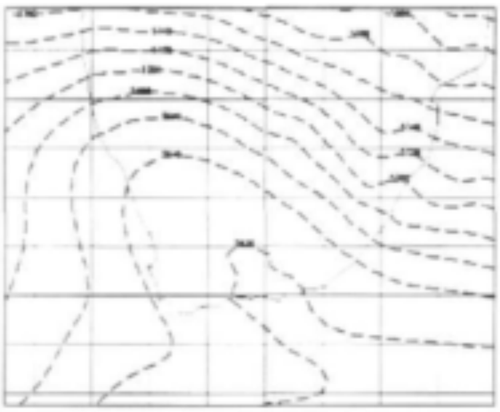

Figure 3.4: The MM5 500hPa geopotential heights (gpm) for 1968 Run 1 on the 1st of September 1968.

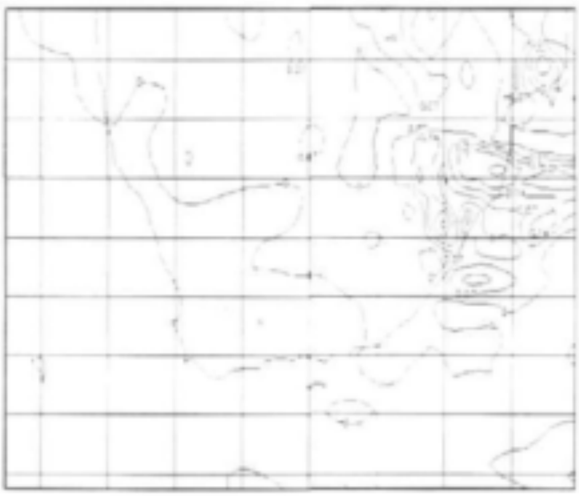

Figure 3.5: The MM5 vertical motion field (ms^{-1}) at 500hPa for 1968 RUN 1 on the 1st of September 1968.

b. 1968 RUN2

The higher vertical resolution run (1968 RUN2) from 30 August 1968 at 0000 UTC to 3 September 1968 at 0000 UTC provided upper geopotential fields, which on visual inspection appear smoother. The way the upper COL is handled is closer to the analysis of Van den Bergh and Hayward as well as to the NCEP analysis. Figure 3.6 depicts the 500hPa geopotential and the vertical motion fields at 1800 UTC on 1 September 1969. Unfortunately the same anomalous perturbations in both fields appear again. Their amplitude seems somewhat reduced. The extreme values for the vertical motion are more or less the same as in the case of RUN1. The use of the higher vertical resolution in the MM5 model RUN2 resulted in marginal improvement but fails to provide reliable input to BARCOZ.

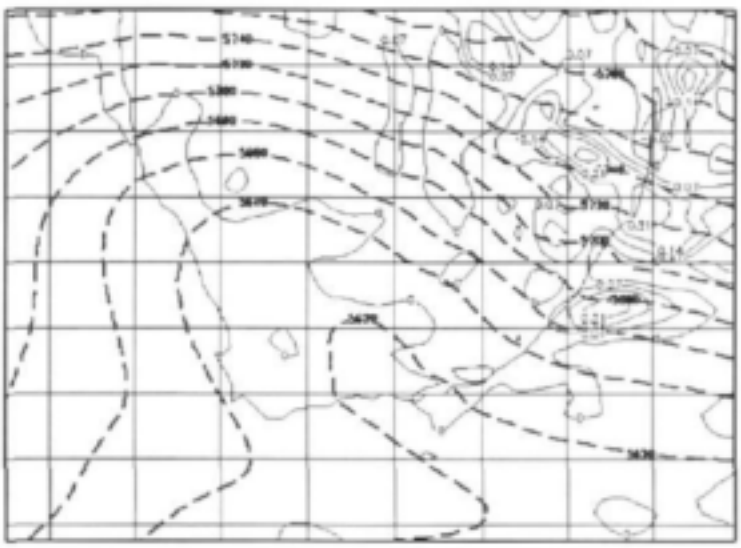

Figure 3.6: The MM5 500hPa geopotential heights (gpm) (dashed) and vertical motion field for Run 2 on the 1st of September 1968.

c. 2002 RUN

This run also took place at the higher vertical resolution and output is available for the period 13 August 2002 at 0000 UTC until 17 August 2002 at 0000 UTC. The upper geopotential fields of these prognoses appear somewhat smoother than the 1968 model runs (not shown). However the perturbations again appear over the east coastal regions. Amplitudes are less but still represent unacceptable variations in the circulation fields. Large amounts of rainfall occurred during this period in the East London region where more than 100 mm fell on one day.

*d. The **Q** Vector*

The high values forecast for the upward motion forced by the anomalous perturbations in the MM5 output resulted in BARCOZ failure. A new approach was indicated. Because realistic values of the upward motion are required by BARCOZ other means to compute the vertical motion (or omega in p coordinates) were sought. One possible way is to use the Quasi-geostophic Omega equation (Holton, 1992). Little will however be gained if the perturbations remain in the geopotential fields predicted by the MM5 model. Another option is to compute the forcing function of the omega equation:

$$f_o^2\partial^2\omega/\partial p^2 + \sigma\nabla^2\omega = -2\nabla\bullet Q \qquad (1)$$

where ω = dp/dt (omega), σ is the static stability parameter and **Q** the so-called **Q** vector. Triegaardt (1992), building on the work of Hoskins (1972) describes three versions of the **Q** vector where the geopotential, the potential temperature or the temperature are variables used to compute the **Q** vector. In this study the temperature will be used because the temperature field is a MM5 model variable directly available in the output fields:

$$Q = i[R/p(\partial vg/\partial y\partial T/\partial x - (\partial vg/\partial x\partial T/\partial y)] + j[R/p(-\partial ug/\partial y\partial T/\partial x - (\partial ug/\partial x\partial T/\partial y)] \qquad (2)$$

Holton (1992) shows that the left hand side of equation (1) is directly proportional to $-\omega$ and therefore:

$$-\omega \propto -2\nabla\bullet\mathbf{Q} \qquad \text{or} \qquad \omega \propto \nabla\bullet\mathbf{Q}$$

This equation simply states that vertical motion is forced by the divergence of the **Q** vector. Because of the negative relationship between omega and vertical motion ($\omega \propto -w$) areas of strong convergence of the **Q** vector ($\nabla\bullet\mathbf{Q} < 0$) coincide with upward motion.

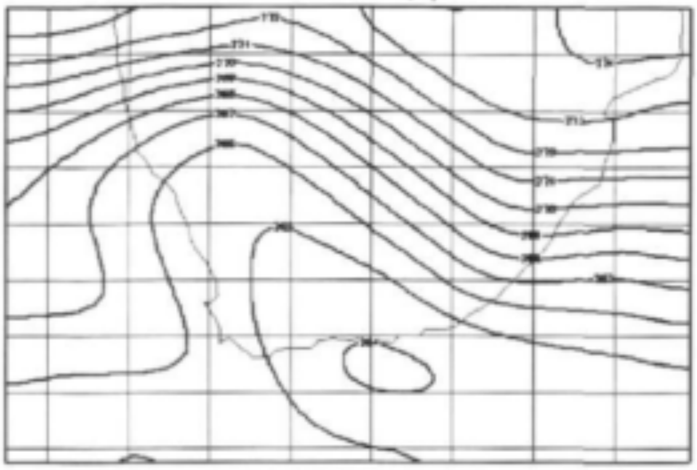

Figure 3.7: The 650hPa temperature (K) for RUN 2 on the 1st of September 1968.

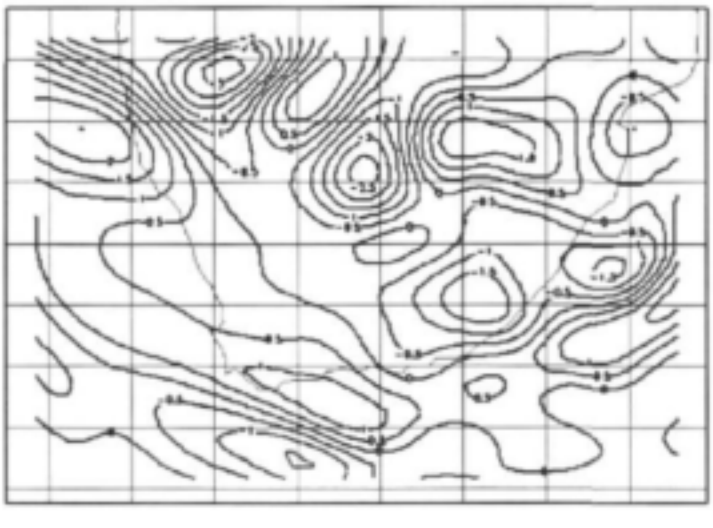

Figure 3.8: The horizontal divergence of the Q vector RUN 2 at 650 on the 1st of September 1968.

It was considered worthwhile to investigate whether the calculation of the **Q** vector *divergence using smoothed values of wind and temperature fields will isolate the synoptic* scale vertical motion field. Figure 3.7 displays the 650hPa temperature prognoses (in K) for 11 September 1968 at 1800 UTC after the nine-point filter was applied to it 10 times. It was also assumed that the model prognostic wind vector approximates the geostrophic wind. The filter was also applied to the wind components 10 times. Figure 3.8 displays the divergence of the **Q** vector computed using equation (2). Here areas with $\nabla \bullet \mathbf{Q} < 0$ indicate areas with upward motion. The large area of upward motion, ahead of the upper COL, is in agreement with accepted quasi-geostrophic theory (Holton, 1992).

This **Q** vector method cannot provide numeric values of the upward motion field and this approach was abandoned.

e. BARCOZ on MM5 prognostic fields

The availability of the MM5 model prognoses, even if suspect, made it possible to test BARCOZ on model output. Data fields were available for every 3 or 6 hrs. As described in Chapter 2, the horizontal resolution of the MM5 model is considerably smaller (0.5°) than that of the NCEP data (2.5°). This required adjustments to the way the BARCOZ field is compiled as well as to BARCOZ specifics (conditions).

Procedural:

- Compute the BARCOZ field for all model output times.
- Accumulate fields for a 24-hr period ending at 0600 UT.
- Use the nine-point filter on the divergence of the gradient of SEC three times.

Atmospheric circulation criteria

- *Vertical motion $w > 0.01\ ms^{-1}$ at 700-, 650- and 600 hPa levels.*
- *Divergence of the gradient of SEC < $-50 * 10^{-13}\ kgkg^{-1}m^{-1}s^{-1}$.*

Figure 3.9 displays the BARCOZ field (Run2) for the 24 hr period ending on 0600 UTC on the 2^{rd} of September 1968. It is clear that BARCOZ, operating on model output, failed to identify the very heavy rains in the Port Elizabeth region on the 1st of September 1968. However it is encouraging that the heavy rains over the East Cape Province were isolated. Unfortunately the poor way in which the MM5 model handled the COL resulted in BARCOZ predicting heavy rain along the east coast.

During the period 14 to 16 August 2002 very heavy rain fell over the East Cape Province centred near East London. More than 500 mm fell at the East London weather office during this period with the maximum of 317 mm on the 15th. Figure 3.10 displays the BARCOZ field for 24 hours ending at 0600UTC on the 16th of August 2002.This field does indicate heavy rain over the Eastern Cape Province. However it follows the MM5 rainfall prognoses (not shown) in predicting heavy rain over the north-eastern parts of the country. This did not happen.

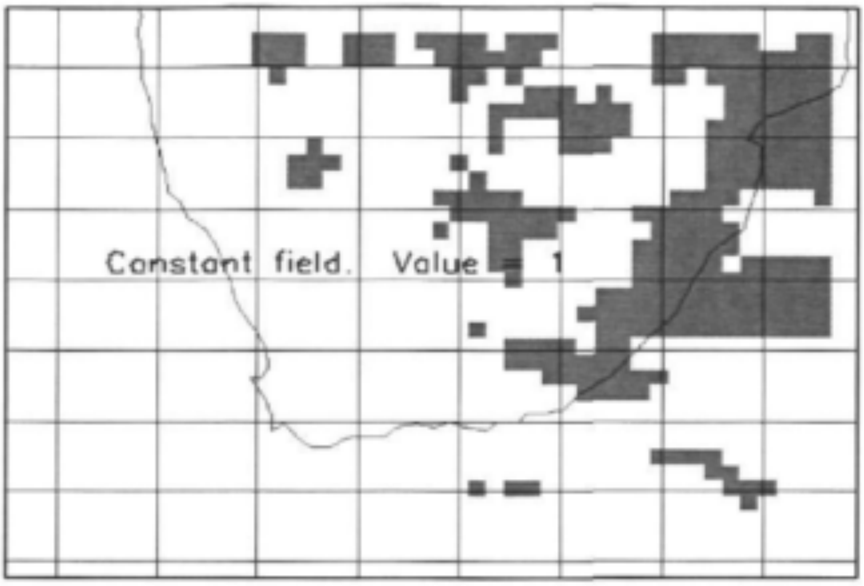

Figure 3.9: The MM5 BARCOZ forecast for the 1st of September 1968.

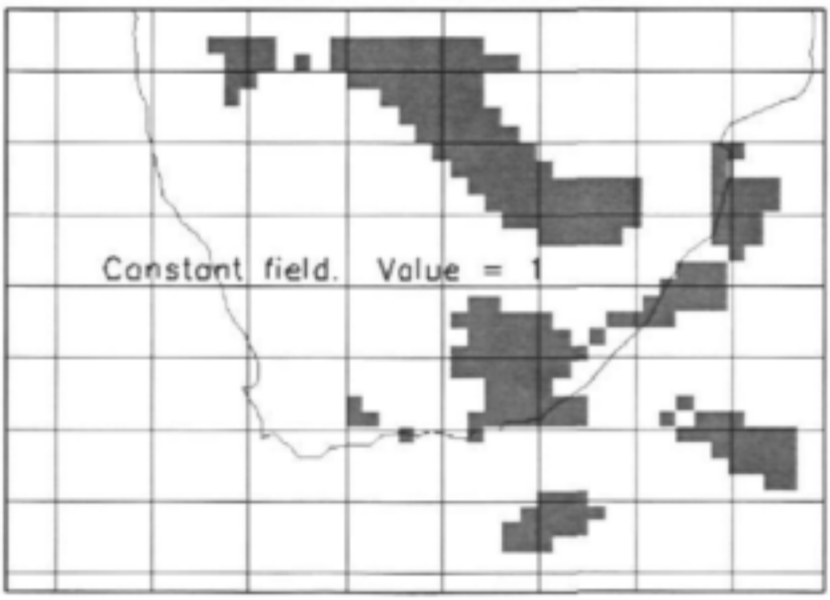

Figure 3.10: Same as figure 3.10 but for the 16th of August 2002.

3.4.2 BARCOZ and the ETA Model

The near stationary, anomalous small-scale perturbations near regions of steep topography of the MM5 model render application of BARCOZ useless. SAWS personnel advised us that the Eta model, which they operate, does not have this failing and they kindly made available prognostic fields from the Eta model. Chapter 2 details the Eta model specifics. BARCOZ application to Eta model prognoses included:

- Surface forcing of the vertical motion.
- Consideration of the horizontal convergence of water vapour flux instead of SEC.

The Eta model did not generate the stationary short waves over the South African escarpment, which had bedeviled the application of BARCOZ in the MM5. The Eta model output fields, as contoured by the GRADS software system and especially near the surface, are also far from smooth. These irregularities did not create serious problems. The model was quite impressive in the way it handled the passage of the weather systems south of the country. The Eta model produced anomalous and sharp geopotential gradients against and near the main escarpment. In the development of BARCOZ parameters the near surface model fields were smoothed lightly with the nine-point filter in order to remove small irregularities.

Inspection of the Eta model vertical motion field over the coastal regions where heavy precipitation occurred revealed that in nearly every case a clear pulse of strong upward motion peaked over the region. This generally built up over a few time steps and maximum vertical motion often exceeded -1 Pas^{-1}. This minimum was generally only maintained over one or two time steps. Most important was the fact that the maximum upward motion (minimum omega) almost always occurred at the 800-hPa level. Consider figure 3.11, which depicts vertical profiles of the vertical motion or omega fields at Margate in KwaZulu Natal on the 4th of April 2002 as predicted by the Eta model. The average rainfall in the Eta grid box where Margate is situated was 36mm. The Eta model prognosis at 1500 UTC on the 4th of April 2002 at this grid point (dashed lines) shows small values of upward motion in the lower troposphere. At 2100 UTC (solid black) the vertical velocity increased to close to -2 Pas^{-1} at 800hPa and at 0300 UTC on the 5th of April the vertical velocity (dotted lines), although still quite favourable, started to decrease in the lower troposphere. It is important to note that for this heavy rainfall event along the coast of Kwa-Zulu Natal the minimum vertical motion exceeded –1 Pas^{-1} and occurred relatively low in the troposphere at 800hPa.

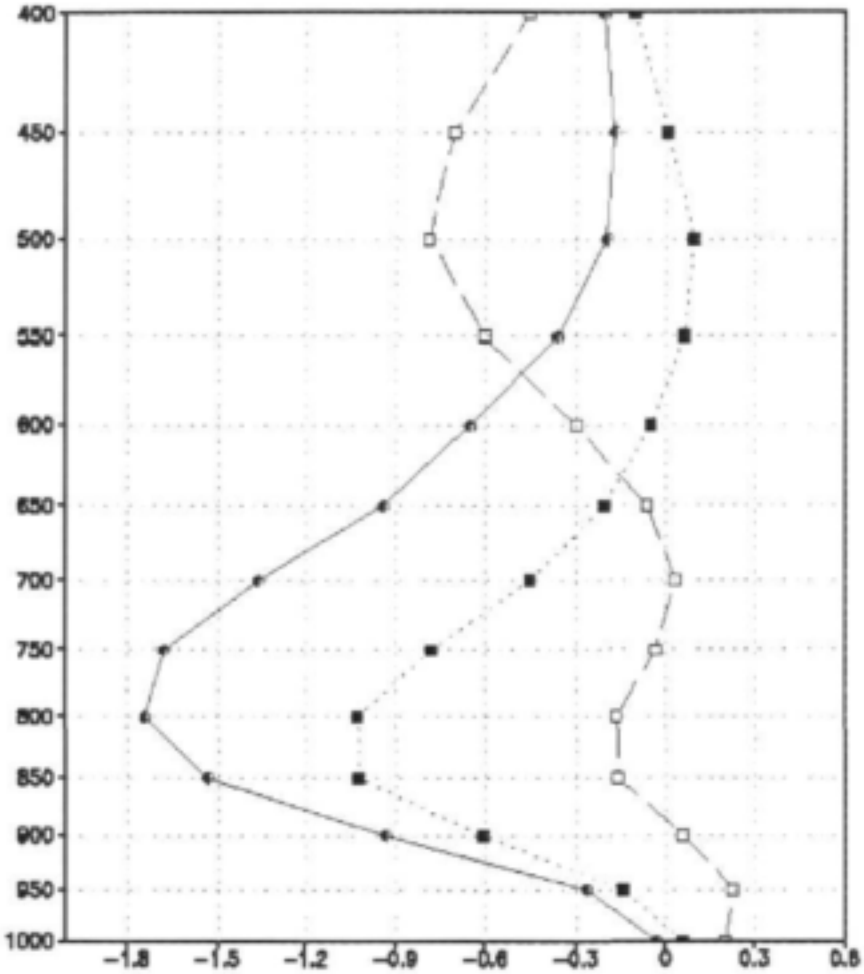

Figure 3.11: Vertical profile of vertical motion (Pas^{-1}) at 1500UTC (dashed), 2100UTC (solid) on the 4th of April 2000 and 0300UTC (dotted) on the 5th of April 2000.

Figure 3.11 depicts the very clear pulse of upward motion with a peak of −1.75 Pas^{-1} at the 800hPa level at 2100UTC. This indicates that most of the cloud and rain processes occurred in the lower troposphere. The vertical motion profile also show that most of the wind and water vapour convergence occurred well below the 850hPa level with divergent motions probably starting by the 700hPa level. The vertical distribution of the omega field depicted by figure 3.11 provides justification for the BARCOZ criteria described in this chapter. The fact that the vertical motion field tends to build to this maximum and then collapse in a few time steps is also in agreement with the observed heavy rainfall temporal pattern.

It is accepted that this is the way the model handles regions of heavy precipitation over the coastal zone. This result is in broad agreement with the views expressed by Triegaardt et. al. (1988). The conditions of BARCOZ were changed to reflect this factor and also considering the scale factors as listed in Chapter 2. .

- Horizontal Wind Divergence ($\overline{\nabla} \bullet \overline{V}$) $\sim 10^{-5}$ s^{-1}
- Water Vapour Flux Divergence ($\overline{\nabla} \bullet q\overline{V}$) $\sim 10^{-6}$ kg kg^{-1}s^{-1}
- SEC ($\overline{\nabla} \bullet q\overline{V}_{SE}$) $\sim 10^{-11}$ kg kg^{-1} m^{-1} s^{-1}

BARCOZ application to the case studies determined the following conditions:

- Omega < - 0.25 Pa s^{-1} at all levels from 900- to 700 hPa
- SEC < -30 x 10^{-9} kg kg^{-1}m^{-1} s^{-1}

SEC is very small and the conditional value for SEC set here is almost two orders of magnitude larger than the scale value. This is necessary in order to reflect regions of significant convergence.

Valid criticism of the BARCOZ system is the artificial parameter referred to as SEC. The problems with SEC are:

- SEC is very small.
- It minimizes fluxes from the SW/NE sector.
- It is a non-standard dynamical expression.

SEC was abandoned as a parameter in operational BARCOZ variants. BARCOZ worked well over the South West Coast, but as detailed in Section 3.5.2 the Eta model does not simulate the lower level wind field very well and therefore any heavy rainfall system, which uses the wind field creates erroneous forecasts.

The fact that heavy rainfall often develops over regions considerably smaller than double model grid boxes (10 000 km^2) and that these real events require large amounts of water vapour convergence resulted in a search for more representative (realistic) means of handling the model water vapour fluxes. However, other variables such as the vertical distribution of vertical velocity remain a very important ingredient of the operational versions of the heavy rainfall identification systems.

3.5 Atmospheric Variables

This section briefly describes the variables researched to identify an improved BARCOZ or coastal heavy rainfall system. Not all of these variables were used in the final operational version of BARCOZ or the coastal heavy rainfall identification systems but are included here as they describe some of the approaches to handle the combination of vertical motion and water vapour in the lower troposphere.

3.5.1 Surface winds and horizontal wind convergence

Unless otherwise stated the surface winds refer to the average 1000-950hPa wind. The averaging endeavours to remove small perturbations in the wind field, which could have resulted in erroneous and large values of surface wind divergence ($\overline{\nabla} \bullet \overline{V}$).

3.5.2 Moisture variables

a. Precipitable water

Huschke (1959) defines precipitable water (W) as the total mass of water contained in a vertical atmospheric column if all the water vapour in the column were to condense out. The precipitable water may be calculated between any two atmospheric pressure levels but one should consider that most water vapour occurs in the lowest levels of the atmosphere. Precipitable water was the preferred moisture variable in the operational version of the coastal heavy rainfall identification systems. This emerged after thorough statistical evaluation. The challenge was in identifying the appropriate critical value of precipitable water for inclusion in the systems.

Figure 3.12 depicts the average 1000-300hPa precipitable water (in mm) for summer (a) and winter (b) for the period October 1999 to March 2002. The 12-hr prognosis of the 0000 UTC Eta model runs for this period was used to calculate the average values. The average value for precipitable water in winter over the South Western Cape is only 11-12 mm while over the East Coast it varies between 15-19mm (Fig. 3.12(b)). There is also a significant difference between summer and winter values. Over the East Coast in summer the average 1200UTC precipitable water values were generally above 30mm and less then 20mm in the South West. It was therefore necessary to adjust the critical value, which forms part of a heavy rainfall identification system for geographical area and season.

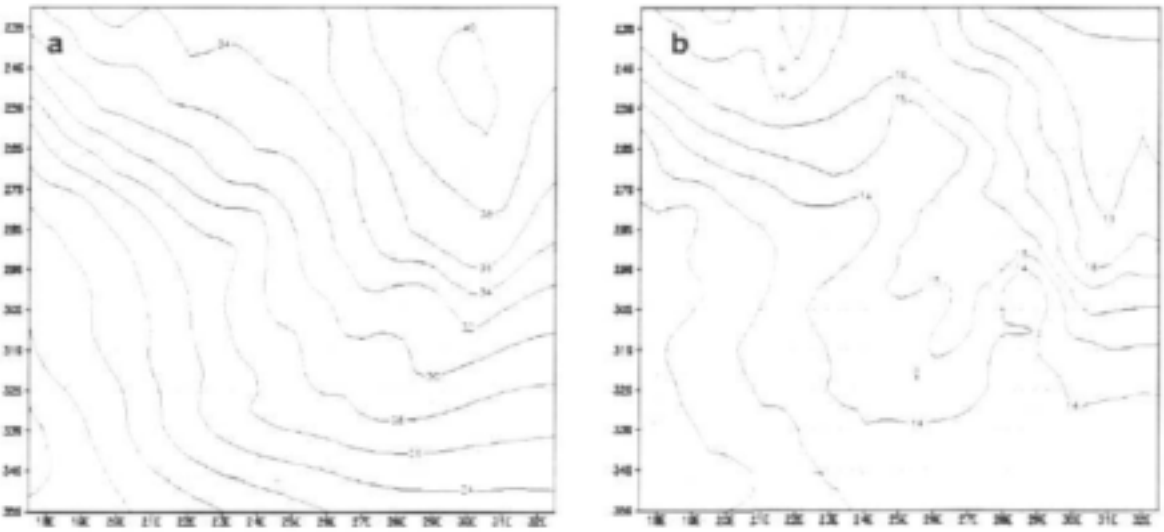

Figure 3.12: The average 1200UTC Eta precipitable water values (in mm) for (a) the summer rainfall seasons and (b) the winter rainfall seasons October 1999 to March 2002

b. Moisture flux convergence

Divergence of the water vapour flux ($\overline{\nabla} \bullet q\overline{V}$) is a conventional way to simulate the large amounts of water vapour required for copious rainfall. This variable is to a large extent dominated by the horizontal wind and the usefulness of moisture flux convergence as part of an objective heavy rainfall identification system relies on how accurately the model predicts the surface winds. Another factor to consider when dealing with moisture flux convergence is how the prognostic fields of a NWP model handle the distribution of moisture on a pressure level. This is especially relevant in the Eta model over the east coast of South Africa. Consider the following examples of moisture flux convergence as simulated by the Eta model on two heavy rainfall days (Fig 3.13). On the 10th of June 2000 a cold front moved in over the South Western Cape (Fig.3.13(a)). The 1000hpa geopotential heights show a short wave trough just west of the country. Note the mixing ratio distribution over the South Western Cape. The highest values occur over the Peninsula, which is consistent with the northwesterly on-shore flow over the area. Over the South Coast where the flow is offshore the values are lower. The contours in figure 3.13a (ii) show moisture flux convergence in the trough west of the country but also over the Peninsula. The moisture flux convergence gives an adequate indication of the water vapour required for heavy rainfall.

The 1000hPa geopotential heights in figure 3.13b show that on the 4th of April 2000 a high-pressure system was situated south of the country. It would be acceptable if a weather forecaster would consider this a strong on-shore flow event. However, consider the surface winds in figure 3.13b (ii). The winds tend to diverge and become parallel to the coast to become easterly in the south and southwesterly in the north. The moisture flux convergence field also indicates that the Eta model did not predict a penetration of moisture into the interior as the convergence occurs offshore. A heavy rainfall identification system which requires surface moisture flux convergence to occur will fail to identify the heavy rainfall which occurred over Kwa-Zulu Natal on this day. Also note how the surface winds diverge around the Lesotho Highlands. The dashed contours in figure 3.13b (i) show the mixing ratio on this day. Note the high value over the northern Kwa-Zulu Natal interior. This distribution of mixing ratio occurs often over this area, with high values over the eastern Lowveld and escarpment of South Africa decreasing towards the south. This distribution has a significant influence on the computation of moisture flux or moisture advection. It is possible that the rapidly rising escarpment over the area has an influence on this distribution and that the error lies in using unrepresentative values at 1000hPa.

Moisture flux convergence is one of the atmospheric criteria, which forms part of the operational coastal zone heavy rainfall identification system over the South Western Cape. However, it was not applied along the East and South coast. In fact unsatisfactory results were found along the South and East coast whenever the surface winds formed part of the heavy rainfall identification system. This includes variables such as horizontal wind divergence or the unit moisture flux (BARLUT).

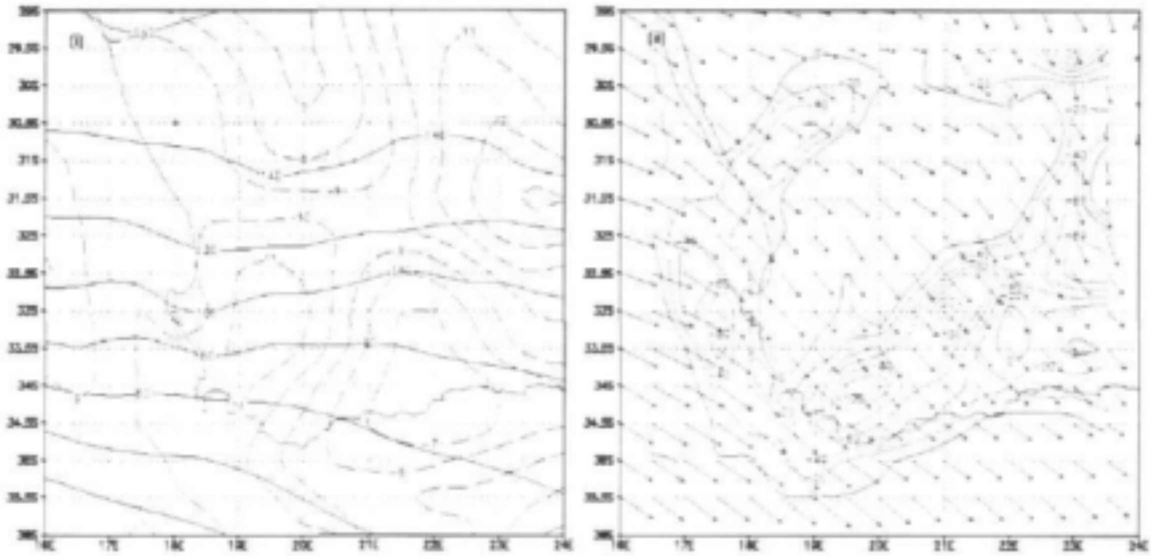

Figure 3.13(a): The (i) 1000hPa geopotential heights (m) and mixing ratio (gkg^{-1}) (dashed) and (ii) the surface wind vectors and moisture flux convergence (s^{-1} $*10^{7}$) on the 10th of June 2000 over the South Western Cape.

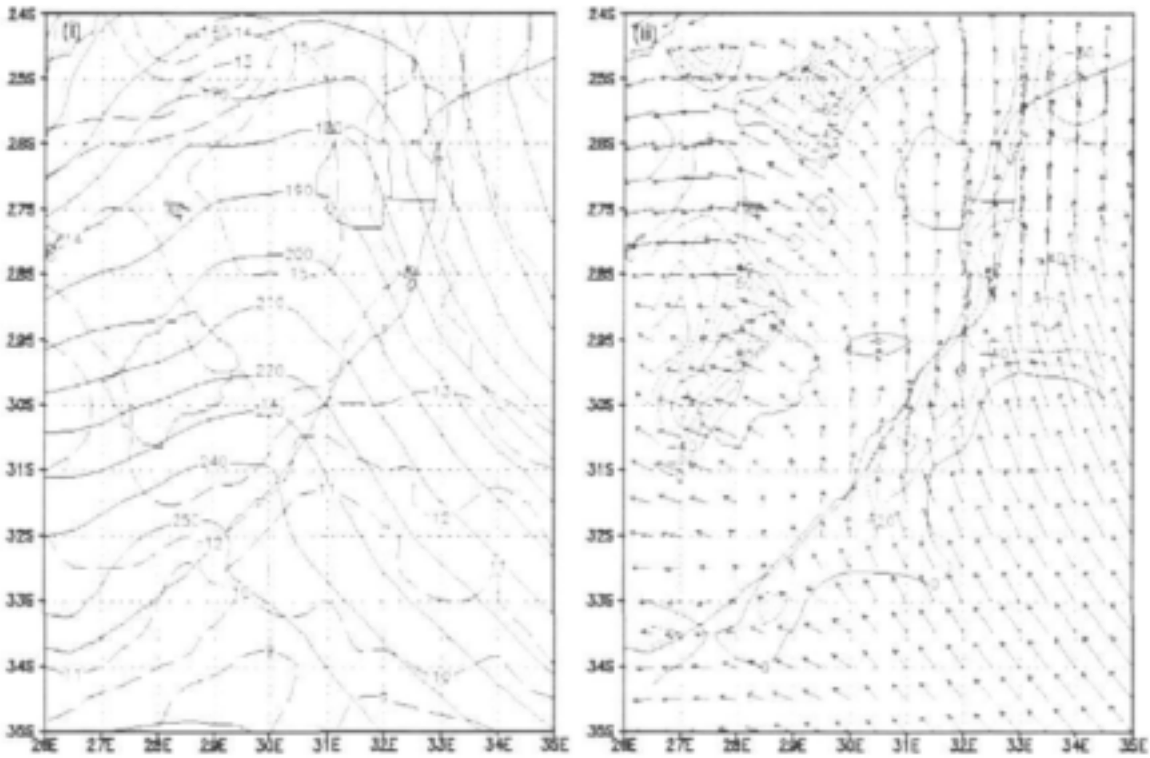

Figure 3.13 (b): Same as figure 3.14 (a) but over the East Coast on the 4th of April 2000.

c. Accumulated Water Vapour Convergence

A rainfall total of 50 mm in 24 hours could be considered a minimum for heavy rainfall. Rainfall, to a depth of 50 mm, represents 50 kg of water accumulated over $1m^2$. If the rain fell in 24 hours this represents rate of water mass accumulation equal to $6 * 10^{-6}$ kg s^{-1}. If the so called precipitable water in the vertical atmospheric column is ignored one may reason that the atmosphere's circulation must converge water vapour at this rate or greater above every $1m^2$ in order to produce 50 mm rain in 24 hours. It is also accepted that not all the water vapour that converges in this way will be available for rainfall production. However for heavy rainfall this rate provides a minimum rate of water vapour convergence.

If the principle of conservation of mass is applied to the mixing ratio and the small vertical motion ignored then:

$$\partial Q/\partial t = -\nabla \bullet (Q\mathbf{V})$$

Where Q is the mass of water vapour. Consider that all the convergence takes place in a vertical column (base $1m^2$) extending from the surface to the 700hPa layer. The total convergence of water **vapour mixing ratio** in this column was computed at each model output time step (3 hrs) by vertically integrating the convergences for all the 50hPa slabs in the column. This represents $\partial \mathbf{q}/\partial \mathbf{t}$ at the specific model output time. This rate was accepted to be constant till the next model output time and a rate could be computed for the 3-hr interval. It is noted that the units of $\partial \mathbf{q}/\partial \mathbf{t}$ are $kgkg^{-1}s^{-1}$ and cannot be compared with the accumulated water mass ($\partial \mathbf{Q}/\partial \mathbf{t}$) without also considering the total mass convergence of air $\nabla \bullet (m\mathbf{V})$ in the column. The product of ($\nabla \bullet (q\mathbf{V})$ and $\nabla \bullet (m\mathbf{V})$) is the accumulation of water vapour mass and can be compared with the mass rate ($\partial \mathbf{Q}/\partial \mathbf{t}$) required to produce the rainfall.

A version of BARCOZ referred to as DIVQRATES was programmed which had the following conditions:

- $\omega_{top} < -0.25$ Pa s^{-1}.
- ω(800 hPa) < -0.25 Pas^{-1}.
- $\partial Q/\partial t > 30$ kg $(3hr)^{-1}$

The first condition requires that upward motion exist over the topography (escarpment). This factor is dealt with in section 3.5.3. The last condition merits some explanation. This 3-hr water vapour convergence rate implies a total of 240mm rain at each model grid point. This however only applies if all the water vapour were converted into rainfall. In real life only a percentage actually reaches the surface as rainfall. The results achieved with DIVQRATES were certainly interesting and the shaded rectangles in figure 3.14 illustrate results for the 9th of November 2000. The numerical values on figure 3.14 show the average 24-hr rainfall per Eta grid box on this day. Heavy rainfall occurred over the north coast of Kwa-Zulu Natal. This version of BARCOZ generally succeeded in identifying the grid points with rainfall in excess of 50mm.

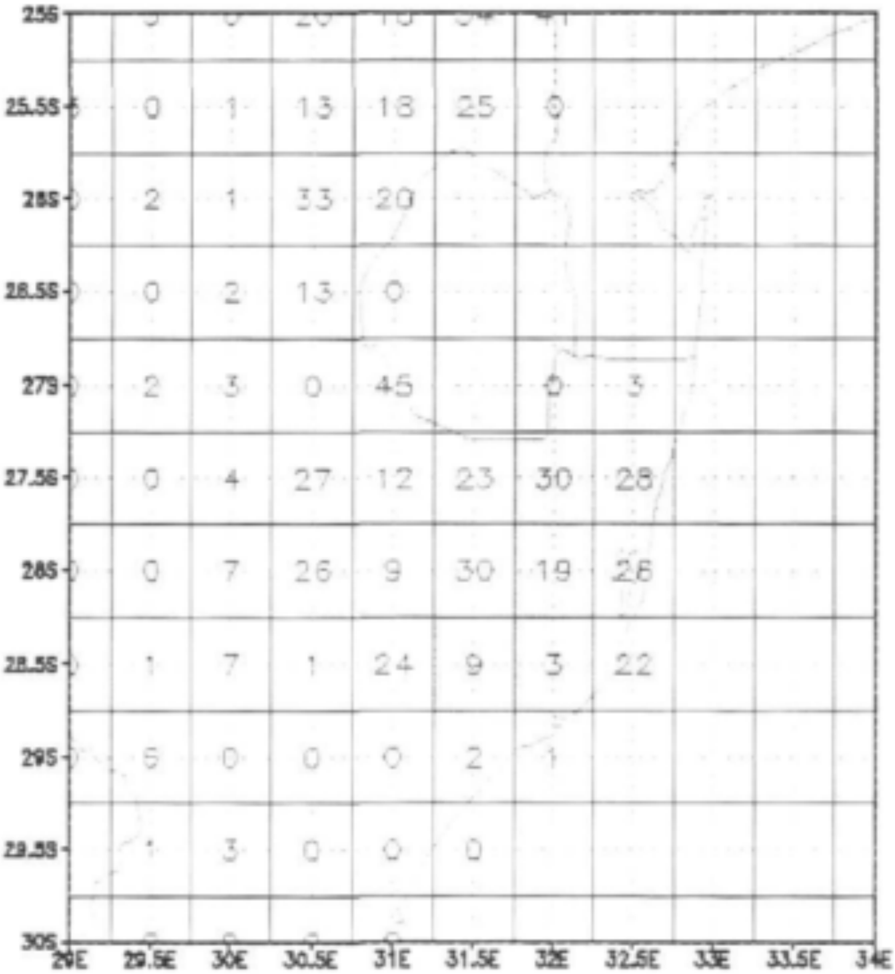

Figure 3.14: DIVQRATES heavy rainfall forecast (shaded) on the 9th of November 2000. The numerical values indicate the average rainfall per Eta grid box on this day.

3.5.3 Vertical motion

Upward motion through the lower and middle troposphere is an essential requirement for the development of heavy rainfall. In this research special emphasis was placed on large values of upward motion in the lower levels of the atmosphere in order to simulate the upward motion caused by surface forcing. A new product, namely topographical uplift, was developed but other critical values for vertical motion were also set to form part of the operational heavy rainfall identification systems.

a. *Vertical distribution of vertical motion*

The vertical profile of vertical motion as depicted by figure 3.11 represents the ideal distribution of vertical velocity for heavy rainfall along the coast. Omega values are all negative in the lower troposphere and decrease with height up to approximately 800hPa where the minimum value of close to -2 Pas^{-1} is reached. This ideal (perfect) situation does not occur very often but in order to identify similar vertical profiles of vertical velocity several conditions for omega were tried.

The first criteria was to stipulate that ω_{top} - ω_{800hPa} >0. This will ensure that there is a decrease of upward motion with height between the surface and 800hPa. The second experiment was to integrate vertical motion from the surface to 750hPa. As lower boundary the lowest value of ω_{top} or ω_{850hPa} was used. This value had to be less that 1.75 Pa^2s^{-1}. After extensive experimentation the decision was reached to use critical values of omega on different pressure levels. Details of the different criteria are provided in Chapter 4.

b. *Topographical Effects*

Tennant and Van Heerden (1994) demonstrated how topography played a role in low-level moisture convergence along the southeast coast. In order to isolate the coastal regions, extending inland to near the top of the escarpment, an artificial topographic field was created, in which all the land areas at 800 m ASL and above were flattened to a constant 800 m level. The ocean was kept at 0 m. The model topography for the coastal zone was left unmodified. This artificial topographic map was used to restrict BARCOZ output to the coastal zone alone and more importantly to restrict the topographically forced vertical motion to the coastal zone.

The role of steep slopes in rainfall production is not questioned but how to model this is very difficult because the model topography, even at 50 km resolution, simply cannot handle the real steep slopes of the coastal and escarpment ranges. Figure 3.15 shows the topography of the Eta model. The model topography gives an adequate, but smooth representation of the topography of South Africa.

The traditional method of computing the vertical motion forced by the topography was used:

$$W_{top} = \overline{V} \bullet \overline{\nabla} Z_{top}$$

with Z_{top} the height of the land surface above sea level (m). Conversion to omega (Pa s^{-1}) followed Holton (1992):

$$\omega_{top} = -\rho g W_{top}$$

In the calculations ρ was taken as 1 kg m^{-3} and g as 9.8 ms^{-2}. Figure 3.16 (a) shows the Eta model topography over the South Western Cape together with the topography gradient vectors ($\overline{\nabla} Z_{top}$). Figure 3.16 (b) shows the surface wind barbs (knots) and the resulting topographical upward motion on the 10th of June 2000. This new topographical uplift became a vital part of the final operational versions of the coastal zone heavy rainfall system.

c. *Enhancing the effect of Surface Forcing*

The technique to reduce the wind vectors to unit vectors, described in paragraph 3.3, was employed to enhance the vertical motion forced by the topography. This approach was taken because the vertical motion forced by the Eta model surface winds and topography was considerably lower than what was expected from theoretical considerations. Both the gradient of the coastal zone topography as well as the surface winds were normalised. The dot product of these two unit vectors was used to compute a factor:

Fact = 1 + grad(normalised topography) • grad(normalised wind)

The enhanced vertical motion was calculated using:

$\omega(\text{Modified}) = \omega_{top} \times \text{Fact}$

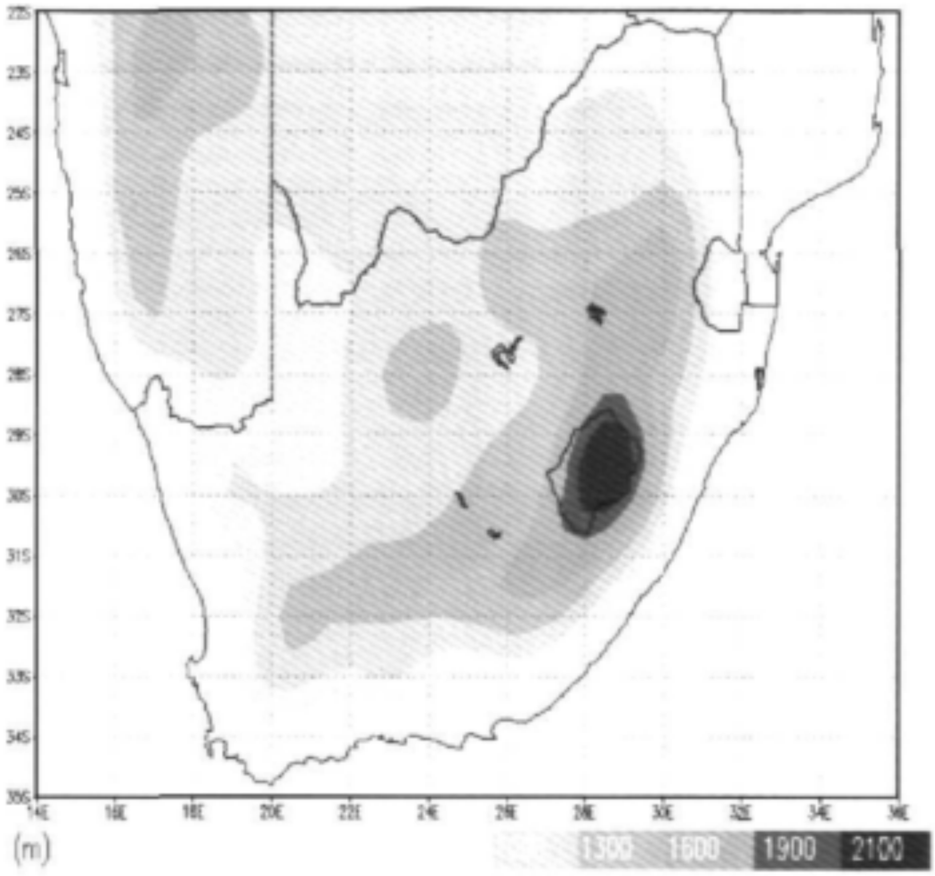

Figure 3.15: The Eta model topography.

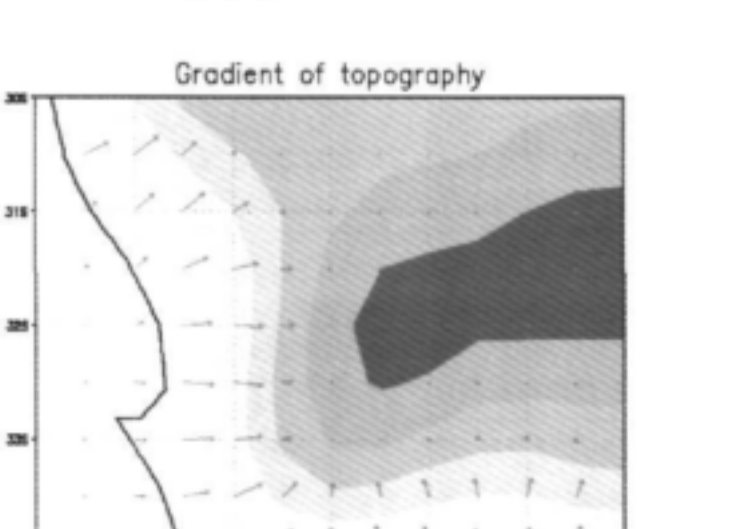

Figure 3.16(a): The Eta model topography over the South Western Cape. The vectors indicate the gradient of the topography.

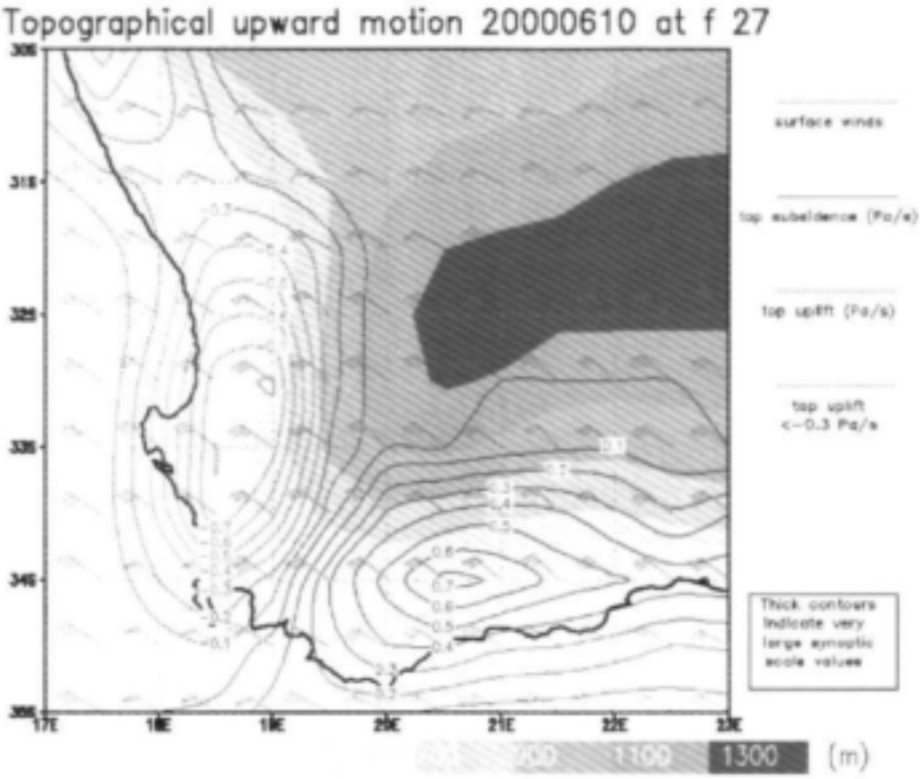

Figure 3.16(b): The surface winds (knots) and topographical upward motion on the 10th of June 2000 over the South western Cape.

3.5.4 Concluding remarks

All of the BARCOZ versions that made use of the topographically driven lower boundary omegas produced lower boundary omega values far below theoretical considerations. A slope of 1:50 is quite realistic along the South African coastal regions. In this case a 10 m s^{-1} upslope wind will produce vertical motion of 0.2 ms^{-1}. This is approximately -2 Pas^{-1}. The omega values calculated by the BARCOZ versions produced numbers about an order of magnitude less.

Careful inspection of the Eta model wind fields below 850 hPa over the coastal zone showed that the model does not handle the upslope motion well. It tends to diverge the flow along the side of escarpment. It also reduces wind speed over the escarpment dramatically and tends to create an area of stagnation on the inland side of the escarpment. The main problem for the BARCOZ versions is that the Eta model deflects the major component of the surface flow tangentially to the escarpment and not across it. Statistical analysis had indicated that areas of heavy rain often coincided with this (erroneous) component of the surface flow. Clearly the

Eta model did not handle strong onshore flow over the south- and south-east coastal zones satisfactorily. This is probably the main reason why the BARCOZ versions with topographically driven vertical motion did not fare well over these areas.

CHAPTER 4

OPERATIONAL HEAVY RAINFALL IDENTIFICATION SYSTEMS

4.1 Introduction

This Chapter describes the final versions of the heavy rainfall identification systems. These systems are all operational, available to the forecasters at the SAWS and utilize the prognostic fields of the Eta model. The atmospheric ingredients which must co-exist to predict heavy rainfall are detailed. The atmospheric criteria of the Tropical Heavy Rainfall Identification System (THERIS) are discussed as well as the operational coastal zone heavy rainfall identification systems.

4.2 Tropical heavy rainfall

The FORFLOOD project (Dyson et al, 2002) details the atmospheric criteria used to create a heavy rainfall forecast for tropical weather systems. In developing THERIS it was considered important that the weather forecaster should first be able to identify the tropical nature of the atmosphere before attempting to predict rainfall from the system. This resulted in the so-called Model for the Identification of Tropical Weather Systems (MITS).

Dyson (2000) and Dyson and van Heerden (2002) identified the dynamical characteristics of a tropical circulation system valid for the interior plateau of southern Africa. Four thermodynamical and circulation criteria apply:

- The continental tropical low should remain upright from the 850- to 400- hPa levels and be displaced by a ridge or anticyclone on the 200- and 300- hPa pressure levels.
- A warm core of 500- to 300- hPa vertically averaged column temperature, must exist above or near the surface low-pressure system.
- Precipitable water values in the 850- to 300- hPa layer should exceed 20 mm and be in the same geographical position as the 200- hPa ridge or anticyclone and must be accompanied by upper tropospheric wind divergence.
- Vertically averaged total static energy (TSE) values in the 850- to 300- hPa layer should exceed 330×10^3 J kg^{-1}.

Dyson (2000) also found that rainfall from tropical systems could be predicted with considerable confidence when upward motion is present from 700 to 400 hPa, the atmosphere is potentially unstable up to the 400-hPa level and precipitable water is greater than 20 mm. Subsequent research by Dyson and Van Heerden (2002) found that by applying these criteria, the rainfall area isolated was often much too large. Stricter thermodynamical controls were applied in the tropical heavy rainfall identification system (THERIS). This system produces a map indicating areas of probable heavy rainfall over southern Africa. THERIS identifies the large-scale environment conducive to the development of heavy rainfall by continental tropical weather systems. THERIS requires the following criteria to be met (Dyson and Van Heerden, 2005):

a. Precipitable water values in the troposphere must exceed 20 mm.
b. Average wind divergence must exist in the 300-200 hPa layer
c. Vertically averaged TSE values in the troposphere should exceed $335 * 10^3$ J kg^{-1}.
d. The atmosphere must be potentially unstable up to at least 300- hPa.
e. Upward motion should exist from 700- to 300- hPa
f. Maximum upward motion must occur below the 300- hPa level.

THERIS was developed and tested on NCEP data and Chapter 5 details the verification results for the summer months of September 1999 to March 2002. THERIS was capable of identifying areas with copious rainfall using this data set.

Applying the same atmospheric criteria to the Eta data revealed that tropical heavy rainfall, as simulated by the Eta model prognosis, is very sensitive to the vertical profile of wind convergence. It was therefore decided to add a circulation criterion for the Eta data.

- Horizontal wind convergence should exist from 750 to 500hPa

Figure 4.1 shows the vertical profile of horizontal wind convergence on the 10th of February 2000. The original THERIS predicted rainfall at both grid points but 43mm occurred at grid point A (solid line) while only 5mm fell at grid point B. Figure 4.1 shows how at grid point A convergence occurs throughout the lower levels of the atmosphere and is replaced by divergence above this. At grid point B wind convergence tends towards zero already at 700hPa and the values remain close to zero up to 400hPa and only above this does divergence occur. The profile at A is the ideal profile of horizontal wind convergence and the additional constraint tries to simulate this profile. The profile depicted by Grid point B is not common in the NCEP data set but this could be because this data set has fewer vertical levels.

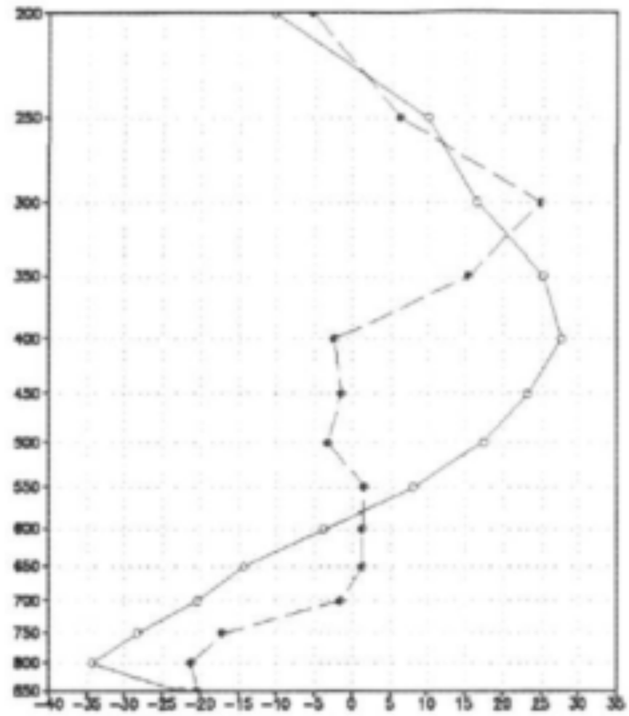

Figure 4.1: Vertical profile of horizontal wind convergence (*10^5 s^{-1}) on the 10th of February 2000. 43mm of rain occurred at Grid Point A (solid) while 5mm occurred at Grid Point B (dashed)

THERIS forecasts were created daily for the 24-hr period, which corresponds to the period the SAWS uses to measure rainfall. THERIS only predicts for Eta model grids where the model topography exceeds 1000m.

The verification results of THERIS on the Eta data are provided in Chapter 5. Dyson and van Heerden (2005) provide a THERIS case study for February 2000. Additional case studies are also provided in the FORFLOOD project (Dyson and van Heerden, 2002) and will not be repeated here. The THERIS forecast for the 8th of February 2000 is shown in figure 4.2. Some rainfall occurred over the entire area identified by THERIS (shaded area Fig 4.2) with the exception of one grid box over the southern part of the THERIS forecast area. The rainfall totals over the southwestern end of the THERIS forecast area were generally below 10 mm. THERIS identified the grid box where the highest average rainfall, 67mm, occurred. All the grid boxes where more than 50 mm occurred were also isolated by THERIS. The average rainfall for the whole THERIS area on this day was 22mm. The highest rainfall recorded at any station was 156 mm and this fell within the THERIS area. Significant rainfall occurred outside the area identified by THERIS especially to the east and northeast of the

THERIS area. The highest average rainfall, which occurred outside of the THERIS area, was 47 mm over the eastern parts of the Limpopo Province.

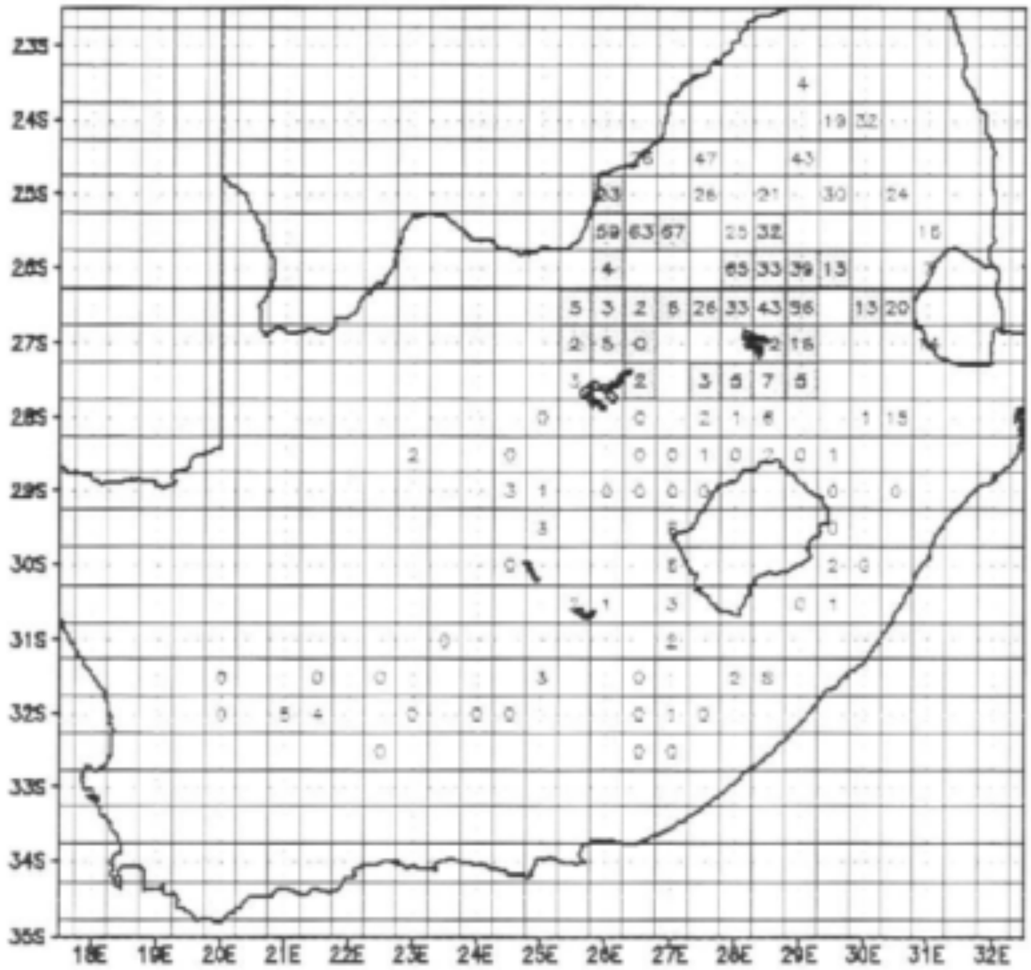

Figure 4.2: Average 24h rainfall, per Eta grid box, on 8 February 2000. The shaded grid blocks are those in which THERIS predicted heavy rainfall.

4.3 Coastal zone heavy rainfall identification systems.

This section describes the criteria selected to develop the operational coastal heavy rainfall identification systems. All the variables were applied to simulate surface forced heavy rainfall. The experimentation conducted during the course of the research revealed some important conclusions. They are:

- The same heavy rainfall identification system cannot be used for the entire coast and for both seasons. Part of the reason for this is the different climate zones along the coast of South Africa. The South West coast receives rainfall predominantly in winter and from extra tropical cyclones. The South Coast tends to get rain throughout the year with local maxima during spring and autumn. The East Coast tends towards summer rain. The climatological features of the model also have a significant influence as was demonstrated when precipitable water was discussed in Chapter 3. Although the same variables may be used in the operational versions of BARCOZ the critical value is area and season dependent.

- The verification results discussed in Chapter 5 show how the Eta model performs excellently over the South West Coast but along the South and East coast results are significantly worse. A possible reason for this is the way the model handles the wind field in areas where the escarpment is steep. The heavy rainfall system developed for the South West Coast gives a 90% hit rate (Chapter 5) but along the East Coast it gave a false alarm more often than it predicted rainfall.

4.3.1 South West Coast

Three heavy rainfall identification systems were developed for the South West Coast. The first referred to as Surface Forced Heavy Rainfall consists of two sets of criteria. A field is created when all three criteria of either set A or Set B are satisfied (see figure 4.3d). The second stipulates critical values of vertical velocity and the third utilises the Eta model precipitation forecast.

a. Surface forced heavy rainfall

i. SET A

- Surface wind convergence must be less than $-20 * 10^{-5}\ s^{-1}$
- Topographical uplift must be less than $-0.25\ Pa\ s^{-1}$
- Precipitable water from 1000-300hPa must be more than 17mm

ii SET B

- Moisture flux convergence of the surface wind must be less than $-20 * 10^{-7}\ s^{-1}$
- Wind divergence at 600hPa must be greater than $20 * 10^{-5}\ s^{-1}$
- Upward motion should be less than $-0.25\ Pa\ s^{-1}$ at 950hPa, 900hPa or the topographical uplift.

b. Vertical velocity less than $-1\ Pas^{-1}$ at any pressure level

c. Eta 24-hr rainfall forecast exceeds 10mm.

The heavy rainfall identification systems are briefly explained by using the Eta model prognosis on the 10th of June 2000.

4.3.1.1 10th of June 2000

Figure 4.3a depicts the average 24-hr rainfall on the 10th of June 2000 over the South West Coast. Daily rainfall totals were generally above 10mm over the Cape Peninsula with more than 30mm over the southern parts.

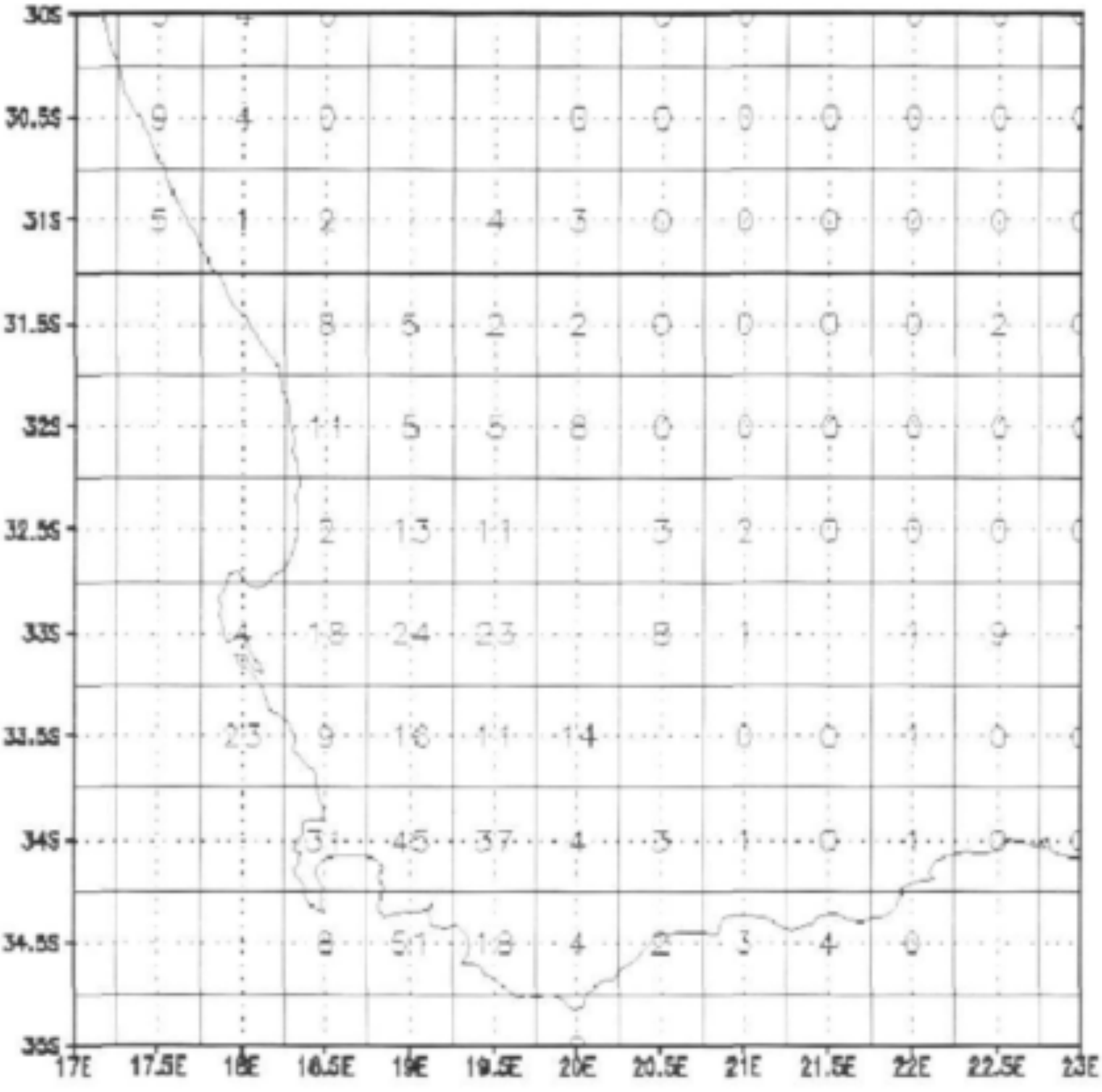

Figure 4.3(a): The average gauge rainfall per Eta grid box on the 10th of June 2000.

Figure 4.3b depicts the atmospheric variables used for SET A. Over the southern parts of the Peninsula the 1000-300hPa precipitable water exceeded 20mm. Over the same area the surface wind convergence was less than $20*10^{-5}\ s^{-1}$ and the topographical uplift was also less than 0.25 Pas^{-1}. The precipitable water field also indicates the cyclonic curvature associated with a well-defined cold front.

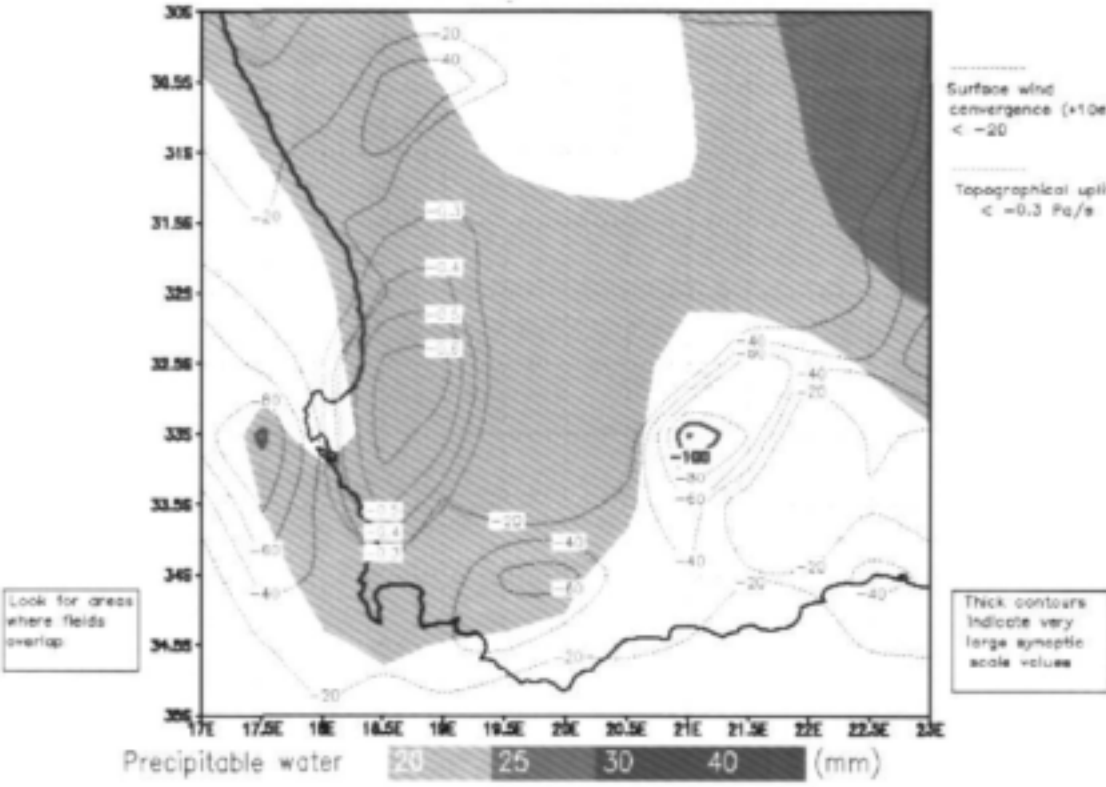

Figure 4.3(b): The Eta model 1000-300hpa precipitable water, surface wind convergence and topographical uplift for the 10th of June 2000.

All the atmospheric variables used in SET B are shown in figure 4.3c. The uplift in the lower levels of the atmosphere was less than –0.25 Pas^{-1} along the West Coast and over the northern parts of the Peninsula. The moisture flux convergence prevailed over the southern parts of the Peninsula with a large area in the west where 600hPa wind divergence occurs.

Figure 4.3d depicts areas where Set A or Set B forecast heavy rain during the 24-hr period. This figure also displays where the Eta model predicted vertical velocity of less than $-1Pas^{-1}$. Comparing figure 4.3d and figure 4.3a, the heavy rainfall identification systems identified all the areas where more than 30mm rainfall occurred. The rainfall totals over the forecasted heavy rainfall area along the west coast were less (5-10mm)

The 24-hr Eta rainfall prognosis is shown in figure 4.3e. The Eta model rainfall forecast generally underestimated the rainfall totals but some rainfall did occur in the area where more than 10mm was forecast.

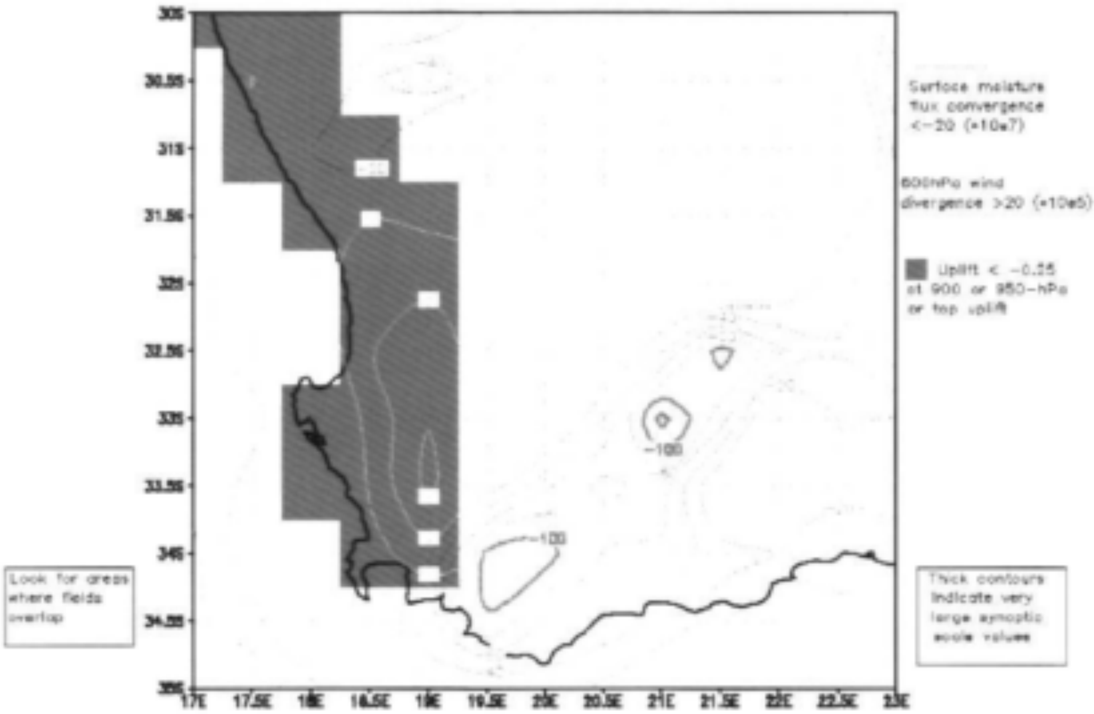

Figure 4.3(c): The Eta model surface moisture flux convergence, 600hPa divergence and surface upward motion on the 10th of June 2000.

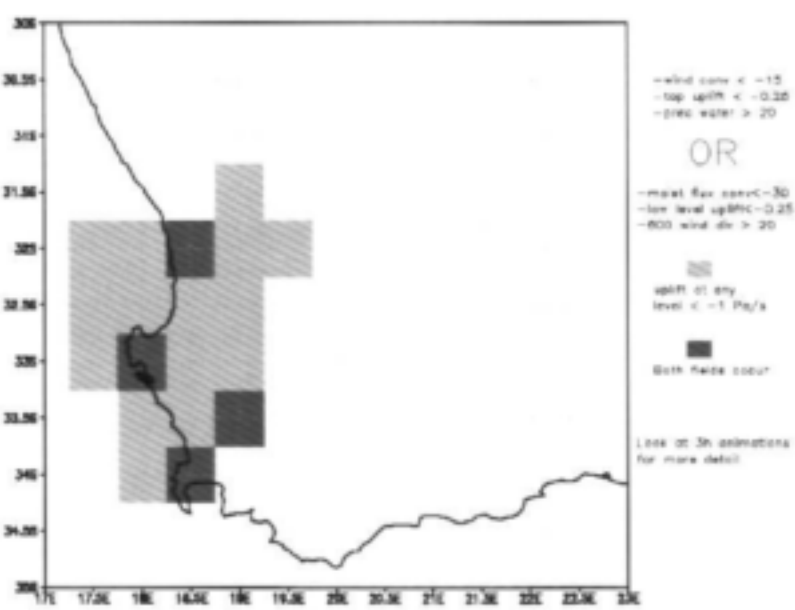

Figure 4.3(d): The Eta heavy rainfall identification systems over the South West Coast on the 10th of June 2000.

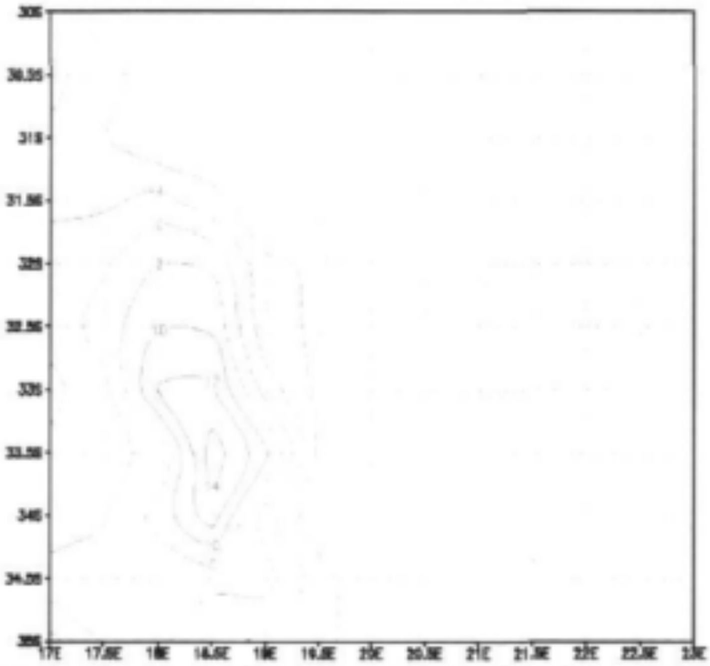

Figure 4.3(e): The Eta model 24-hr rainfall prognosis on the 10th of June

4.3.2 South and East Coast

The Surface Forced Heavy Rainfall system defined for the South West coast performed badly along the South and East coast. This is most likely because of the way the Eta model handles the surface winds over the area. A different set of criteria had to be developed for the South and East coast. However, the basic principles still apply and those atmospheric variables which simulated the forced rising of moisture laden air was identified. The three heavy rainfall identification systems for the East and South Coasts are

a. Surface forced heavy rainfall

The South and East coast Surface Forced Heavy Rainfall system applied the following criteria

- The 1000-650hPa precipitable water should be more than 22mm (East Coast) and more than 17mm (South Coast).
- Vertical velocity should be less that $-0.22Pas^{-1}$ from 950 to 800hPa.
- Horizontal wind convergence should exist at the 950,900 and 850-hPa levels

- Horizontal wind convergence should decrease with height (larger negative values) from 1000 to 900hPa.

OR

- Horizontal wind convergence at the 950 and 900hpPa levels should be less than -20 * 10^{-5} s^{-1}.

The criteria stipulating that horizontal wind convergence should decrease with height from 1000 to 900hPa allows for horizontal wind divergence at a 1000hPa but require horizontal wind convergence at the pressure levels from 950 to 850hPa. In this way this heavy rainfall identification system tries to compensate for the surface divergence which often appears in the Eta model 1000 hPa wind fields

b. Vertical velocity less than –0.5 Pas^{-1} at 950hPa

c. Eta 24-hr rainfall forecast exceeds 10mm.

4.3.2.1 4th of April 2000

In Chapter 3.5.2 it was shown how the surface moisture flux convergence did not occur along the coast of Kwa-Zulu Natal for the heavy rainfall event of the 4th of April 2000. Widespread rainfall occurred on the 4th of April 2000 with the largest totals along the coast of Kwa-Zulu Natal (Fig. 4.4a).

Figure 4.4b shows the heavy rainfall forecast over the East Coast applying the criteria stipulated above. The heavy rainfall forecast was confined to the coastal areas and rainfall occurred over the entire area (Fig.4.4a).

The 1000-650hPa precipitable water field shows values in excess of 25mm over the coast of Kwa-Zulu Natal (Fig.4.4c). Comparing figure 4.4c with figure 3.14b illustrates why precipitable water was the preferred moisture variable in the heavy rainfall identification systems. High values of precipitable water are shown over the area where heavy rainfall occurred but surface moisture flux convergence did not occur over the coast and adjacent interior of Kwa-Zula Natal.

At the Eta grid point near Durban (30°S 31°E) 31mm of rainfall occurred. The vertical distribution of horizontal wind divergence is shown in figure 4.4d. Horizontal wind convergence occurred at the 950, 900 and 850-hPa levels and there was a decrease in convergence from 1000 to 900hPa (larger negative values). Note that at 1000hPa horizontal wind divergence occurred. The vertical velocity was less than -0.22Pas^{-1} from 950 to 800hPa and was in fact also less than -0.5 Pas^{-1} at 950hPa (Fig 4.4e). The 24-hr Eta rainfall also predicted rainfall values larger than 10mm over the area (not shown).

Figure 4.4(a): The average gauge rainfall per Eta grid box on the 4th of April 2000.

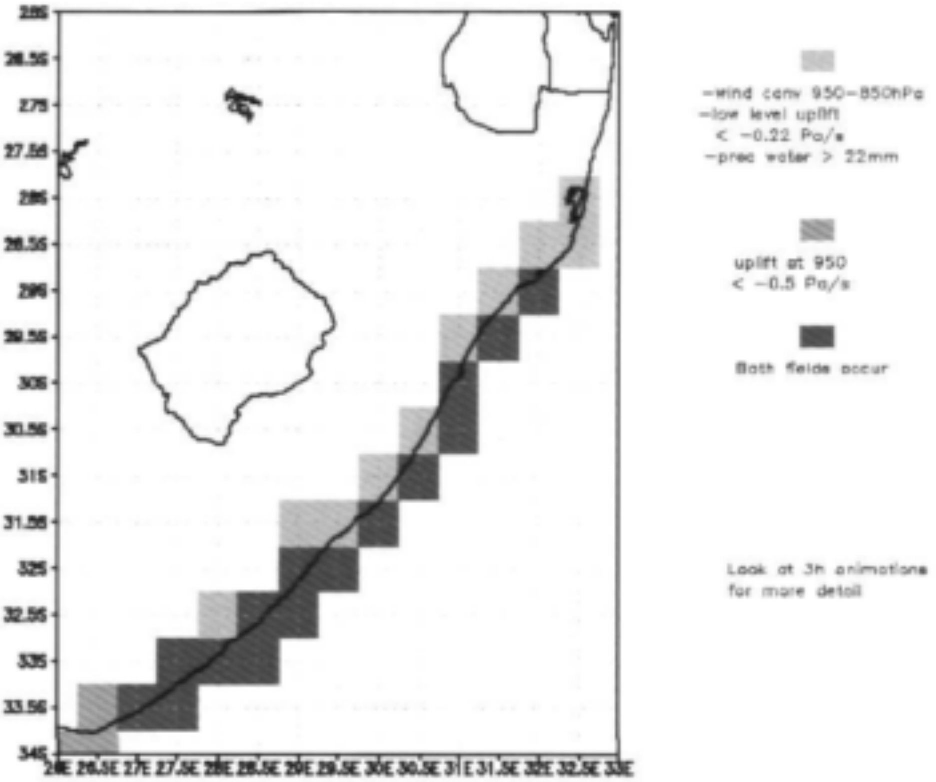

Figure 4.4(b): The Eta heavy rainfall identification systems over the East Coast on the 4th of April 2000.

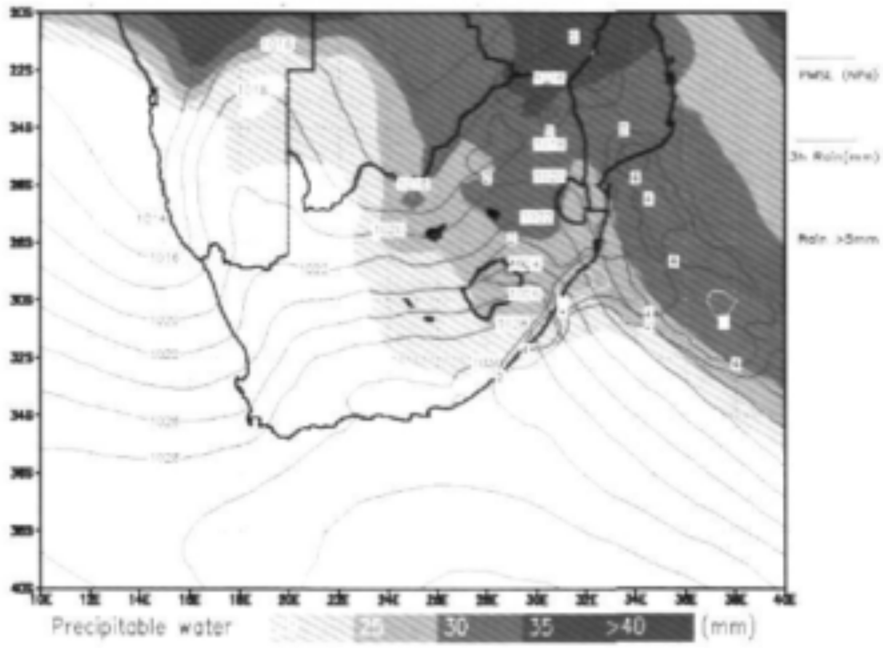

Figure 4.4(c): The Eta model (1000-650hPa) precipitable water on the 4th of April 2000.

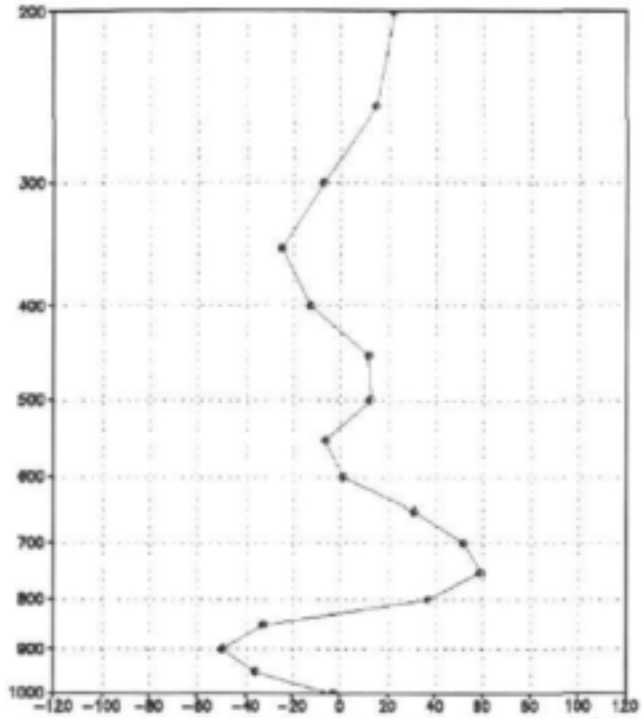

Figure 4.4(d): The vertical profile of horizontal wind divergence (*10^5 s^{-1}) at Durban on the 4th of April 2000.

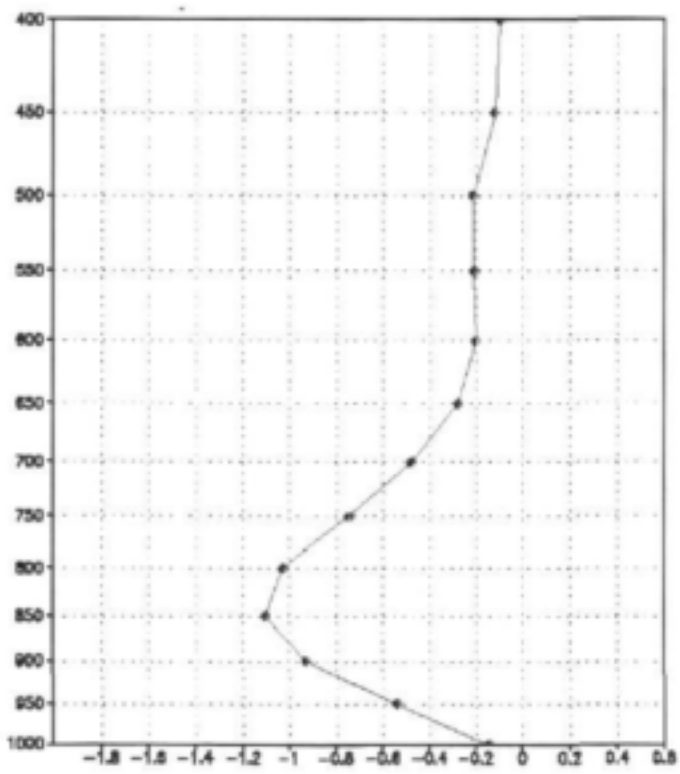

Figure 4.4(e): The vertical profile of vertical velocity (Pas^{-1}) at Durban on the 4th of April 2000.

CHAPTER 5
VERIFICATION

5.1 Introduction

The first heavy rainfall identification systems were developed on NCEP data. The operational versions were developed on the prognostic fields of the Eta model. The verification results for both data sets are discussed here. The NCEP data set is considered to be one of the best available numerical representations of the atmosphere and the results utilizing this data set serve to verify the ability of the heavy rainfall identification systems to pinpoint areas of heavy rainfall. Interpreting the verification results for the Eta model is far more complex. The results reflect the quality of the heavy rainfall identification systems that are also a function of the ability of the Eta model to produce true prognostic fields. The statistical results may therefore provide a mixed signal of the quality of heavy rainfall identification systems.

5.2 Statistical aspects

A detailed discussion on verification methods used in meteorology is available in Murphy and Epstein (1967), Murphy and Winkler (1984), Murphy et al. (1985), Murphy and Winkler (1987), Murphy (1995), Sanders (1963) and Stanski et al. (1989). Verification is only useful if it leads to some decision considering the product being verified. In meteorology, verification has two goals: an administrative goal, to monitor the overall quality of a forecast and track any changes in the quality, and a scientific goal, to identify strengths and weaknesses of a forecast so as to direct research and development (Stanski et al. 1989).

The rainfall forecasts generated by the heavy rainfall identification systems are of an objective nature as they combine various atmospheric criteria, which must all co-exist to identify areas of possible heavy rainfall. They do not rely on the interpretation or experience of a weather forecaster. One of the common methods in verifying the quality of a rainfall forecast is the use of contingency tables (Stanski et al., 1989). Statistical scores such as the probability of detection, false alarm ratio, percentage correct forecasts, threat score as well as the Heidke skill score can be calculated from the contingency tables.

The authors did not consider the use of contingency tables ideal to verify the heavy rainfall identification systems because rainfall and indeed heavy rainfall also develop from weather systems not investigated in this report. The verification is performed daily and all rainfall is incorporated into the statistical results. Poor results regarding the probability of detection, as calculated from the contingency table, were obtained. At the start of the research the authors decided to develop the heavy rainfall identification systems by limiting the number of false alarms and in this way build the confidence of weather forecasters. In an ideal world identification of the relevant weather systems should be the first step and thereafter only the appropriate days should be used to calculate the statistical scores. However, to develop the software to do a daily weather system identification objectively is beyond the scope of this research. To our best knowledge this has not yet been achieved elsewhere.

Consider the contingency table (Table 5.1). The results shown here are for THERIS forecasts using the NCEP data set (summer days only). The table shows the results for THERIS forecasting rainfall amounts exceeding 0mm. The false alarm rate was only 3%, the percentage correct forecasts were 38% but the probability of detection was a mere 9%. THERIS predicted rainfall for 308 grid points during the three summer rainfall seasons and was wrong on only 8 occasions. The large number of observations when THERIS did not predict any rainfall (second row of the table) skews the results.

Table 5.1: The two-way contingency table for THERIS forecasting rainfall amounts exceeding 0mm in the NCEP data. Columns represent the number of forecasts and the rows the number of observations.

	Y	N	Total
Y	300	3032	3332
N	8	1574	1582
Total	308	4606	4914

In order to provide an indication of the quality of the forecast generated by the heavy rainfall identification systems it was therefore decided to utilize cumulative distribution functions (Wilks, 1995).

5.3 Verification results from the NCEP data

NCEP data is of such a high quality that it may be considered a perfect prognosis. The results shown here may therefore be taken as an indication of the quality of the heavy rainfall identification systems. A total number of 942 days were used in the verification. Of these 546 were summer days and 396 winter days.

The NCEP data has a coarse horizontal resolution of 2.5°. As discussed in Chapter 2, the geographical area represented by a single NCEP grid point (box) is approximately 62.500

km^2. This is a very large area and a single NCEP grid point may cover an area over South Africa with large topographical and climatological variation. Consider grid point No. 27 over the interior of Kwa-Zulu Natal (Fig 5.1). The grid point covers a section of the Maluti and Drakensburg Mountains in the west but also the coastal areas of Kwa-Zulu Natal and the Eastern Cape in the east. The weather systems responsible for heavy rainfall over this large and diverse area could be very different. To identify the appropriate vertical level in the NWP data where atmospheric variables such as horizontal wind divergence must be considered is not easy and could not be determined on theoretical grounds alone. The whole process therefore presented a considerable challenge.

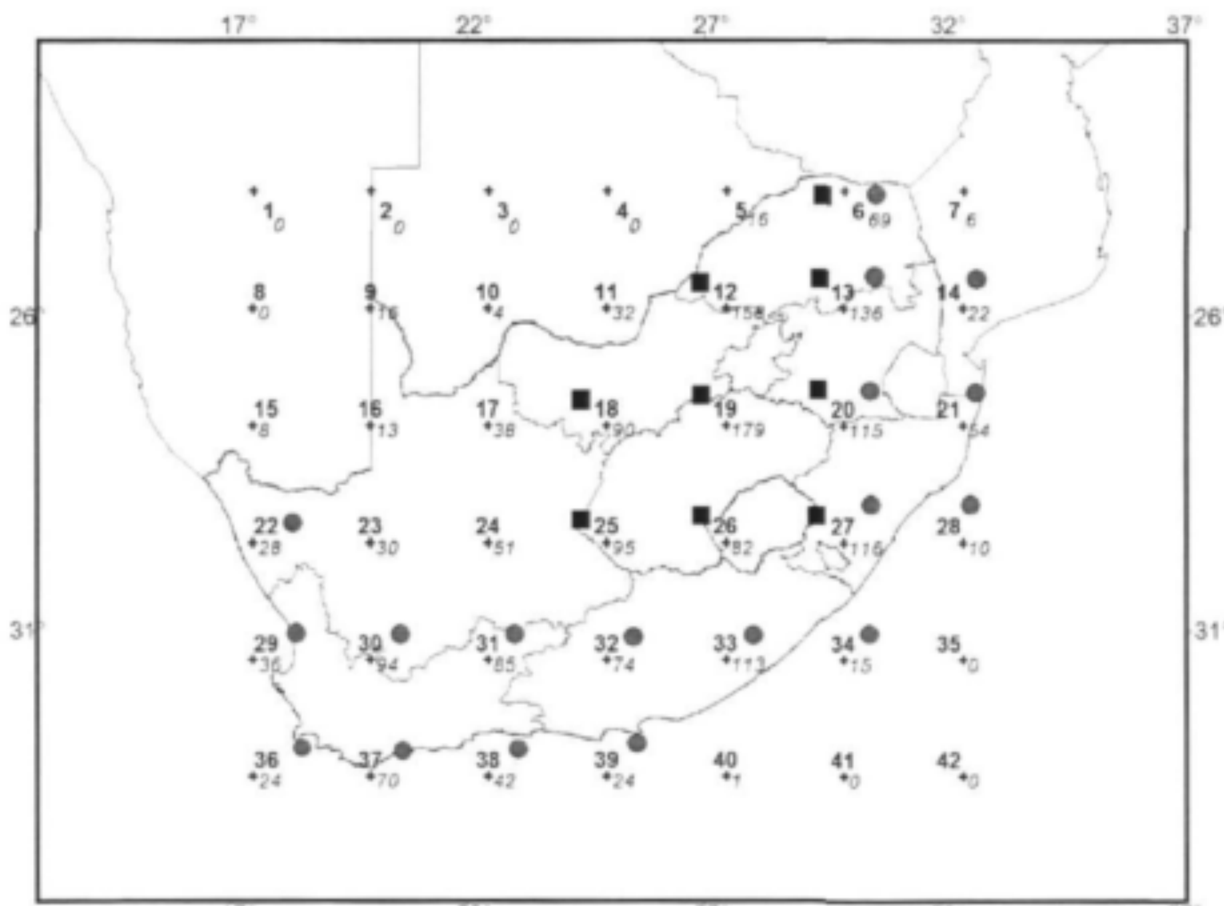

Figure 5.1: The geographical position of the 42 NCEP grid boxes over South Africa. The smaller print shows the number of rainfall station per NCEP grid point. The THERIS forecast area is indicated by black rectangles while grey circles show the coastal forecast area.

The large geographical area that a single NCEP grid box covers also presented the complication that some rainfall is measured in this grid box nearly every day and especially so in summer. Table 5.1 indicates that out of a possible 4914 grid boxes used in the verification, rainfall occurred (average rainfall more than 0mm) on 3332 occasions. This is approximately 67% of the time. Using smaller grid boxes and over areas with similar climatological characteristics may give significantly different results.

The uneven distribution of SAWS rainfall stations over South Africa provides another problem in computing verification statistics. Figure 5.1 shows the number of rainfall stations per NCEP grid box in September 1999. The NCEP grid boxes with the most rainfall stations are located in highly populated areas such as Gauteng and Kwa-Zulu Natal. In the NCEP grid boxes that contain only a part of South Africa the number of rainfall stations is generally less than 10 i.e. grid points 7,10 and 28 (Fig 5.1). The number of rainfall stations per NCEP grid box also did not remain constant over time. During the three-year period used in the verification the number of rainfall stations available have decreased.

Considering these limitations but also bearing in mind the importance of the geographical position of a particular grid point in a heavy rainfall identification scheme the following criteria were applied:

- The THERIS forecast was verified only for grid boxes where 50 or more rainfall stations were active in a grid box. To ensure that THERIS is evaluated for inland areas of South Africa only, those grid boxes where the land surface elevation approximates the 850hPa level were used. Due to the highly variable spread of summer convective precipitation a smaller number of rainfall stations could result in unrealistic grid box average rainfall. The black rectangles in figure 5.1 depict the NCEP grid boxes where THERIS was verified (NCEP THERIS forecast area).
- The Coastal Zone heavy rainfall forecast was verified for those grid boxes indicated by grey circles in figure 5.1. These grid boxes were chosen because they, at least, partially cover the coastal plain up to the adjacent escarpment. A further criterion set was that at least 10 rainfall stations should be present in any NCEP grid box. This was required to include grid boxes 28 and 34 where respectively only 10 and 15 rainfall stations were operational (NCEP coastal forecast area).

5.3.1 THERIS verification results.

The details of the criteria used to create a THERIS forecast are described in Chapter 4. The verification was performed each day for the summer rainfall seasons (October to March) during the period.

The average rainfall over the entire NCEP THERIS forecast area for all days during this three-year period was 3mm (Table 5.2). Grid point no. 13 over the escarpment of Mpumalanga had the highest average daily rainfall at 5mm. There were approximately 130 rainfall stations operational in this grid box. At the same grid point the daily average maximum rainfall of 62mm was also the highest out of the 9 grid boxes. This high value demonstrates the difficulty in verifying THERIS for heavy rainfall events. In this grid box there was at least one station that recorded more than 50mm on 256 days out of the possible 527 days. For the entire NCEP THERIS forecast area the average maximum rainfall for all days was also quite high at 40mm. In the very large grid boxes the average percentage of rainfall stations that recorded some rainfall was 23%.

Table 5.2: The average daily rainfall, average daily percentage of rainfall stations recording rainfall and the average daily maximum rainfall in the NCEP THERIS forecast area for all summer days. The shaded cells give the results for the days that THERIS forecasted.

	All days			THERIS forecast				
Grid number	Average	Percentage	Maximum	Ave	Percentage	Maximum	No. of forecasts	No. of stations
6	4	20	43	18	43	100	25	69
12	3	23	44	8	47	75	60	152
13	5	26	62	14	50	133	32	132
18	2	18	29	5	35	53	33	89
19	3	24	35	6	43	57	62	171
20	4	26	41	8	47	69	45	114
25	2	15	22	5	35	39	14	95
26	3	23	30	6	45	49	26	81
27	4	31	54	8	46	82	11	116
Average	3	23	40	9	44	73	308	
							Total	

The shaded cells in Table 5.2 show the results for the NCEP THERIS forecast area when THERIS predicted heavy rainfall in a NCEP grid box. The average rainfall over the entire area was 9mm. This is 6mm more than the average rainfall for all days. The average maximum rainfall for the entire area (73mm) was close to double the value for all days. Table 5.2 clearly shows the skill in THERIS to predict above normal and heavy rainfall.

THERIS was originally developed to forecast heavy rainfall from tropical weather systems. If the verification for THERIS is performed for all summer days the rainfall from extra-tropical systems is also incorporated into the results. The difficulty lies in designing an objective method to isolate 'tropical' days. Dyson and van Heerden (2001) identified atmospheric criteria, which are all associated with tropical weather systems. One of the vital criteria set was that the average 500-300hPa column temperatures should form a warm core near the lower level tropical low. Their research results did not, unfortunately, determine a critical lower value for the temperatures of the warm core. In order to isolate tropical weather systems it was decided to only consider the rainfall on days when the average column temperature in the 500-300hPa layer exceeded -19°C.

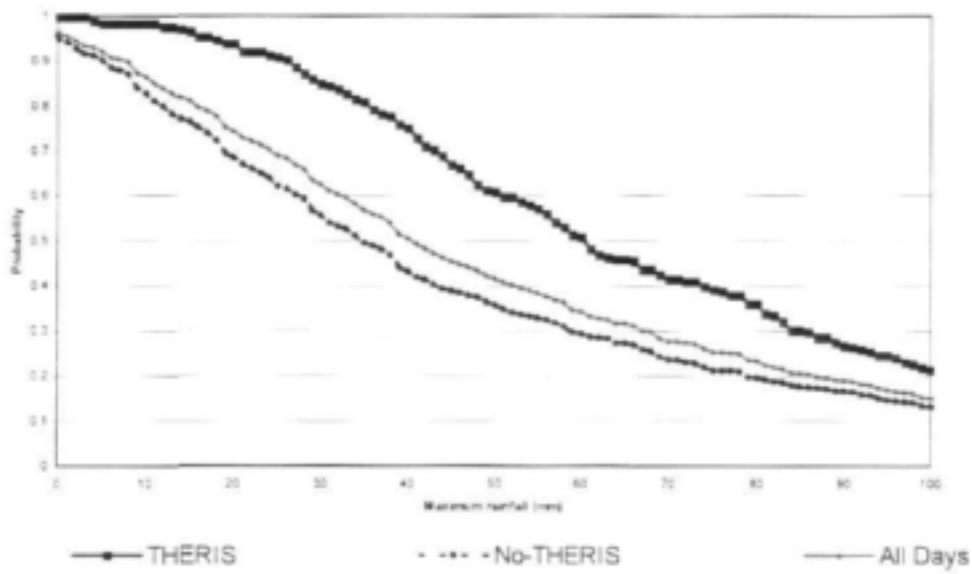

Figure 5.2: Exceedence distribution function of average maximum rainfall for all the NCEP grid boxes when THERIS forecast heavy rainfall for the summer rainfall seasons, October 1999 to March 2002 (thick black). The thin black line is the exceedence distribution function of rain for all grid points when THERIS did not forecast any heavy rainfall (No-THERIS forecast) during the same period and the grey line is for all days during the period (All Days).

Applying this constraint the cumulative distribution functions (Wilks, 1995) were used to test the reliability of THERIS forecasts for tropical continental rainfall. The results for the maximum rainfall per NCEP grid box during the entire summer rainfall period are shown in figure 5.2. The exceedence distribution function was first calculated for all days (All Days) during this period to give a representation of the climate over the NCEP THERIS forecast area (grey line in figure 5.2). The thick black line shows the results for all the THERIS forecasts and the dashed line for all the times when THERIS indicated that heavy rainfall would not occur (No THERIS). The horizontal lines show the fraction of maximum rainfall values (the ordinate values) with maximum rainfall equal to, or more than, the value on the abscissa. Figure 5.2 shows that the probability for at least one station in a NCEP grid box to exceed 0mm is more than 90%. This is true not only when THERIS identified a grid box as an area of heavy rainfall but also for No THERIS and All Days. There is a 94% probability that at least one station in a NCEP grid box will record more than 20mm when THERIS forecast while for No THERIS and All Days the probability is approximately 70%. The grey contour in figure 5.2 shows that there was a 50% probability that the maximum rainfall in a grid box would exceed 40mm. When THERIS forecast heavy rainfall the probability was 75%. As the maximum rainfall threshold increases the lines tend to converge but even for the 80mm threshold the probability for a THERIS forecast is still 10% higher than for All Days.

5.3.2 BARCOZ and BARLUT verification results

The details of BARCOZ and BARLUT are given in Chapter 3. Results for summer (October to March) and winter (April to September) are detailed here.

Table 5.3 shows the average rainfall, average maximum rainfall and the percentage of rainfall stations that recorded rainfall for the NCEP coastal forecast area for the summer months. The average rainfall for all days was 3mm. When BARCOZ indicated heavy rainfall the average rainfall was 14mm and in the case of BARLUT forecasts 10mm. BARCOZ forecasted 248 times while BARLUT made a heavy rainfall forecast only 179 times. BARCOZ frequently forecasted heavy rainfall for the interior regions of Kwa-Zulu Natal as well as the Eastern Cape (grid points 27 and 33). The average rainfall whenever BARCOZ forecasted was 13mm in grid box 27 and 9mm in grid box 33. These figures are significantly higher than the average rainfall for all days in these two grid boxes (Table 5.3).

The average maximum rainfall for all the days is 24mm. For BARCOZ forecasts it is 58mm and 50mm for BARLUT forecasts. The highest average maximum rainfall occurred in grid box 6 (140mm) (Limpopo Province) and in grid box 27 (121mm) when BARCOZ forecasted heavy rain.

Table 5.4 depicts the winter month results for BARCOZ and BARLUT. The average daily rainfall for all days in winter is 1mm. In grid boxes 36 and 37 (South Western Cape) the average daily rainfall is more than 2mm. When BARCOZ forecasted heavy rain the average rainfall was 8mm and in the case of BARLUT 6mm. BARCOZ forecasted heavy rainfall on 84 and BARLUT on 33 occasions. The largest number of BARCOZ forecasts was again over Kwa-Zulu Natal. The average rainfall as well as the average maximum rainfall shows that BARCOZ had some skill in identifying heavy rainfall events.

Table 5.3 The average daily rainfall, average daily percentage of rainfall stations recording rainfall and the average daily maximum rainfall in the NCEP coastal forecast area for all summer days. The shaded cells give the results for the days that BARCOZ forecasted and the lightly shaded areas when BARLUT forecasted.

	All Days			BARCOZ forecasts				BARLUT forecasts				
Grid number	Average	Percentage	Maximum	Average	Percentage	Maximum	Nr of forecasts	Average	Percentage	Maximum	Nr of forecast	Nr of stations
6	4.3	20.2	42.6	31.9	45.5	139.9	13	19.1	52.4	113.8	17	69
7	3.3	19.3	7.4	34.1	70.3	51.2	12	16.0	62.4	30.3	7	6
13	4.5	26.2	62.5	7.6	44.2	69.0	5	12.1	53.6	98.9	16	132
14	3.5	22.1	19.8	14.6	52.3	60.1	7	8.3	62.5	36.3	6	22
20	3.5	26.0	41.4	7.1	48.5	60.7	19	9.0	51.4	67.7	20	114
21	4.1	25.2	33.4	20.3	58.5	88.3	17	14.9	54.4	68.2	9	55
27	4.3	31.3	54.2	13.3	60.5	121.1	36	8.8	51.6	69.6	19	116
28	5.0	33.6	14.2	37.4	90.3	66.7	20	5.0	43.8	12.5	4	10
30	0.6	6.3	8.6				0	7.0	51.0	41.0	2	92
31	1.0	9.4	12.7	0.2	4.6	6.6	5	7.3	44.7	46.4	12	85
32	1.5	13.2	17.0	2.8	22.7	22.7	18	4.8	35.4	33.2	26	74
33	2.9	23.0	38.1	8.9	51.2	76.4	35	8.1	46.1	73.4	19	113
34	3.8	21.9	19.8	15.8	58.2	59.7	20	6.8	43.3	24.0	13	15
36	0.6	11.8	2.6	0.0	4.7	0.7	3				0	24
37	1.0	13.2	8.2	7.6	41.4	28.8	12	6.5	58.0	40.0	2	69
38	2.0	19.3	12.5	11.2	42.1	39.3	13	6.0	29.0	23.0	3	40
39	1.9	19.2	10.2	5.6	46.9	33.8	13	24.0	61.8	71.5	4	24
Average	2.8	20.1	23.8	13.6	46.4	57.8	248	10.2	50.1	53.1	179	
							Total				Total	

The results for the maximum rainfall per NCEP grid box during the entire summer rainfall period are shown in figure 5.3. The exceedence distribution function was first calculated for all days (All Days) during this period to provide a representative rainfall climate for the NCEP coastal forecast area (grey line in figure 5.3). The solid black line shows the results for all the BARCOZ forecasts and the dashed line for all the BARLUT forecasts. The probability that at least one station in a NCEP grid box will receive more than 0mm for All Days is approximately 70%, for BARCOZ forecasts it is 91% and for BARLUT forecasts 98%. There is only a 33% probability for All Days that at least one station a NCEP grid box will exceed 20mm while it is 75% for BARCOZ forecasts and more than 80% for BARLUT forecasts. For the higher rainfall thresholds the lines converge and for the 90mm rainfall threshold there is a

5% probability for All Days while the probability for both BARCOZ and BARLUT is more than 20%.

Table 5.4 Same as Table 5.3 but for all the winter days.

	All Days			BARCOZ forecasts				BARLUT forecasts				
Grid number	Average	Percentage	Maximum	Average	Percentage	Maximum	Nr of forecasts	Average	Percentage	Maximum	Nr of forecast	Nr of stations
6	0.5	6.0	8.5				0	7.0	45.5	39.0	2	69
7	0.3	5.5	0.8				0				0	6
13	0.7	7.3	14.9				0	11.0	40.3	76.7	3	136
14	0.5	6.5	4.2				0	0.3	20.0	2.3	3	22
20	0.8	7.3	11.7	8.0	42.0	46.7	10	2.4	22.0	30.0	5	115
21	1.3	9.4	15.3	10.7	45.9	84.2	10	8.5	57.0	86.3	4	54
27	1.2	10.0	16.6	11.0	53.7	64.5	17	6.0	42.5	45.0	2	116
28	1.9	15.4	5.7	12.3	55.0	31.2	17	3.0	37.0	10.5	2	10
30	1.3	13.9	13.8				0				0	94
31	0.5	7.1	6.8				0	0.0	4.0	10.0	1	85
32	0.7	8.0	8.0	4.0	24.8	19.5	4	11.0	67.7	45.3	3	74
33	1.1	11.1	13.9	10.0	39.5	53.7	6	20.0	68.0	75.0	1	113
34	1.5	9.5	7.7	11.9	38.8	33.0	8	7.2	49.2	20.8	5	15
36	3.0	32.1	10.5	0.0	0.0	0.0	2				0	24
37	2.1	22.2	16.4	0.0	0.0	0.0	1	2.0	33.0	16.0	1	70
38	1.2	17.3	8.0	7.5	51.0	37.0	2				0	42
39	1.3	15.5	6.9	6.9	27.4	33.4	7	1.0	24.0	5.0	1	24
Average	1.2	12.0	10.0	7.5	34.4	36.7	84.0	6.1	39.2	35.5	33	
							Total				Total	

Figure 5.4 shows the results for winter in the NCEP coastal forecast area. Comparing figures 5.3 and 5.4 the results for BARCOZ and BARLUT are not as good in winter as they are in summer.

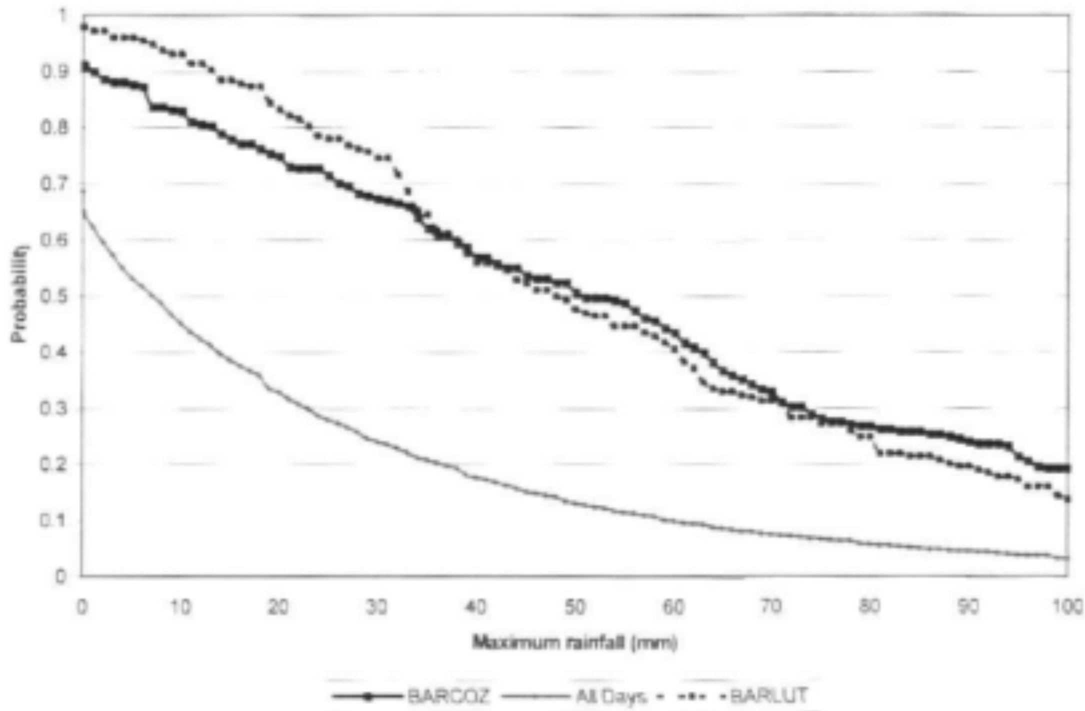

Figure 5.3: Exceedence distribution function of average maximum rainfall for all the NCEP grid boxes when BARCOZ (thick black) and BARLUT (thin black) forecast heavy rainfall for the summer rainfall seasons, October 1999 to March 2002. The grey line is the exceedence distribution for all days during the period (All Days)

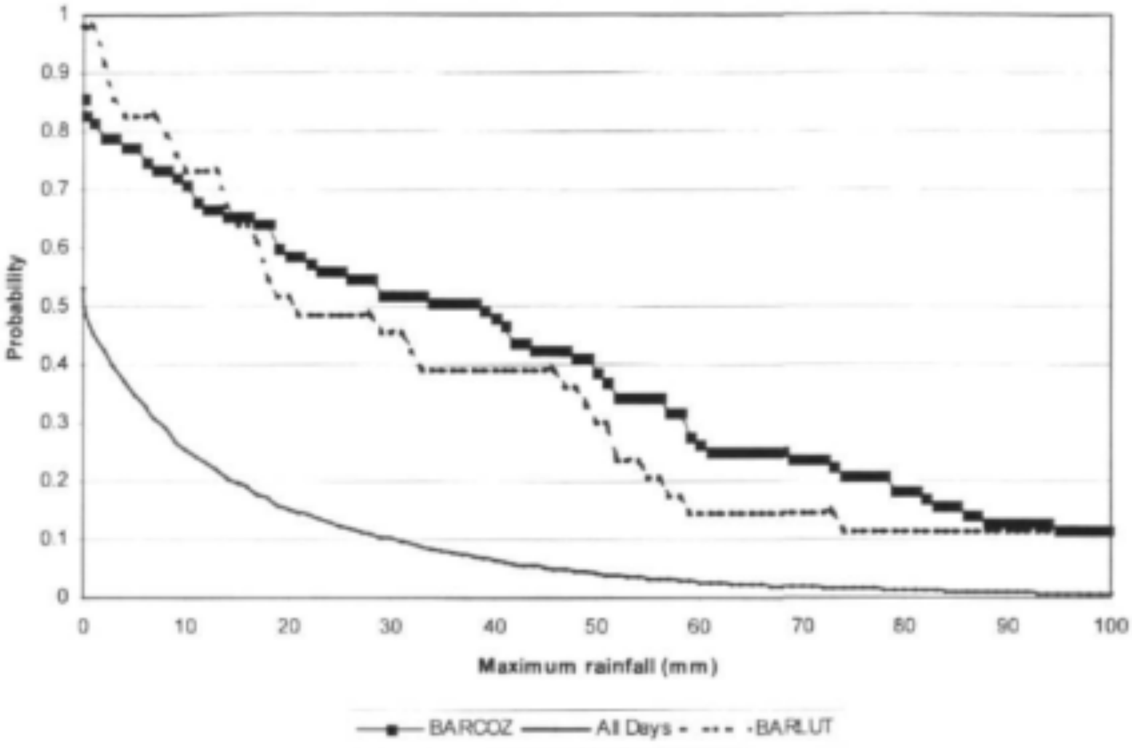

Figure 5.4: Same as figure 5.3 but for all the winter days.

5.4 Verification results from the Eta data

Chapter 2 describes how the heavy rainfall identification systems were calculated daily for Eta data. The 3-hr prognostic fields from 0600 UTC on day 1 to 0600 UTC on day 2 were individually subjected to the heavy rainfall systems and a single field created which indicate the areas where heavy rainfall is probable in the 24-hr period. This period corresponds with the 24-hr period the SAWS uses for daily rainfall measurement. The verification results discussed provide an indication of the quality of the heavy rainfall identification systems but also give an indication of the quality (reliability) of the prognostic fields of the Eta model.

There was a total of 764 days available for analysis. A total of 179 days was lost due to failure of the SAWS Eta data archive. This left 427 summer days and 337 winter days for statistical analysis. Eta data were unfortunately also unavailable for January, February and most of March 2002.

The Eta model has a horizontal resolution of 50km and a single Eta grid box therefore represents a geographical area of approximately 2500 km^2. The heavy rainfall identification systems were compared to the SAWS-measured gauge rainfall for the same geographical area. During the years 1999 to 2002 there were approximately 1500 rainfall stations recording rainfall over South Africa. Unfortunately the rainfall stations are concentrated in the populous areas of South Africa and in many Eta grid boxes over South Africa no rainfall stations were operational (Fig. 5.5). There are only a few Eta grid boxes where more than 10 rainfall stations are operational, notably over Gauteng, the eastern Free State, the south coast and the southern parts of the Cape Peninsula. One of the major challenges in verifying the products generated by the prognostic fields of the Eta model is that SAWS rainfall stations are present in only 168 of the 806 grid boxes depicted in figure 5.5.

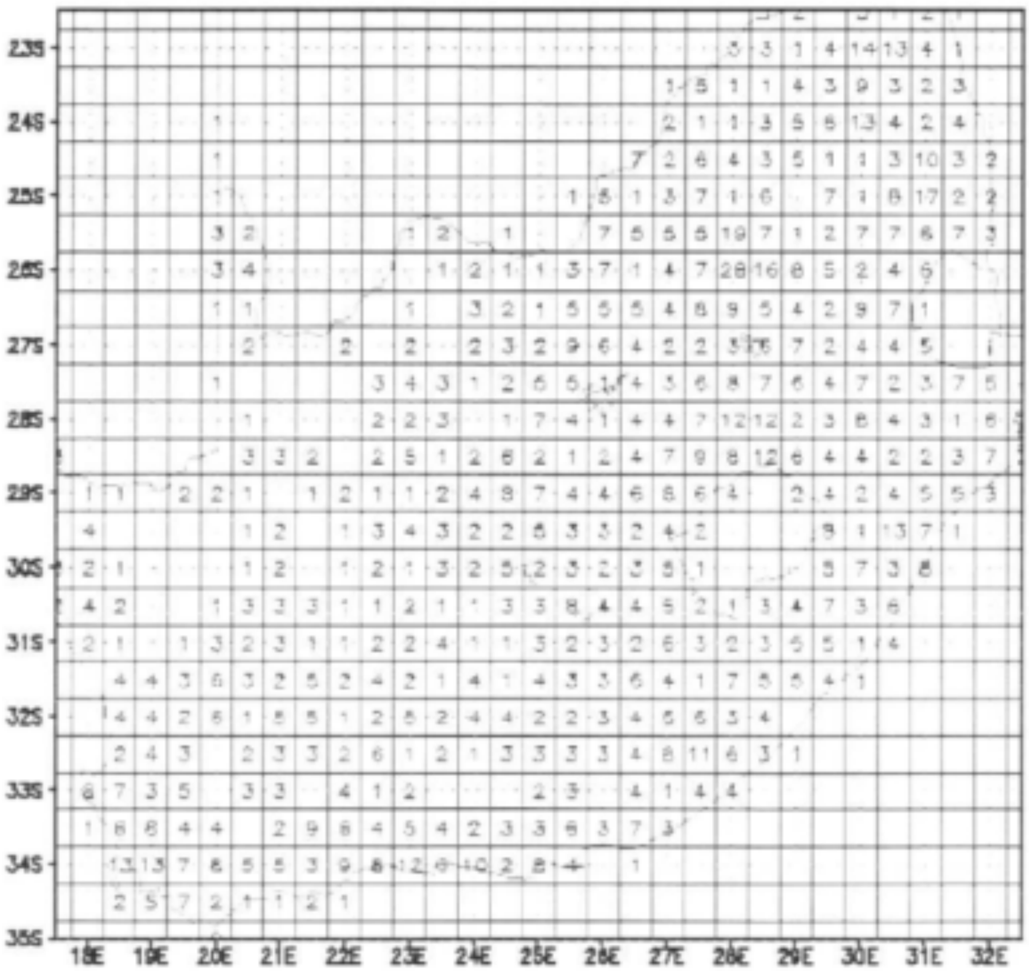

Figure 5.5. Geographical distribution of Eta grid boxes over South Africa. The numerical values indicate the number of rainfall stations per grid box.

Verification was performed only for Eta grid boxes where four or more SAWS rainfall stations were operational and in addition to this the following criteria were set

- The THERIS forecasts were verified only where the model indicated an altitude in excess of 1000m. Figure 5.6 depicts the geographical position of the Eta grid boxes where THERIS was verified (Eta THERIS forecast area). This left 102 Eta grid boxes for daily verification of the THERIS forecasts.

- The coastal forecast area is depicted by the shaded rectangles in figure 5.7. The additional criterion stipulated here was that the model indicated an altitude less than 800m.

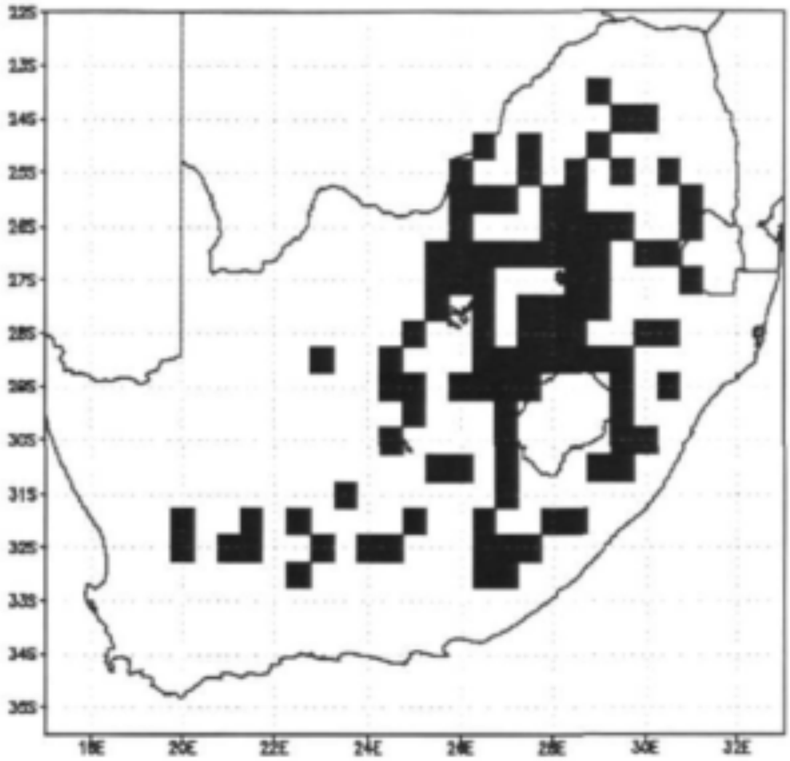

Figure 5.6 The geographical position of the Eta THERIS forecast area. The shaded blocks show Eta grid boxes with at least four South African Weather Service rainfall stations and with the Eta model topography above 1000m ASL.

It should be noted that the discontinuity with regard to the 1000 and 800 m boundaries has nothing to do with weather systems or climate but merely serves to differentiate between inland and coastal regions.

Direct comparison between the verification results from the Eta and NCEP data should be avoided because the two data types are significantly different. NCEP provides the so-called perfect prognosis while Eta provides prognostic fields from an operational NWP model which at times diverges from reality. The horizontal resolution of the two data sets is also very different. In the NCEP data 1mm of rainfall in a grid box will result in 62,5 million m^3 of water while in the Eta data 1mm of rainfall is 2,5 million m^3 of water.

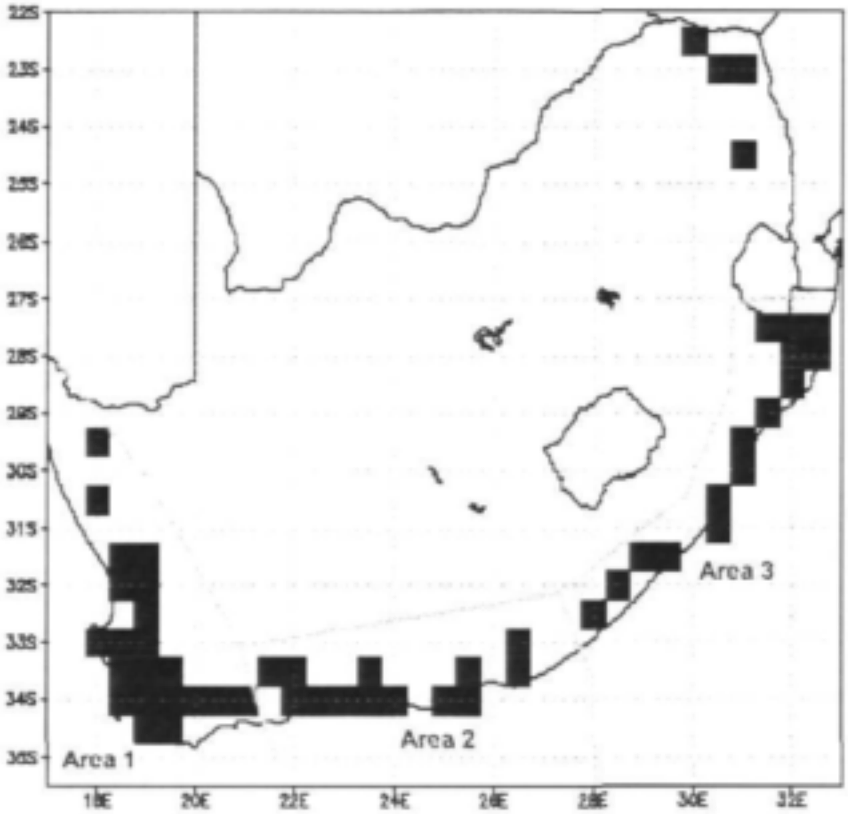

Figure 5.7: The geographical position of the Eta coastal forecast area. The shaded blocks show Eta grid boxes with at least four South African Weather Service rainfall stations and with the Eta model topography less than 800m ASL. Area 1 shows the grid boxes used for the South Western Cape, Area 2 the South Coast and Area 3 the East Coast.

5.4.1 THERIS verification results

Chapter 4 describes how the atmospheric criteria are defined and used to create a THERIS forecast in the Eta model. This set of criteria was slightly modified from the version of THERIS, which runs on the NCEP data. The verification was preformed daily for all the grid boxes in Eta THERIS forecast area as depicted in figure 5.6.

Figure 5.8 depicts the results of the verification of THERIS heavy rain forecasts (black line) using exceedence distribution functions. There is an 83% probability that the average rainfall in a Eta grid box will exceed 0mm whenever THERIS forecasts heavy rain. The grey line on figure 5.8 represents the results for all days and all cells during the summer season. Comparing the two lines, it is clear that for all the rainfall thresholds, a THERIS forecast gives a significant higher probability of occurrence of rainfall. The probability of THERIS identifying rainfall values exceeding 30mm is less than 10%. However, during the entire period and considering all the cells, rainfall exceeding 30mm occurred only 1% of the time.

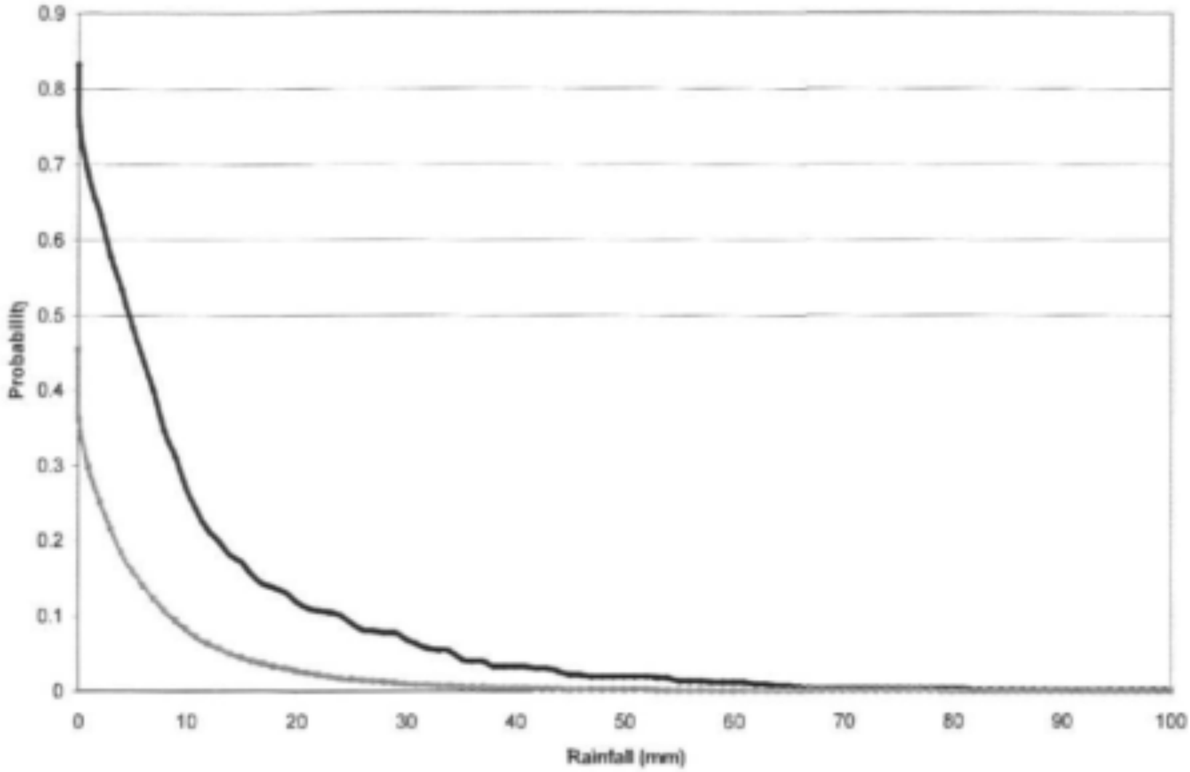

Figure 5.8 Exceedence distribution function of average rainfall for all the Eta grid boxes when THERIS (black) forecasted heavy rainfall for the summer rainfall seasons, October 1999 to March 2002. The grey line is the exceedence distribution for all days and all grid boxes during the period (All Days)

Considering the proportion of THERIS forecast days to all days as a function of rain depth per day for the whole of summer (Fig. 5.9) gives some indication of the quality of THERIS forecasts for the higher rainfall thresholds. Note the improvement in the proportion as the rainfall threshold increases. This is useful when set against the fact that only 45% of all cells over summer experienced 1mm or more rain on average.

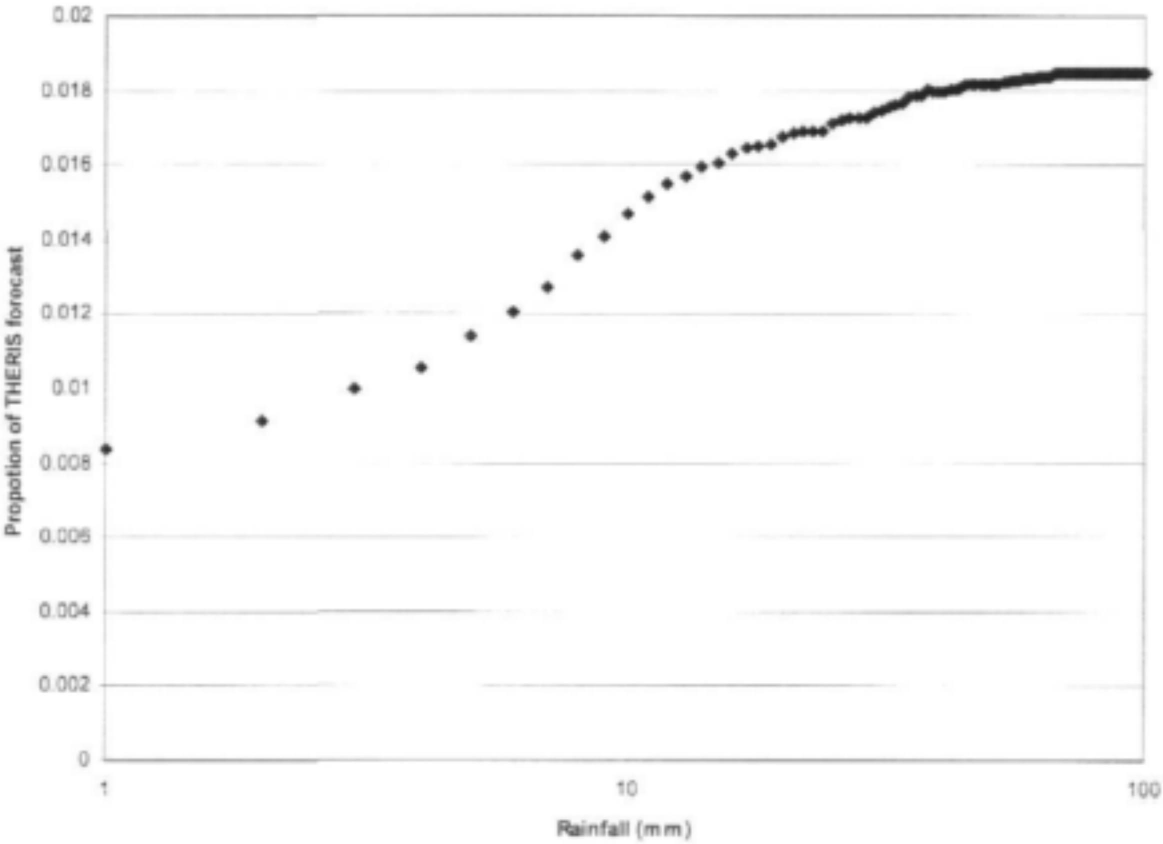

Figure 5.9: Proportion of THERIS forecast days to all the days for the summer rainfall seasons of October 1999 to March 2002.

5.4.2 Coastal zone heavy rainfall verification results.

Chapter 4 describes the development of several heavy rainfall identification systems for the coastal zone. None of them performed adequately for the entire coastal zone. Three different versions of the coastal heavy rainfall identification system (BARCOZ versions) were eventually selected for statistical analysis. They were evaluated individually for the South Western Coast, the South Coast and the East Coast (Fig. 5.6). It was also necessary to adjust the criteria between summer and winter.

a. *South West Coast*

The verification was performed in 23 Eta grid boxes over the South Western Cape (Fig. 5.6) and for three heavy rainfall identification systems. The latter are:

1). Surface forced heavy rainfall

A field is created when all three criteria of either Set A or all three criteria of Set B are satisfied.

SET A

- Surface wind convergence must be less than $-20 * 10^{-5}\ s^{-1}$
- Topographical uplift must be less than $-0.25\ Pa\ s^{-1}$
- Precipitable water from 1000-300hPa must be more than 17mm

SET B

- Moisture flux convergence of the surface wind must be less than $-20 * 10^{-7}\ s^{-1}$
- Wind divergence at 600hPa must be greater than $20 * 10^{-5}\ s^{-1}$
- Upward motion should be less than $-0.25\ Pa\ s^{-1}$ at 950hPa, 900hPa or the topographical uplift.

2). Vertical velocity at any pressure level is less than $-1\ Pas^{-1}$

3). Eta 24-hr rainfall prediction is more than 10mm

Table 5.5: Exceedence distribution probability of exceeding the average rainfall threshold for: surfaced forced heavy rainfall; vertical velocity < $-1\ Pas^{-1}$; and Eta rainfall forecast > 10mm, for the winter rainfall seasons October 1999 to March 2002 over the South West Coast. The average rainfall whenever the heavy rainfall identification system is forecast is given in the last row.

Average Rainfall threshold (mm)	**Probability of exceeding rainfall threshold (%)**		
	Surface forced heavy rainfall	Vertical velocity < -1 Pas^{-1}	Rainfall > 10mm
0	91	98	100
5	67	75	91
10	46	53	72
20	21	21	38
30	10	9	17
40	4	3	7
50	1	1	2
Average rainfall when forecast (mm)	9	11	16

The results of the verification for these three products (1, 2 and 3) using exceedence distribution functions are shown in table 5.5. All three products perform very well in identifying average rainfall greater than 0mm. When the Eta 24-hr rainfall forecast predicts more than 10mm, there is a 100% probability that some rainfall will occur. There is a 72% probability that rainfall will exceed 10mm for this same product while the probability of the surfaced forced heavy rainfall and vertical velocity products for 10mm is close to 50%. The probabilities decrease rapidly for average rainfall thresholds larger than 20mm. Table 5.5 also show the average rainfall values whenever there is a positive prediction using any one of the three identification systems.

b. South Coast

The three heavy rainfall identification systems tested for the South Coast during winter are:

1). Surface forced heavy rainfall

- The 1000-650hPa precipitable water should be more than
- Vertical velocity should be less that $-0.22 Pas^{-1}$ from 950 to 800hPa.
- Horizontal wind convergence should exist at the 950,900 and 850-hPa levels
- Horizontal wind convergence should decrease with height (larger negative values) from 1000 to 900hPa.

OR

- Horizontal wind convergence at the 950 and 900hpPa levels should be less than $-20 * 10^{-5} s^{-1}$.

2). Vertical velocity at 950hPa should be less than $0.5 Pas^{-1}$

3). Eta 24-hr rainfall prediction is more than 10mm

There were 14 Eta grid boxes over the South Coast area used in the verification. The verification results for winter rainfall are shown in figure 5.10. The exceedence probabilities for all winter days and all cells are indicated with the thick grey line. On any particular day in winter there is only a 25% chance for some rainfall to occur on the South Coast. The surface-forced heavy rainfall system (solid black) as well as the vertical velocity criterion of less than $-0.5 Pas^{-1}$ fares well for the lower rainfall thresholds but results are not as good for rainfall exceeding 10mm. The poor performance of these systems could partly be due to the small number of heavy rainfall events in winter over this area. However figure 5.10 clearly shows that the Eta model precipitation exceeding 10mm is by far the best heavy rainfall system for the South Coast.

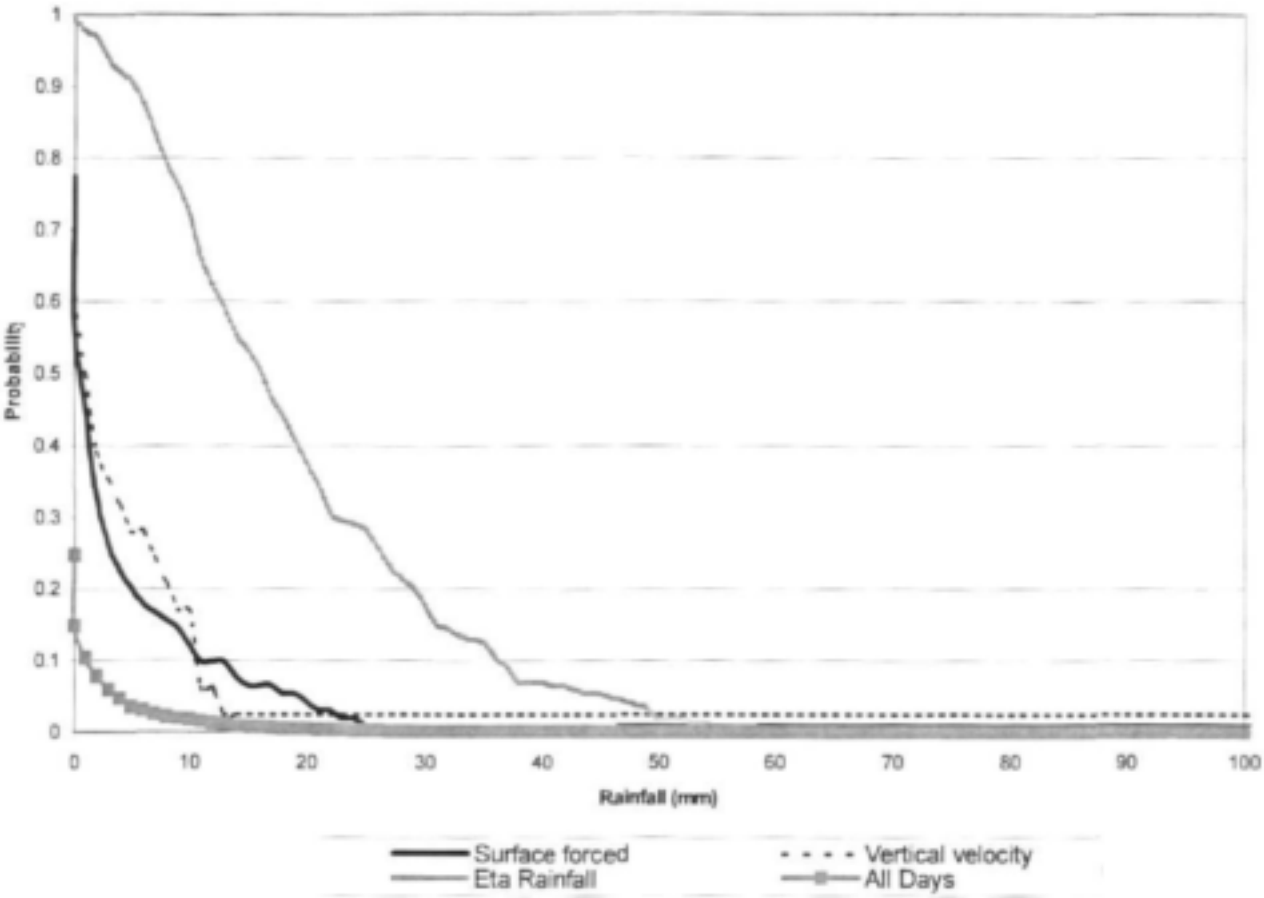

Figure 5.10 Exceedence distribution function of average rainfall for all the Eta grid boxes when the three heavy rainfall systems forecasted heavy rainfall for the winter rainfall seasons, October 1999 to March 2002 for the South Coast. The thick grey line is the exceedence distribution for all days and all grid boxes during the period (All Days)

c. *East Coast*

The heavy rainfall identification systems over the East Coast applied the same criteria as over the South Coast with the exception that the precipitable water in the 1000-650hPa level should exceed 22m. There were 23 Eta grid boxes used in the verification over the East Coast.

The results for winter over this area are shown in figure 5.11. The three heavy rainfall systems perform adequately for the lower rainfall thresholds but are less adequate for the higher rainfall thresholds. The results for the higher rainfall thresholds may be misleading as it happened less than 1% of all days that the average rainfall exceeds 30mm. There were in total 21 events where the average rainfall in a cell exceeded 30mm. The surface-forced rainfall system identified 10 of these events, the vertical velocity system 5 and the Eta precipitation system 18 of these events. The results are better than for the South Coast but not as good as those for the South West Coast.

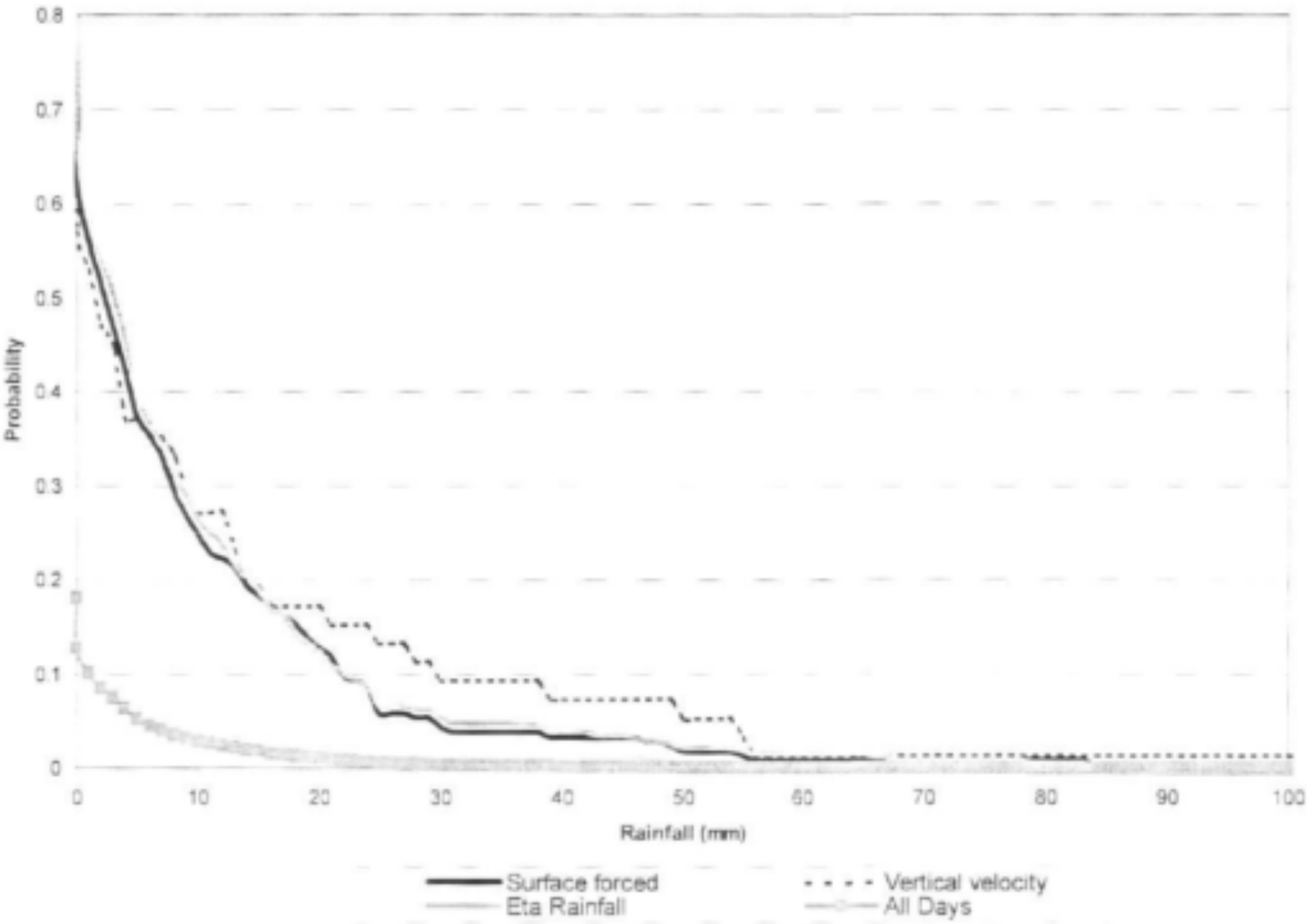

Figure 5.11 Exceedence distribution function of average rainfall for all the Eta grid boxes when the three heavy rainfall systems forecasted heavy rainfall for the winter rainfall seasons. October 1999 to March 2002 for the East Coast. The thick grey line is the exceedence distribution for all days and all grid boxes during the period (All Days)

CHAPTER 6

COMPARISON OF THE RAINFALL PROGNOSIS OF A NUMERICAL WEATHER PREDICTION (NWP) MODEL TO SATELLITE RAINFALL FIELDS

(Contribution by Mr Luis Fernandes)

In this chapter a method is proposed to improve the quality of the precipitation forecasts of a NWP model. The method integrates real time measured rainfall data and the rainfall forecast from a NWP model. The aim of this research was to investigate if the adjustment method could improve the rainfall forecast. Recent advances in the quality of remotely sensed rainfall observations as well as improvement in NWP models will result in improved results of this method.

6.1 Introduction

Numerical Weather Prediction (NWP) models provide a precipitation forecast often referred to as the Quantitative Precipitation Forecast (QPF). Unfortunately the QPFs often fail to predict the actual rainfall amounts accurately. This chapter describes a method of integrating measured rainfall (satellite rainfall) and the rainfall from a NWP (MM5) in real time in order to improve the QPF.

Laurent et al. (1997) explained that satellite rainfall estimates are essential, to compensate for low-density or lack of ground-based rainfall measurements. Cloud top temperatures, obtained from a geostationary satellite, can be used to estimate rainfall using threshold and other techniques. This in turn produces estimates of the rain rates at each satellite pixel. The scientific justification for this method is based on the observation that the area, height and duration of a storm are related to its volume rain rate. Geerts (1998) discusses how visual and infrared (IR) images are used in satellite rainfall estimations. Higher albedos in the visual image indicate more water droplets and/or ice, and the deeper the cloud tends to be, the more likely rainfall is on the ground. The lower the IR brightness temperature, the higher the cloud top and therefore a greater chance of rainfall. Combinations of both channels give the best results. This method of using both visible and IR rain rate retrieval works best at lower latitudes since at higher latitudes, the satellite view is more slanted, and high reflectivity from snow and ice contaminate the cloud reflectivity. Deep convective precipitation is also less common in the higher latitudes (Geerts, 1998). Arkin, cited in Laurent et al. (1997) describes a statistical relationship between thermal IR temperatures and precipitation over the tropics.

The satellite data used in this report is from the Meteosat 7 geostationary satellite, obtained, courtesy of the SAWS, Bethlehem, through Eumetsat (SAWS, 2002).

Spatial Interpolation and Mapping of Rainfall (SIMAR) is a joint project between the Weather Service, Water Research Commission and The University of KwaZulu-Natal. The project proposes the development of an integrated rainfall mapping system for South Africa. The integration of remotely sensed rainfall derived from weather radar and meteorological satellite with gauge rainfall measurements comprises the system. The SIMAR satellite rainfall fields were used to make specific model forecast adjustments of the 24-hour MM5 NWP rainfall forecasts. (Deyzel et al., 2004 and Pegram, 2004)

6.2 Numerical weather prediction and rainfall data

The South African Weather Service (SAWS) carried out two separate MM5 model runs for this project. Cumulus parameterisation and the Grell scheme were used for both. The first model run was initialised at 1200 UTC on 18 March 2003 and provided prognostic fields every 6-hours up to 36-hours ahead (0000 UTC on 20 March 2003). The second model run was initialised at 1200 UTC on the 19th and the last prognostic field was for 0000 UTC on 21 March 2003. In this paper only prognoses for the first 24-hours in each model run were used. The period used from the first model run was from 1200 UTC on the 18th to 1200 UTC on the 19th (Run 1). From the second model run the 24-hour period used was from 1200 UTC on the 19th to 1200 UTC on the 20th (Run 2). The rainfall prognosis for each run was obtained in six 6-hour accumulations, with a horizontal resolution of 15 minutes.

Satellite rainfall data for the whole month of March 2003 were obtained from the METSYS offices in Bethlehem, in 1- hour accumulations. The data were in ASCII format and had a resolution of 1 minute.

The NCEP reanalysis data were used for comparisons, and images of the reanalysis data were obtained from the Climate Diagnostics Centre (2003).

The satellite and NWP data needed to be transferred from ASCII format into Idrisi and Arcview GIS for further analysis. Once this was done, the satellite data's resolution was changed from 1 minute to 15 minutes (Fig. 6.1 (a) and (b)); which is the resolution in which the MM5 data were obtained. This was necessary, since the GIS applications used do not allow grids or maps of differing resolutions to be analysed together. When this function is performed, the mean of the values of the smaller, one-minute pixel is used as the new value of the larger 15-minute pixel. This does result in some loss of data, but in this instance the loss was not too severe. In figure 6.1a, individual pixels can be identified, whereas in figure 6.1b the field is much smoother. Some isolated patches of rainfall, such as the ones observed off the east coast (Fig. 6.1a), are no longer present after the pixel size was changed (Fig.6.1b). Although there is loss of data, the geographical distribution of precipitation is still captured and the amounts remain within the same range (not shown).

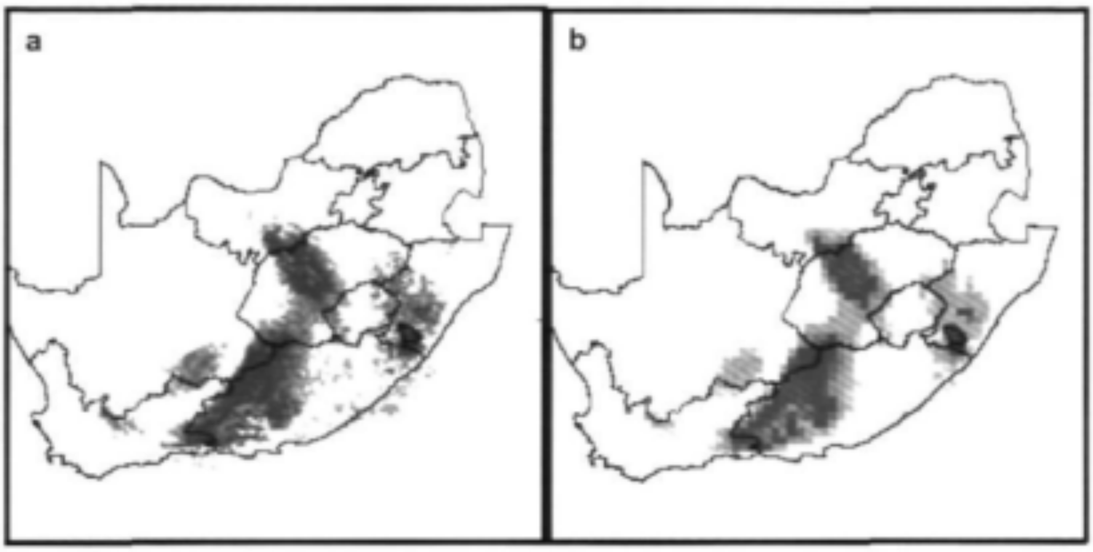

Figure 6.1: Satellite rainfall image on 20th March 2003 at 0600 UTC at 1-minute resolution (a) and at a 15-minute resolution (b).

Since the MM5 data were over a larger domain than the satellite data, there were some areas of the two data sets, which did not overlap. In order to obtain a proper comparison between the data sets MM5 and satellite rainfall fields were considered for the regions where the fields overlapped.

In order to make visual comparisons between the forecast and observed accumulated rainfall, the 1-hour satellite accumulations were then added over the same 6-hour accumulation periods as the MM5 forecasts. This was also done to obtain 24-hour rainfall accumulations, over the periods of Run 1 and Run 2, for both types of data.

6.3 Integrating MM5 and satellite rainfall

The following method was used to adjust the MM5 24-hour rainfall prognosis, with the satellite observations. Firstly, the satellite rainfall accumulation for the first six hours of each model run was subtracted from the MM5 rainfall prognosis for the same time (1200 to 1800

UTC). The result was a difference image with positive values where the model over forecast, and negative values were the model under forecast. An example of this is shown in figure 6.8. This difference map was then subtracted from the MM5 24-hour rainfall accumulation. The resulting image was an adjusted 24-hour model forecast after six hours of observations. This procedure was then repeated for a second time, using the 6-hour accumulations that follow directly after those used in the first step (1800 to 0000 UTC). Furthermore, the difference of these accumulations is then subtracted from the adjusted 24-hour forecast after 6-hours of observations; unlike the first step, which uses the accumulated 24-hour rainfall forecast. The final result is an adjusted 24-hour model forecast, with all errors from the first 12 hours of the forecast removed. This process is graphically described in figure 6.2

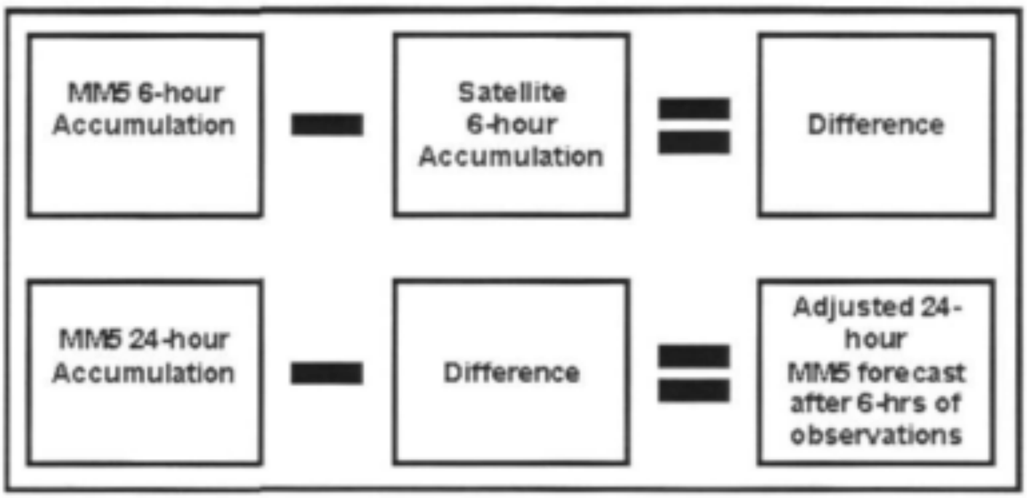

Figure 6.2: Adjustment method of model precipitation prognosis, using satellite rainfall data.

The Root Mean Square Error (RMSE), for Run 1 and Run 2, of the adjusted model precipitation forecast and the original MM5 24-hour rainfall accumulation was calculated, to investigate the error difference between the two model forecasts:

$$RMSE = \sqrt{\frac{\sum_{i=1}^{N}(F_i - O_i)^2}{N}}$$

For the purposes of this study, F_i represents the value of one pixel of the MM5 forecast and O_i represents the value of one pixel of the 24-hour observed satellite rainfall. N is the number of pixels in the grid.

Stanski et al. (1989) stated that the RMSE is a quadratic scoring rule, which gives the 'average' magnitude of errors, weighted according to the square of the error. They go on by discussing that the RMSE gives greater weights to large errors than to small errors in the average. Therefore, the RMSE is used when large errors are particularly undesirable, such as in the case of heavy rainfall forecasts (Stanski et al., 1989).

6.4 Results and discussion

Making a visual comparison, for Run 1, between the 24-hour accumulations of the model rainfall prognosis (Fig. 6.3a) and the satellite rainfall (Fig. 6.3b), the most noticeable difference is the extent to which the model has over forecast. Although the satellite data does indicate that the highest rainfall, between 10 and 25 mm, occurred over the KwaZulu-Natal (KZN) south coast and interior, the model forecast up to 300 mm over this area. The model also forecast up to 75mm over the escarpment in eastern Mpumalanga, which does not reflect on the satellite rainfall. The satellite data shows rainfall over southern Gauteng that was not forecast by the MM5 model. For the period of Run 2 a similar pattern is observed (Fig. 6.4a and 6.4b). Once again the model over forecasts rainfall on the KZN south coast and the escarpment in Mpumalanga. From the model runs there seems to be a trend, for these two days, as to where the MM5 model over forecasts rainfall. The greatest rainfall errors occur near to regions of steep topography. This will be discussed later in this section.

The model prognosis (Run 1) for the 500hPa heights on the 18th at 1200 UTC (Fig 6.5) shows the upper air trough south west of the country. The position and depth of the trough compares well to the NCEP reanalysis data for the same time (Figure not shown). Noticeable features of the model prognosis are the small perturbations in the geopotential heights, especially over the eastern escarpment. On the 19th (Run 2), the MM5 and NCEP (not shown) images (Fig 6.6) indicate that the upper air disturbance moved over the western interior of the country and developed into a COL. The model did predict the position of the centre of the low relatively well; however, it also predicted it to be deeper than the reanalysis data indicates. The MM5 prognosis also shows the low extending southeastward, and once again there are perturbations along the eastern escarpment, except they are far more pronounced than on the previous day. There appears to be a correlation between topography and where the model produces these large perturbations. The result is that these features have a large effect on the rainfall prognosis. When comparing the model's 24-hour accumulated rainfall prognosis for Run 2 (Fig. 6.4a) to its' 500hPa height prognosis (Fig. 6.6) on the 19th at 1200 UTC, it is evident that the highest rainfall was forecast to the east of these perturbations.

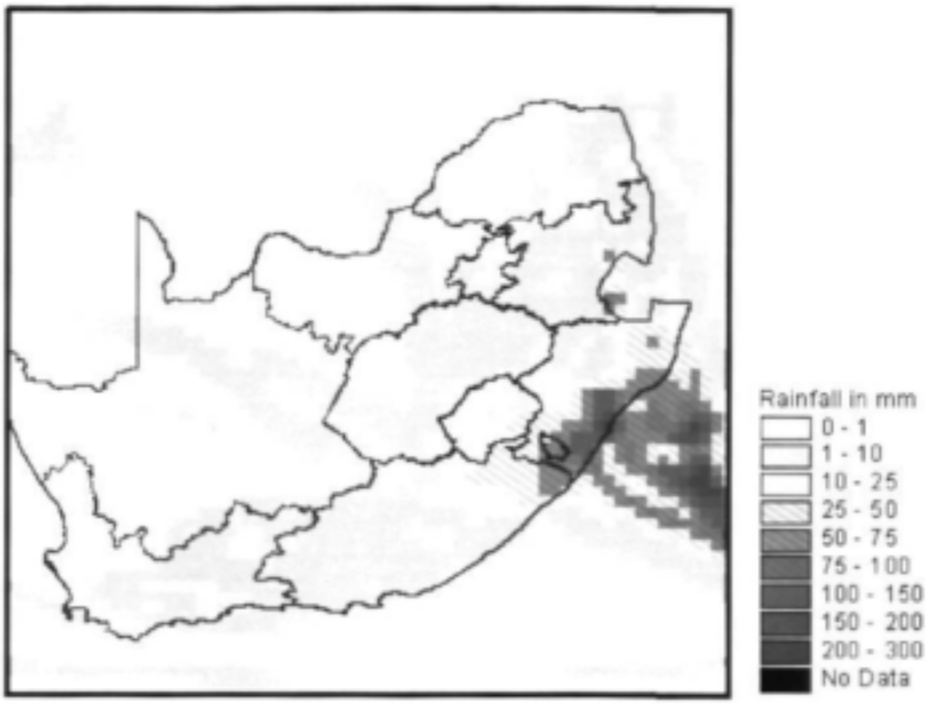

Figure 6.3(a): MM5 24-hour rainfall accumulation for the time period of Run1.

Figure 6.3(b): Satellite 24-hour rainfall accumulation for the time period of Run1.

Figure 6.4(a): MM5 24-hour rainfall accumulation for the time period of Run2.

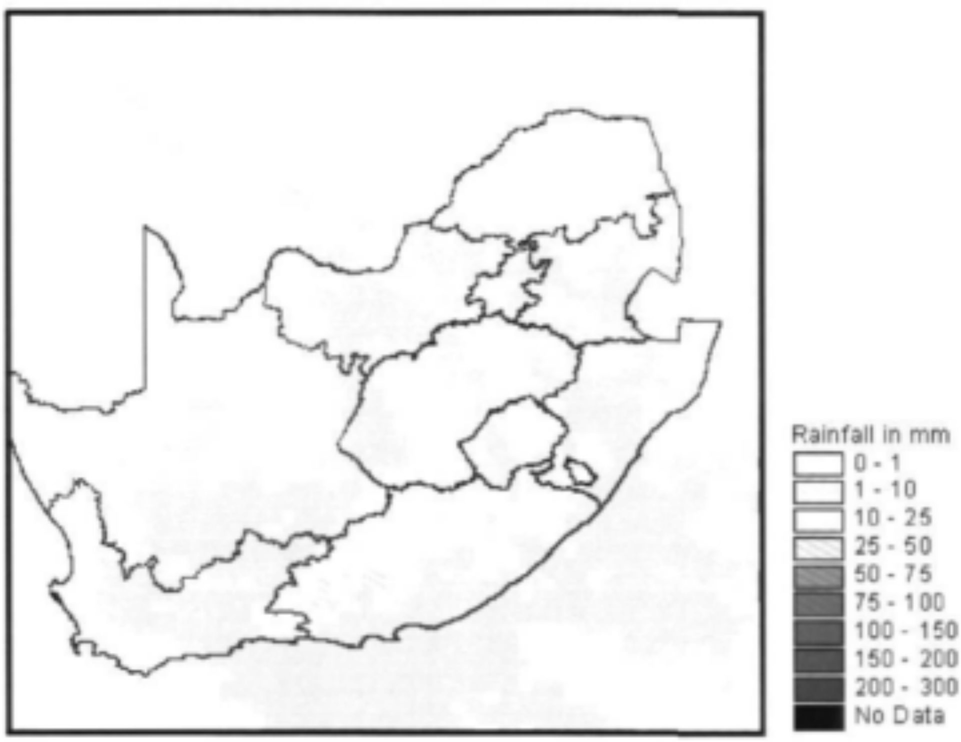

Figure 6.4(b): Satellite 24-hour rainfall accumulation for the time period of Run2.

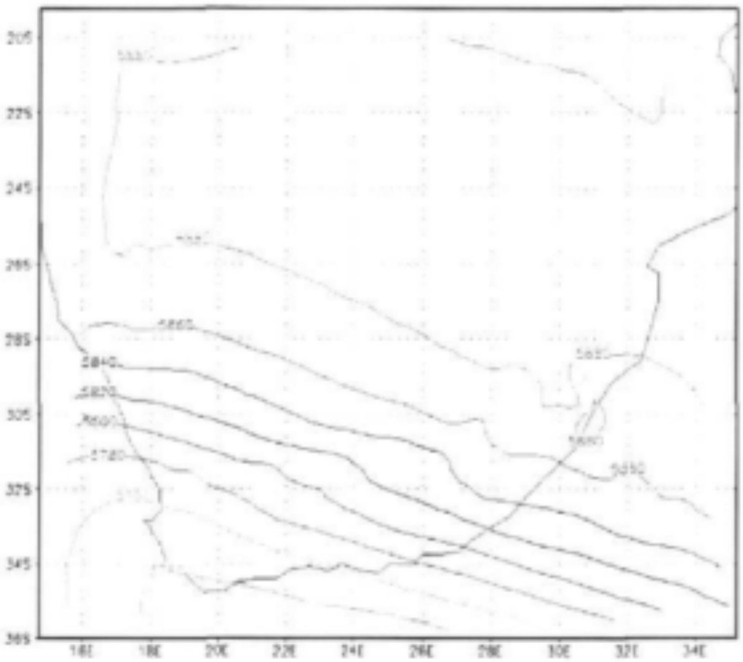

Figure 6.5: MM5 prognosis for the 500hPa heights for the 18th March at 1200 UTC for Run1.

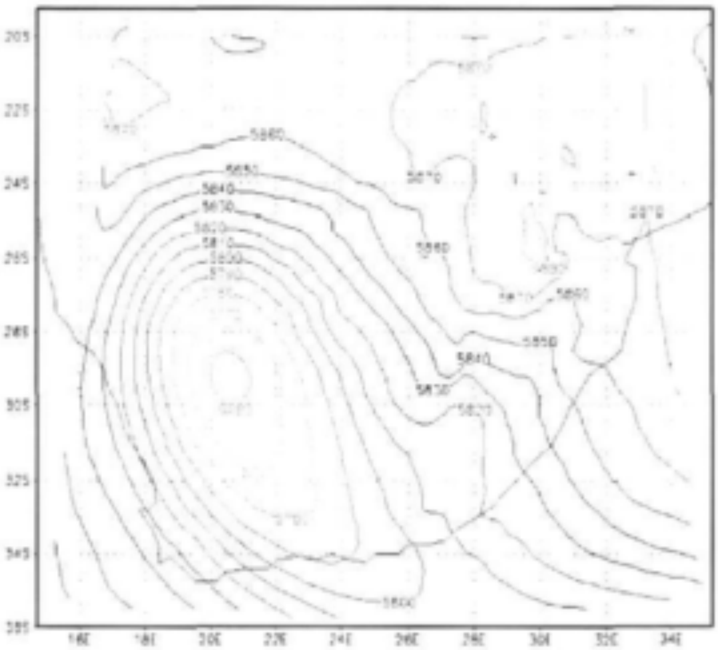

Figure 6.6: MM5 prognosis for the 500hPa heights for the 19th March at 1200 UTC for Run2.

A prominent feature on the model prognosis in addition to the large perturbations, for the sea-level pressures at 1200 UTC on the 20th (Fig. 6.7a), is the low pressure on the KZN south coast. When looking at the 500hPa heights for the same time (Fig. 6.7b), it can clearly be seen that the low pressure is still present at this level. The Coastal Low workshop, cited in Taljaard (1995), defines a coastal low as "a small area of relatively lower pressure which appears in the lower levels of the atmosphere (below 700hPa) along the coast...". From this we can conclude that the model was not forecasting a coastal low.

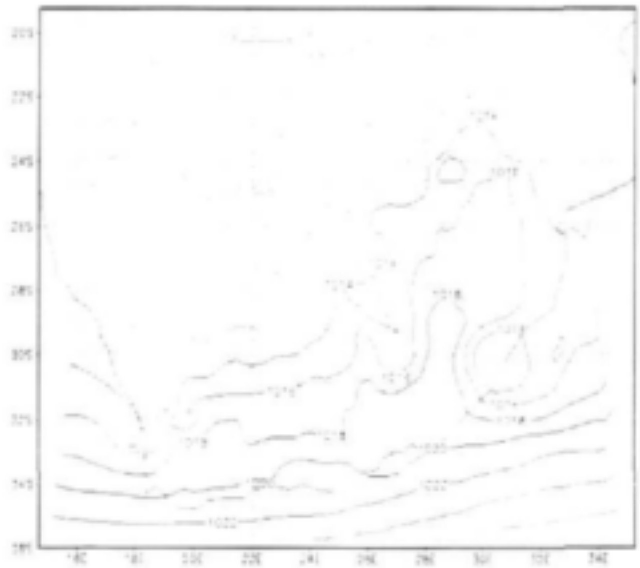

Figure 6.7(a): MM5 prognosis for the sea level pressure for the 20th March at 1200 UTC for Run2.

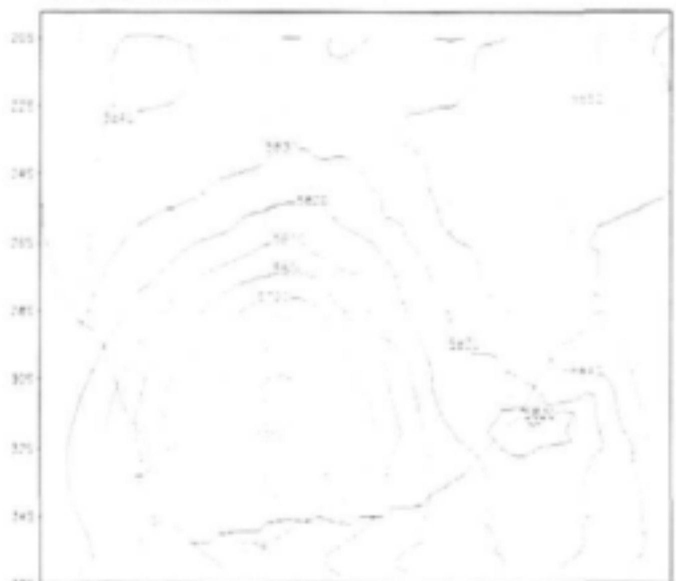

Figure 6.7(b): MM5 prognosis for the 500hPa heights for the 20th March at 1200 UTC for Run2.

In order to investigate the effects of this low on the rainfall, the 6-hour difference map, (6-hour satellite accumulation subtracted from the 6-hour accumulated rainfall forecast) from 0600 UTC to 1200 UTC, for the 20th (Fig. 6.8) was analysed. This figure shows that the model over forecast up to 150mm of rain in the region of the low. The cyclonic curvature of the low can also be identified by the rainfall in figure 6.8 over southern KwaZulu-Natal. The model prognosis indicated the development of this low, which did not occur in reality; and this low had a major effect on the model's rainfall forecast over the area.

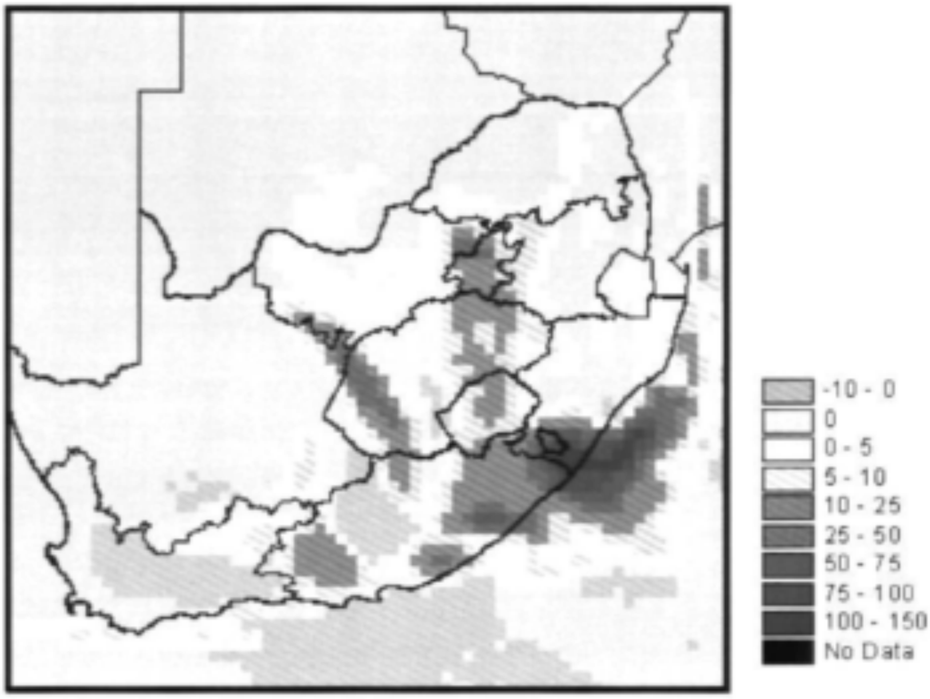

Figure 6.8: Difference between MM5 and satellite 6-hr rainfall accumulations, from 0600 to 1200, UTC on 20 March 2003, for Run2.

The adjustment method described in paragraph 6.3 was applied to RUN1 and RUN 2. The results for the adjusted MM5 QPFs are shown in figures 6.9 and 6.10. When comparing the adjusted (Fig. 6.9) and unadjusted (Fig. 6.3a) 24-hour forecasts for Run 1, the most striking difference is the heavy rainfall that has been removed from the KZN south coast in the adjusted forecast. After the adjustment between 25-75mm is now forecast for this coast where before the adjustment the rainfall prediction was in the vicinity of 200mm. Similarly (Fig. 6.10 and 6.4a), there is a dramatic reduction of rainfall over the coastal areas of KwaZulu-Natal, for the period of Run 2. However, very heavy rainfall is still forecast for the coast of KZN, even after the adjustment.

The RMSE results for the adjusted and unadjusted 24-hour rainfall forecasts are indicated in Table 6. These results indicate that on both days, there was an improvement of over 5 mm, over the entire grid. The results also show that the average error over the grid was greater for Run 2 than for Run 1. However, the improvement was also greater over the period of Run 2.

Table 6: RMSE of adjusted and unadjusted rainfall forecasts for the 18th and 19th March 2003.

Date	Unadjusted	Adjusted	Improvement
Run1	20.18 mm	14.94 mm	5.24 mm
Run2	25.03 mm	19.19 mm	5.84 mm

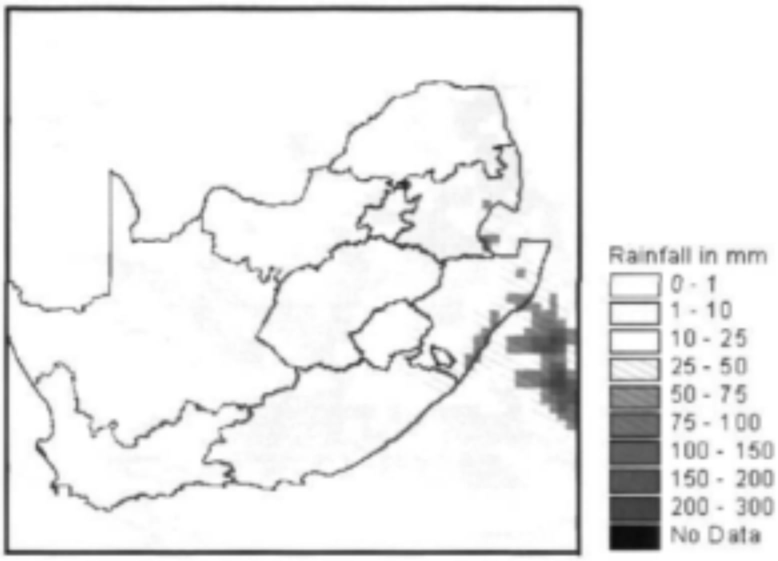

Figure 6.9: Adjusted 24-hour model forecast for Run1.

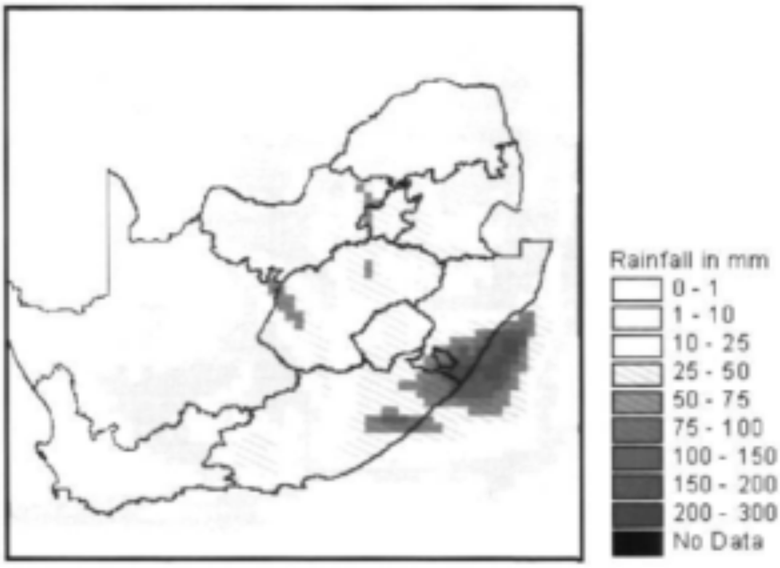

Figure 6.10: Adjusted 24-hour model forecast for Run2.

6.5 Conclusions

The rainfall prognoses from the MM5 model run for the two case studies were not accurate and provided unrealistic rainfall figures over the East Coast. After adjusting the MM5 rainfall prognoses with satellite rainfall the errors were somewhat diminished.

The method of adjusting the rainfall of a NWP shows some promise. It is possible to obtain NWP rainfall prognoses of a higher quality. The launch of the Meteosat Second Generation satellite and improved RADAR coverage over South Africa will also provide observed rainfall fields of a higher quality. Provided the observed rainfall fields are available in time steps of 3-6-hrs this method could aid in providing predicted rainfall fields of a high quality.

CHAPTER 7

OPERATIONAL IMPLEMENTATION OF HEAVY RAINFALL IDENTIFICATION SYSTEMS

This chapter briefly describes the operational implementation of the heavy rainfall identification systems. All products are available for the weather forecasters of the South African Weather Service and run on the prognostic fields of the Eta model. The products were originally made available on PCGRIDDS display software available to the forecasters. Due to limitations in PCGRIDDS the products are currently available on the SAWS web site for use and display by the forecasters in Pretoria and the regional offices. A large amount of graphics are available on the web site and only a few selected fields are displayed here as illustration. The web site is available on the intranet of the SAWS.

The details of all the heavy rainfall identification systems are provided in Chapter 4 and will be summarised here.

7.1 Heavy rainfall identification systems

The first product available for operational use is the Tropical Heavy Rainfall Identification System THERIS. This system isolates summer heavy rainfall over the interior of South Africa.

The coastal zone heavy rainfall identification systems are available for the different coastal zones of South Africa. The criteria used for the different coastal zones are detailed in Chapter 4 but they all have common features:

- A product which simulates heavy rainfall due to surface forcing
- A product that utilizes the vertical velocity of the Eta model.
- A product that uses the Eta model precipitation forecast

7.2 Operational implementation on PCGRIDDS

PCGRIDDS is currently being used in the SAWS forecasting offices to display NWP products. PCGRIDDS is useful as it allows the weather forecaster to display or manipulate the NWP fields without too much trouble. However, the PCGRIDDS software has some limitations. It does not allow for the full data set available from the Eta model to be ingested.

This means that only a limited number of variables are available. In addition PCGRIDDS cannot display all the available data on all the pressure levels. The problem is exacerbated at the regional offices due to a limit on the file size that can be transmitted to the regional offices. This results in even fewer variables and vertical levels being available at the regional forecasting offices. Nevertheless due to the forecasters' familiarity with PCGRIDS the heavy rainfall systems were made available in this format.

The following products are available on PCGRIDDS

1. MITS (Model for the Identification of Tropical Weather Systems).
2. THERIS
3. BARCOZ

In these products the atmospheric variables which make up the heavy rainfall identification system are displayed first and then finally a field that shows the heavy rainfall forecast area is displayed. The forecasters can display this at 6-hr intervals up to 48-hrs or may choose to display a single 24-hr heavy rainfall forecast field. It was considered wise to provide the atmospheric flow fields, which make up the criteria of the heavy rainfall identification systems and not to provide only the heavy rainfall forecast as a single end- product or black box. It must be remembered that the forecasters are all scientists, some with many years of experience and that they need to know precisely what they are dealing with. Having access to all the fields and criteria builds confidence when and if the forecaster has to subjectively decide to accept or reject the forecast.

7.3 Operational implementation on the SAWS web

In addition to the limitations of PCGRIDDS detailed above, PCGRIDDS is not a good research tool. It is extremely difficult, for instance, to isolate the coastal zone or the area where the model topography is less than 800m. It was therefore decided to do all development with the display system GRADS and to make all the relevant images available on the SAWS web site. This allows for all the Eta variables used in the heavy rainfall identification systems and at all 19 vertical pressure levels as well as the products derived from these fields to be available at all the forecasting offices in South Africa. Water managers should, prior to the use of the products, receive some basic training.

The procedure to make the heavy rainfall product available is:

1. The required Eta variables are ingested into a file, which can be manipulated by GRADS.
2. GRADS scripts are run and the relevant images are created.
3. The images are written to the appropriate directory on the SAWS computers and are available to view on a web site.

This entire procedure is automated and the updated images on the web site become available after the conclusion of the 0000UTC Eta model run. At present data is only available for the 0000UTC run and only for 30-hrs ahead. This can easily be expanded to include the 1200UTC run and the entire 48-hr forecast.

7.3.1 Theoretical basis

The first page on the web site gives a summary of the dynamical and thermodynamical variables used in a forecasting environment. They are:

- Cartesian co-ordinate system
- Isobaric co-ordinate system
- The continuity equation
- Hydrostatic equation
- Hypsometric equation
- Baroclinicity
- Wind divergence
- Moisture flux convergence
- Mixing ratio and saturated mixing ratio
- Relative humidity
- Precipitable water
- Topographical uplift

These topics are made available to demonstrate the theoretical principles used in identifying the atmospheric criteria, which forms part of the heavy rainfall identification systems.

7.3.2 Regional stations

Separate products were developed for all the forecasting offices in South Africa. These products are tailor-made for the area of responsibility of a forecasting office and were chosen in collaboration with the forecasters from the relevant office. All products are available from

0600UTC on the current day to 0600UTC on the following day. The products include predicted heavy rainfall fields for the 24-hr period or animations which provide detail for every 3-hrs. The following products are available for the different offices.

a. *Cape Town*

i. 24hr heavy rainfall fields

The surface forced heavy rainfall identification system as well as the heavy rainfall prediction using vertical velocity less than –1 Pas^{-1} is displayed (details in Chapter 4).

ii. 24hr Eta precipitation

The statistical results as detailed in Chapter 5 are also summarised and displayed together with the heavy rainfall forecast. This gives the forecaster some guidance on the accuracy of the forecast and the average rainfall associated with the different heavy rainfall forecasts.

iii. Animations

- Surface forced heavy rainfall

The appropriate atmospheric fields, which form the ingredients for the heavy rainfall identification system are displayed at 3-hr intervals. The forecasters may then determine the time during this 24-hr period when heavy rainfall is likely to occur. Figure 4.3d depicts the heavy rainfall forecasts on the 10th of June 2000.

- The 1000-300hPa precipitable water

This field is animated simultaneously with the sea level pressure and the 3-hr precipitation forecast. An example of this is provided in figure 4.3b.

- Topographical uplift

The topographical uplift is displayed simultaneously with the surface wind barbs in knots. Figure 3.16b shows the topographical uplift on the 10th of June 2000.

- Vertical cross section at 34°S, 32°S and 19°E

Vertical cross sections from 1000 to 400hPa are displayed where relative humidity, horizontal wind divergence and vertical motion (Pas^{-1}) are depicted. This field is especially useful over the Cape Peninsula as it shows the movement from the west of weather systems responsible for rainfall. An example of a vertical cross section at

32°S is provided in figure 7.1. Significant values of vertical velocity are plotted in bold in order to focus the forecasters' attention on this.

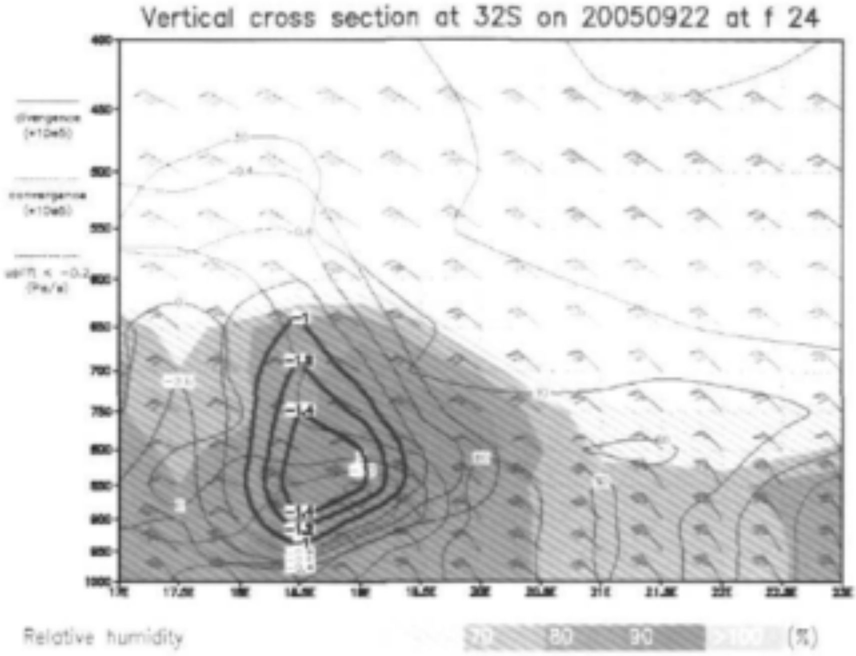

Figure 7.1: Vertical cross section at 32°S and from 17°E to 23°E on the 10th of June 2000. The figure shows the relative humidity (%), horizontal wind divergence (*10^5 s^{-1}) and vertical velocity (Pas^{-1}).

b. *Durban*

i. 24hr heavy rainfall fields

An example of a heavy rainfall forecast is provided in figure 4.4b on the 4th of April 2000.

ii. 24hr Eta precipitation

iii. Time sections near coastal cities Margate, Durban and Richards Bay as well as near the inland towns Vryheid, Jozini, Giants Castle and Ladysmith.

These fields are vertical cross sections where the location is fixed but the time varies. Over the interior the height of the freezing level is also available to facilitate the forecasting of snow. An example of a time section at Vryheid on the 8th of August 2001 is shown in figure 7.2. Note how the height of the freezing level drops significantly between 1500UTC and 1800UTC. A similar field is available in the PCGRIDDS software and is very popular with the weather forecasters. However, as *all the Eta prognostic fields and vertical levels are incorporated, detail is provided here which is not available in PCGRIDDS.*

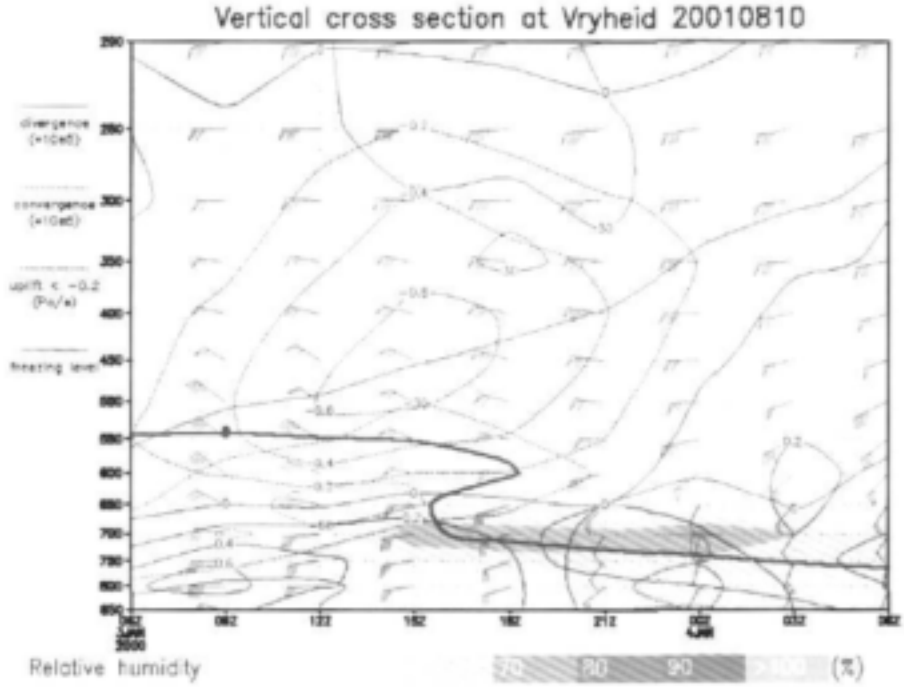

Figure 7.2: Time section at Vryheid on the 10th of August 2001. The figure shows the relative humidity (%), horizontal wind divergence ($*10^5\ s^{-1}$), vertical velocity (Pas^{-1}) and the height of the freezing level.

iv. Animations

- The 1000-650hPa precipitable water

An example is provided in figure 4.4c for the 4th of April 2000.

- The 850-300hPa precipitable water

This field is displayed together with the 500hPa geopotential heights and 700hPa vertical velocity. The precipitable water between 850-300hPa is displayed as it gives a more appropriate representation than including the values in the layer between 1000 and 850hPa over the interior of South Africa. Figure 7.3 depicts these variables on the 4th of April 2000

- Topographical uplift

The escarpment rises very quickly over the interior of KwaZulu Natal and the 1000-950hPa winds are not considered ideal to use here. The Eta model provides 10m *horizontal winds and the wind barbs plotted on this figure are the 10m winds and not the average 1000-950hPa winds as were used over the Cape Town area.*

- Vertical cross section at 34°S
- Vertical profiles of vertical velocity and horizontal wind divergence near Margate, Durban and Richards Bay

The surface-forced heavy rainfall forecasts are generated using these two variables and the forecaster may determine when the favourable conditions occur for heavy rainfall.

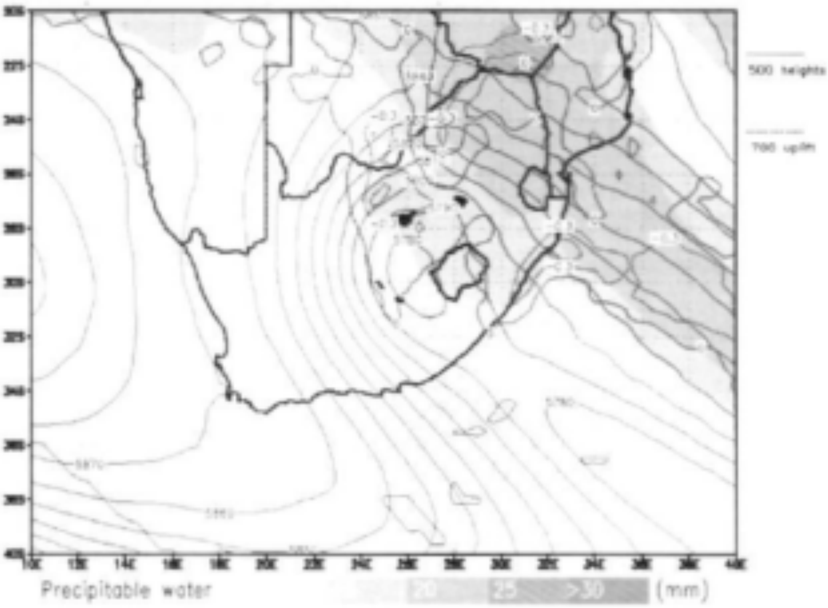

Figure 7.3: The 850-300hPa precipitable water (mm), the 500hPa geopotential heights (gpm) and 700hPa vertical velocity (Pas^{-1}) on the 4[th] of April 2000.

c. *Port Elizabeth*

The same fields are available for the Port Elizabeth forecasting office but the vertical cross sections were done near George, Port Elizabeth, East London and Port St Johns along the coast as well as near Queenstown, Umtata, Lady Grey and Graaff-Reinet.

d. *Pretoria*

The forecasters in Pretoria have to issue forecasts for the whole of Southern Africa but they are also responsible for generating specific forecasts for the four northern Provinces of South Africa. Designing useful products for the Pretoria office was a considerable challenge. Several products are nevertheless available and figure 7.4 depicts the THERIS forecast for the 10th of February 2000.

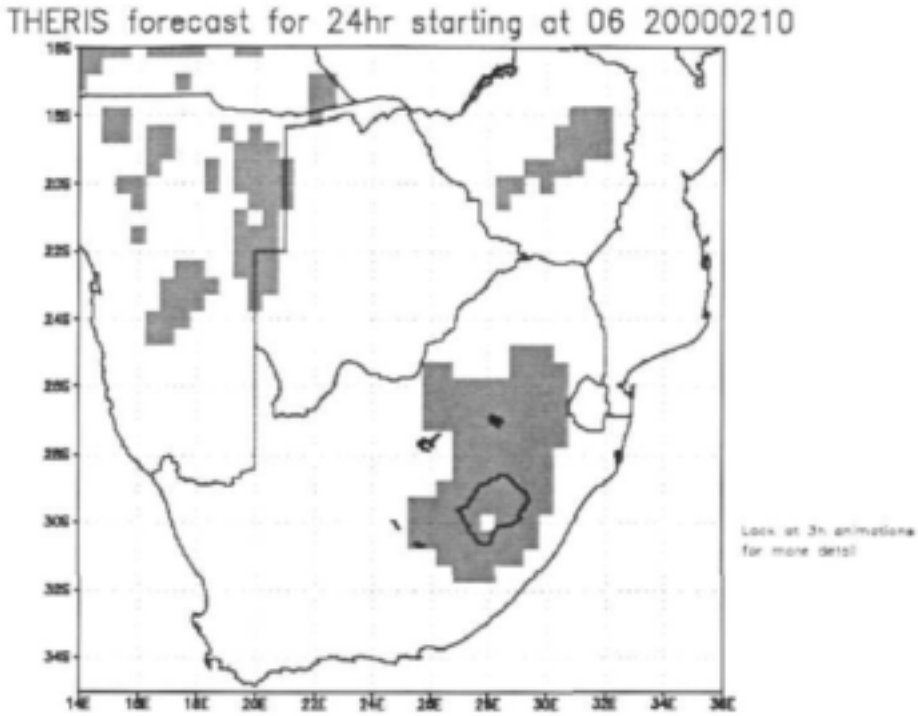

Figure 7.4: THERIS heavy rainfall forecast on the 10th of February 2000

7.4 Concluding remarks

Providing atmospheric variables on the Internet has several advantages. The Internet is available nearly everywhere and provided that limited infrastructure exists the fields are available almost instantaneously. This is especially important for countries in Africa that are not capable of accessing NWP fields by other means.

In this research the products were designed with the active participation of weather forecasters and were designed to provide new and ready-made forecasting products. The heavy rainfall identification systems are available for operational use, research and experimentation. It is also relatively easy to add additional forecasting products. An example of this is the experimental snow forecast developed by Mr. L Fernandes and M Todd (Fig. 7.5).

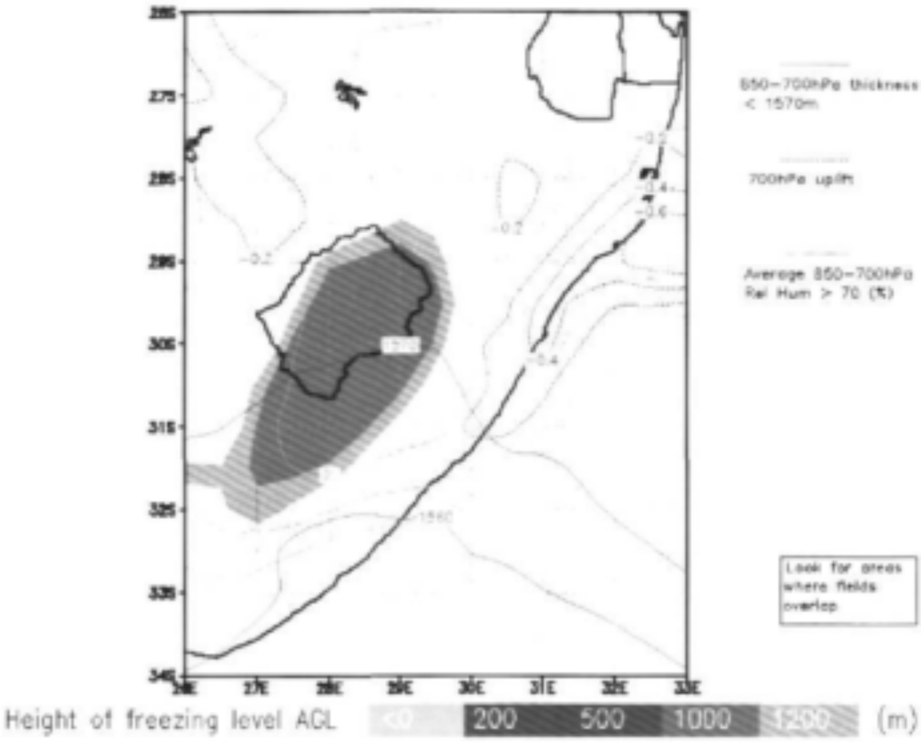

Figure 7.5: The height of the freezing level AGL (m), the 850-700hPa geopotential thickness (gpm), 700hpa uplift (Pas^{-1}) and the average 850-700hPa relative humidity (%) on the 4th of April 2000.

CHAPTER 8

CONCLUSIONS

For the convenience of the reader the main aims of the project as well as the secondary aims as agreed to by the WRC Steering Committee will be briefly detailed below followed by a report on how these aims were met. The work was performed in terms of a contract between the University of Pretoria and the Water Research Commission referred to as: **WRC RESEARCH PROJECT NO. 1333 (PROGRAIN).**

8.1 Aims of the Project

The main aim of this research was the production of a predicted rainfall field over southern Africa for a period 6 to 48 hours ahead.

In order to achieve this goal, secondary aims of the project were defined.

- Isolate heavy rainfall in specific weather systems
- Model the enhancement of heavy rainfall by steep orography
- Perform model ensemble rainfall forecasting
- Incorporate observed rainfall rates
- Hold workshop(s) to disseminate the knowledge gained.
- Develop an operational rainfall forecast verification scheme.

The WRC Steering Committee (15 July 2003) agreed that the secondary goal 'Model ensemble rainfall forecasting' be dropped. This step was necessary because the funding approved by the WRC was considerably less than the original amount requested. This also had an effect on some of the other secondary goals in that all were not completed as originally planned. This in part also holds true for the development of the operational rainfall forecast verification scheme. Some preliminary work was done but an operational verification system was not completed.

Weather systems causing heavy rainfall along the coastal plains and adjacent escarpment of South Africa were the main focus of this research. The weather systems are extra tropical cyclones and the ridging Atlantic Ocean High. These surface weather systems may or may not be accompanied by an upper air trough or even a COL. The initial research was conducted on NCEP data and the heavy rainfall identification systems had to be implemented and tested on the prognostic fields of operational NWP models. This was a considerable challenge. Analysis of the MM5 prognosis revealed serious problems along the escarpment of South Africa and this data set had to be abandoned. The SAWS Eta model was consequently used. Obtaining the archived data from the SAWS and developing the software to write the data into a format for manipulation in GRADS was a very time consuming exercise. The work program did not make adequate provision for this process. This resulted in not all the weather systems stipulated in the research proposal being investigated. Nevertheless, a thorough investigation was completed on coastal zone heavy rainfall using the prognostic fields of the Eta model.

8.2 General concluding remarks and recommendations

A system exists which can delineate areas where heavy rainfall can be expected with a considerable degree of accuracy. All the components of these systems are based on well-proven meteorological dynamics but depend on the accuracy of the data fields generated by the analyses or prognoses using NWP models. This heavy rainfall identification and forecasting system consists of computer programs combining and applying atmospheric dynamic concepts to the data. These programs are able to synthesize many variables and parameters derived from the data. To integrate all this information in the short time available is beyond the capacity of a meteorologist.

All the heavy rainfall identification systems were developed for the operational meteorologist and delineate areas of possible heavy rainfall. The systems use the prognostic fields of the Eta model and products are made available for use anywhere over the Eta domain by disseminating them through the web site of the SAWS. Countries to the north of South Africa can benefit by this, especially for the prediction of tropical heavy rainfall.

THERIS (tropical heavy rainfall identification system) was adapted to run on the Eta model. Verification of THERIS for three summer seasons on the Eta model prognosis revealed that THERIS is capable of pinpointing heavy rainfall from tropical weather systems.

Coastal zone heavy rainfall identification systems were developed for three coastal areas of South Africa: the South West Coast, the South Coast and the East Coast. A thorough investigation into the prognostic fields of the Eta model revealed that the atmospheric flow fields are simulated very well over the South West Coast but the model does not fare as well over the South and East Coast. This is possibly due to the way the Eta model handles the topography. However, by identifying the appropriate variables in the Eta model prognosis, heavy rainfall identification systems were developed for all three areas. The criteria used to isolate heavy rainfall are season and area dependent. It was also shown how Eta model variables such as vertical velocity or the rainfall prognosis could be used to aid in the identification of heavy rainfall areas.

The atmospheric variables used in the coastal heavy rainfall identification systems are all in the lower levels of the atmosphere. A variable, not directly available from the Eta model output, referred to as the topographical upward motion, was developed. The topographical upward motion simulates the upward motion forced by the surface wind blowing against the topography. This 'new' variable forms an important part of the coastal heavy rainfall identification systems.

It was demonstrated how the Eta model upward motion and wind convergence all below 800hPa are important for the formation of heavy rainfall along the coast. The operational meteorologists do not often refer to variables at the 950 or 900hPa pressure levels when forecasting heavy rainfall. This research has shown that heavy rainfall along the coast is often associated with large values of wind convergence and vertical upward motion at these levels. It is important that the weather forecaster has access to the entire Eta data set or that the relevant and important atmospheric variables in the production of heavy rainfall are displayed adequately. The operational products from this research endeavours to do exactly this. It was shown how along the East Coast and South of South Africa upward motion of -0.5 Pas^{-1} is a good predictor for heavy rainfall. In the current display system, PCGRIDDS, the variables at 950hPa are not available.

All systems were originally developed on NCEP data and the verification results show a good performance in identifying heavy rainfall areas. Applying these systems on the prognostic fields of the Eta model did not always give the same positive results. Some insight was gained into the differences between the data sets and the significant influence the horizontal resolution has in computing variables such as divergence or vertical velocity where spatial derivation is required.

All heavy rainfall identification systems are available on the SAWS web site for use in the forecasting offices in South Africa. In addition to the heavy rainfall forecasts extra forecasting products were developed for use at the regional offices in South Africa. This was done in consultation with the weather forecasters, which ensured their active participation in the project. The visit of Ms Liesl Dyson to all the offices was useful and provided some insight into the forecasting needs and challenges over the different areas of South Africa.

Students at the University of Pretoria undertook several research projects during the duration of the PROGRAIN project (Chapter 6 and 7). The SAWS employed most of these students as weather forecasters. The involvement of the young forecasters in the successful implementation and use of the heavy rainfall identification systems cannot be stressed enough. They were exposed to these systems as students, they conducted research as part of this project and they are now the individuals in the different forecasting offices who use the products.

An extensive data archive was created. The daily Eta model prognosis, NCEP data and SAWS gauge rainfall were obtained for September 1999 to March 2002. All these data were written into GRADS format and can be used readily.

All heavy rainfall systems were verified for the period between September 1999 and March 2002. The Eta model precipitation forecast was also validated for the same period. The heavy rainfall systems all have some skill in predicting heavy rainfall. The best results were achieved over the South West coast in winter but THERIS also fared well in identifying heavy rainfall days over the interior in summer. In the final operational product available to the weather forecaster on the SAWS web site, a summary is provided of the statistical results for all the different heavy rainfall systems. By providing these products the weather forecaster will have an understanding of the quality of these systems for past events.

The Eta model 24-hr precipitation forecast is available on the SAWS web site. However the preparation of a proper quantitative precipitation forecast (QPF) proved not to be possible in this project. Uncertainty about the accuracy of the Eta rainfall prognosis prevented the creation of a reliable first guess rainfall field. In future improved NWP generated rainfall fields could serve as a basis in the creation of a QPF. A method was explored to adjust the precipitation forecast of a NWP model by incorporating real time precipitation data. This method showed some potential and it is recommended that experiments be conducted into combining the SIMAR rainfall fields and the Eta model rainfall prognosis.

This research endeavoured to identify areas of heavy rainfall objectively. This required a thorough analysis of the prognostic fields of the Eta model and in this way some of the strengths and weaknesses were identified. Atmospheric variables associated with heavy rainfall were identified, some of them new and some on levels not commonly used by weather forecasters. Research of this nature serves a very important purpose in the weather forecasting process. The weather forecasters may grow to understand the strengths and weaknesses of the model better or they are encouraged to explore new variables. Objective systems such as the products developed here serve an important purpose. However, it is the opinion of the authors that no objective system can ever replace the subjective interpretation of an experienced weather forecaster.

Research results to pinpoint heavy rainfall from baroclinic systems, but well inland, were disappointing. It is speculated that summer continental baroclinic systems are modified by daytime convection and develop many features typical of tropical systems. The tropical temperate trough (TTT) may be an example of a mixed tropical, baroclinic system, producing considerable rainfall, yet not easy to detect with THERIS. The project was too short and not enough data on continental systems were available to develop a heavy rainfall detection system suitable for the TTT and other continental baroclinic systems. However, results from BARCOZ, analysing particularly active baroclinic systems, indicate that the convergence of water vapour and vertical motion remains fundamentally important. Preliminary results also indicate further research on these systems should consider atmospheric stability and related factors.

The SAWS appreciates the value of these products and they are already being used in Pretoria, Cape Town, Durban and Port Elizabeth. Finally, it is our belief that the output fields of this system should be disseminated to the Department of Water Affairs, Flood Management Group for independent evaluation and in time perhaps also to some civil authorities and Disaster Prevention Groups.

8.3 The way forward

In order for the heavy rainfall identification systems to come to its full use, the support of the weather forecasters as well as of their managers is required.

The Internet provides a powerful tool for the dissemination of NWP products and this should be explored further and additional products developed.

The following research projects and development tasks deserve urgent funding:

- Development of an "operational" heavy rainfall prediction scheme that specialises in continental weather systems with mixed (baroclinic/tropical) properties. The extensive experience gained during this project indicated that this is indeed possible and advantageous. This should be started as soon as possible.

- The current operational NWP models at the SAWS do not predict convective rainfall adequately. Research is required to optimise the output of the available NWP models to predict convective precipitation better.
- Research during the PROGRAIN project had also indicated that heavy rainfall prediction is region dependant. It is proposed that a project be funded to regionalise the prediction system and at the same time to target specific areas such as: the Umgeni river catchment; the Vaal river catchment; the Breede river catchment as well as smaller regions with large urban settlements such as Gauteng Province. If this work is funded it will be important to involve Water and Disaster Mitigation managers right from the start.
- It is a simple fact that the quality of heavy rainfall precipitation products is all utterly model dependant. It is therefore vitally important that the developers of the current products have the means and the support to update and improve the systems when new model updates are implemented.
- During the course of the PROGRAIN excellent rapport was established with Managers and Forecasters of the SAWS. All steps should be taken to continue this and to extend this to other Water Managers.
- One of the student projects explored the interactive modification of the model's rainfall prognoses using satellite data. Results were very promising and it is important to develop this, using the full SIMAR product, into an operational rainfall prognoses modification scheme. This can then become part of the greater operational rainfall systems.
- Operational rainfall prediction evaluation schemes should be developed alongside the proposed new heavy rainfall systems.
- One of the principal disappointments was that the NWP model predictions of the lower troposphere's flow fields did not allow the important principle of water vapour convergence to come to its right. With the new generation of regional NWP models becoming available this aspect needs to be re-visited.

The authors are convinced that large advances were made and that this project was a very cost effective effort and delivered a useful product to the benefit of all the country's citizens.

CHAPTER 9

CAPACITY BUILDING

This project provided opportunities for Capacity Building. However the nature of the research determined that the involvement of previously disadvantaged persons was limited to students in meteorology at the University of Pretoria as well as weather forecasters from the South African Weather Service.

9.1 Individuals

Table 9.1 lists the individuals who have completed research projects under the auspices of the PROGRAIN project from 2002 to 2005.

Ms H.G. Marx, co-author of the WRC project FORFLOOD (Dyson et al, 2002), was the principal author of a research article published in the WATER SA in 2003. Details are provided in section 9.3.

Table 9.1: Individuals who completed research projects for the PROGRAIN project.

Name	Degree	Gender	Previously Disadvantaged	Outputs
H. G. Marx (Pretoria)	BSc (Hons) Meteorology (2000)	Female	No	Publication Water SA 2003
L. Clark * (Pretoria)	BSc (Hons) Meteorology (2002)	Female	No	SASAS 2002
A Moatse * (Pretoria)	BSc (Hons) Meteorology (2002)	Male	Yes	SASAS 2003
L Burger (Cape Town)	BSc (Hons) Meteorology (2003)	Female	No	SASAS 2003
L Fernandes * (Pretoria)	BSc (Hons) Meteorology (2003)	Male	No	SASAS 2003
L. Masimini (Port Elizabeth)	BSc (Hons) Meteorology (2004)	Male	Yes	SASAS 2002 & 2003
M Roux (Durban)	BSc (Hons) Meteorology (2004)	Male	No	SASAS 2003
M Martin	BSc Meteorology (2004)	Female	No	SASAS 2005

During the three-year period of the PROGRAIN project several students completed research projects. This research was done as part of the requirements for a B.Sc or B.Sc (Hons) Meteorology degree (Table 9.1). *All these projects resulted in presentations at the South* African Society of Atmospheric Sciences conferences. Full details are given in section 9.3.

The research conducted by Mr Masimini (Chapter 3) and Mr Fernandes (Chapter 6) forms an important part of this research report while Chapter 9.4 details the research results of the remainder of the students. Ms Martin is currently completing her B.Sc (Hons) Meteorology degree; the remainder of the individuals listed in Table 9.1 are all currently employed as weather forecasters or researchers at the South African Weather Service. The involvement of the weather forecasters greatly facilitated the operational implementation of the heavy rainfall identification systems at the SAWS. The research conducted as part of PROGRAIN also resulted in three of these individuals (asterix, table 9.1) being employed by the University of Pretoria as part time lecturers.

Table 9.2: Individuals who completed the Classical Weather Forecasting Techniques course.

Name	Degree	Gender	Previously Disadvantaged
C. Fillis R Malala M Motsepe T Nethavhani N Ngubo	BSc (Hons) Meteorology (2002)	Male Male Male Male Male	Yes Yes Yes Yes Yes
SJ Gaebee D Makhubele MP Mbedzi SI Mbuya TM Moloi H Mtongori T Ndarana AR Nduganda TI Ngwana HO Senga	BSc (Hons) Meteorology (2003)	Female Male Male Male Male Female Male Male Male Female	Yes Yes Yes Yes Yes Yes Yes Yes Yes Yes
NS Nake M P Todd D van der Mescht	BSc (Hons) Meteorology (2004)	Female Male Male	Yes No No
S Du Toit A E Ramulifho L N Somazembe. M A Tladi M S Tshifaro	BSc (Hons) Meteorology (2005)	Female Male Female Male Male	No Yes Yes Yes Yes

In addition to the individuals who conducted research as part of the PROGRAIN project table 9.2 lists the individuals who completed the subject WKD 715: Classical Weather Forecasting Techniques from 2002 to 2005. The content of this honours course contains the research results from the PROGRAIN project and the students benefited directly by being exposed to recent research findings. The students were exposed to these components and they were taught the atmospheric dynamics behind them all. In this way they gained deeper understanding of the atmospheric circulation features, which cause copious rainfall. The systems will remain a component of the forecasting course and in this way ensure that future forecasters will have the competence to make full use of the systems developed. The course material for the 2005 class is taken directly from the operational web site described in Chapter 7. Mr Fernandes and Mr Todd designed an experimental snow forecasting method. This product is also available operationally on the SAWS web site.

The individual forecasters in Pretoria, Cape Town, Durban and Port Elizabeth also benefited by a series of talks, which explained the fundamental principles, which underlies the heavy rainfall identification systems.

9.2 Institutions

9.2.1 University of Pretoria

The University of Pretoria has benefited from this project in numerous ways. The financial assistance has ensured the employment of research assistants, who played an invaluable role in the success of the project. The research results obtained have influenced the course content of subjects presented at the honours level considerably and have helped to maintain an internationally recognised standard. This in turn has ensured a continued growth in the student numbers at the honours level and establishment of contact with weather services in Southern Africa and abroad.

During August and September 2004 Ms Liesl Dyson visited the National Severe Storm Laboratory (NSSL) in the USA as well as the University of Alberta in Edmonton, Canada. Dr Harold Brooks was her host at the NSSL where she had opportunity to interact with the researchers as well as forecasters in the Storm Prediction Centre (SPC). The interaction between their researchers and forecasters is excellent. Each year there is a Spring Program where new research is introduced and tested in the forecasting office. The researchers in turn receive immediate feedback from the forecasters to improve and change techniques in relation to forecasting severe weather. The heavy rainfall forecasting techniques developed as part of this WRC project were presented to the staff of the NSSL and in subsequent discussions, useful advice was given especially in the verification of heavy rainfall. This contributed to a paper on THERIS, by the co-project leaders, being accepted for publication in the prestigious journal Weather and Forecasting, published by the American Meteorological Society.

Mr Julian Brimelow (ex University of Pretoria student, now Research Meteorologist at the University of Alberta) hosted Ms Dyson in Canada where useful discussions ensued about the forecasting of severe storms as well as forecasting techniques best suited for mountainous terrain. Mr Brimelow also serves as external examiner in the subject Classical Weather Forecasting techniques.

9.2.2 South African Weather Service

The research results emanating from this project have also directly profited the SAWS. The weather forecasting students (potential SAWS employees) completing the honours course have been trained in the latest available techniques.

Chapter 8 details the operational heavy rainfall identification systems. All these forecasting products are now available operationally on the SAWS web site. On request of the weather forecasters from the regional offices product were specifically designed for use in the appropriate area of South Africa. These products are new.

Ms L Dyson visited all the forecasting offices in South Africa where the weather forecasters were trained in the use of the heavy rainfall identification systems.

During 2004 a series of talks were given to the forecasters in Pretoria. On the advice of Ms De Coning the same lecture was given twice a week in order to reach all the forecasters who work in shifts. In total 10 lectures had to be given. Mr Ndambambi, Mr Hunter and Ms De Coning all went to great lengths to ensure the full participation of the forecasters. Some of the heavy rainfall identification systems became operational during 2004 on the software PCGRIDDS. The feedback from the forecasters has generally been positive and it is especially the younger forecasters (listed in table 10.1 and 10.2) who used these systems frequently and operationally. It appears that the THERIS product was not used as extensively as the BARCOZ product, probably because baroclinic systems linked to the mid-latitude westerlies are more frequent over South Africa.

During August 2004 Ms Dyson visited the Cape Town, Durban and Port Elizabeth regional forecasting offices. Using the same approach as in Pretoria, she visited the forecasting offices on two consecutive days in order to train all the weather forecasters. Mr Pretorius (Durban), Mr Stander (Cape Town) and Mr Van Niekerk (Port Elizabeth) were extremely helpful during these visits and ensured the full participation of all the weather forecasters. The rationale was to start off with some basic factors and theory and then work towards the heavy rainfall systems. In this way the dynamical principles of the heavy rainfall systems became familiar to the forecasters. The interaction with the forecasters was very good and some lively debate ensued regarding the interpretation of some of the variables.

9.3 Conferences and articles

The following research products resulted from the PROGRAIN research project

2002

1. Dyson L.L and van Heerden (2002) A Model for the Identification of Tropical Weather Systems. *Water SA*, **28** No. 3, *249-258pp* .
2. Clark L and Dyson L.L. (2002) Forecasting heavy rainfall over the Southwestern Cape: A case study. *18th Annual conference of the S. Afr. Soc. Atmos. Sci.*
3. Masimini L and Dyson L.L. (2002) The Retrograding Cut-Off Low of the 25 January 1981. *18th Annual conference of the S. Afr. Soc. Atmos. Sci.*
4. Van Heerden J and Dyson LL (2002). Relationship between water vapour convergence and vertical motion during large scale heavy rainfall events. *18th Annual conference of the S. Afr. Soc. Atmos. Sci.*

2003

1. Marx H.G., Dyson L.L. and van Heerden J. (2003). Verification of Rainfall Forecasts for the Vaal Dam Catchment for the Summer Rainfall Seasons of 1994 to 1998. *Water SA*, **29** No. 2, 195-200.
2. Burger, L. & Dyson, L.L 2003: Localised flooding over Gauteng in December 2002. *19th Annual conference of the South African Society of Atmospheric Sciences.*
3. Dyson, L.L. 2003: Verification of heavy rainfall identification systems. *19th Annual conference of the South African Society of Atmospheric Sciences*

4. Fernandes, L. & Dyson, L.L. 2003: Comparison Between SIMAR Rainfall and MM5 Rainfall Prognosis for The Rainfall, March 2000. *19th Annual conference of the South African Society of Atmospheric Sciences*

5. Masimini, L. & Dyson L.L. 2003: Improving A Heavy Rainfall Forecasting Systems Along The South East Coast. *19th Annual conference of the South African Society of Atmospheric Sciences*

6. Moatshe, A.B. & Dyson, L.L. 2003: Heavy rainfall along the south-east and the east coast during the period 15th to 20th July 2002. *19th Annual conference of the South African Society of Atmospheric Sciences.*

7. Roux M.S. & Dyson, L.L. 2003: Severe Thunderstorm Environments Over South Africa. *19th Annual conference of the South African Society of Atmospheric Sciences*

8. Van Heerden J 2003. Predicting heavy rainfall with the MM5 model. *19th Annual conference of the South African Society of Atmospheric Sciences.*

2005

1. Dyson L.L and van Heerden 2005. A Tropical Heavy Rainfall Identification System. *Article accepted for publication. Weather and forecasting*

2. Martin M.S. and Dyson L.L. 2005. Widespread Heavy Rainfall in the Drakensberg Mountains. *21st Annual conference of the South African Society of Atmospheric Sciences.*

9.4 Student Contributions

A number of students made use of the opportunity this project provided to do research and contributed to the achievement of the aims of this project. The most important results and contributions beneficial to this project are reported here. Students who conducted research under the direction of the Project Leader during the course of the project are:

Ms Lee-Ann Clark	UP/SAWS
Mr Abel Moatshe	UP/SAWS
Ms Lynette Burger	UP/SAWS
Mr Marcel Roux	UP/SAWS
Ms Melissa Martin	UP
Mr Luthando Masimini	UP/SAWS
Mr Luis Fernandes	UP/SAWS

The ingenious concept developed by Mr. Luthando Masimini is reported fully in Chapter 3. The important research on adapting the MM5 rainfall prognoses by using satellite imagery by Mr. Luis Fernandes forms Chapter 6. Research by most of the other students contributed to the project in a more indirect way. Several interesting heavy rainfall case studies were completed and are reported here in a very condensed manner.

9.4.1 Severe rain caused by cyclogenesis

(Contribution by Ms L Clark)

9.4.1.1 Introduction

During the 3rd July 2001 Cape Town experienced the wettest conditions in 44 years (Pretoria News, 2001). During a week of continuous rainfall, 250 homes in the Gugulethu and KTC informal settlements were flooded, and 3500 people were displaced (Star, 2001). Again on 22 July 2001, more than 1300 people were displaced and 295 shacks destroyed by yet more flooding in Cape Town (Pretoria News, 2001). A map of the rainfall distribution on the 3rd July is given in figure 9.1.

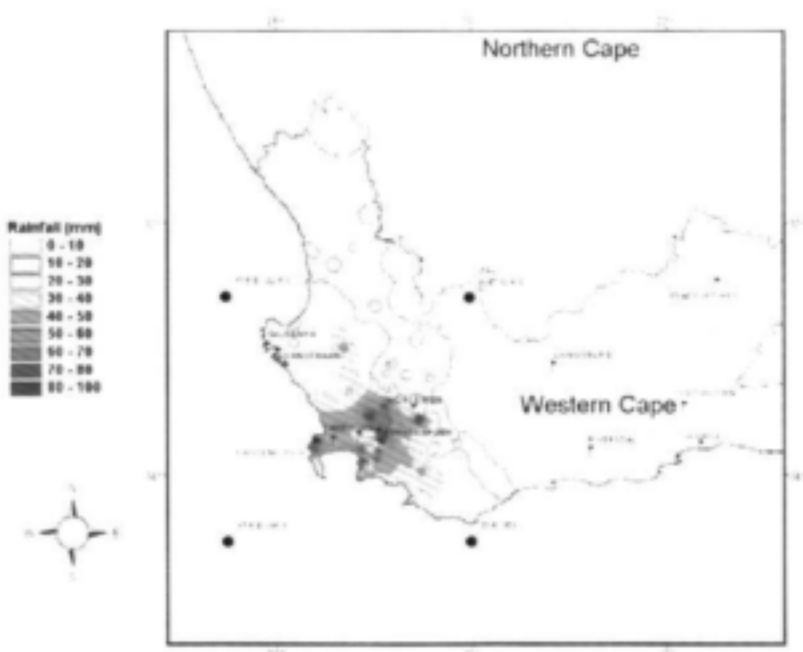

Figure 9.1: Rainfall distribution on 3 July 2001

The Western Cape Province receives most of its rainfall in winter (May-August) (Schulze, 1965) caused predominantly by cold fronts (Taljaard, 1985). On 3 July 2001, very high rainfall rates occurred over the Cape Peninsula when 57mm of rain fell over Cape Town in 6-hrs. Franschoek and Kirstenbosch also received about 75mm.

Cyclogenesis is the process, which describes the development of a mid-latitude cyclone. This occurs when an upper trough of wavelength 5000km or less interacts with a surface frontal zone (Conway, 1997). The low-pressure system develops at the surface in the presence of vertical wind shear and thermal instability (Conway, 1997). This study shows that two types of cyclogenesis occurred almost simultaneously. Firstly, a cold front approaching the Southwestern Cape was still intensifying when the heavy rainfall event occurred. This system developed from a main frontal cloud band. Secondly considerable enhancement of convective activity took place in the cold air behind the front.

9.4.1.2 NCEP analysis and METEOSAT Infra Red imagery

This heavy rainfall event was investigated by utilizing NCEP data as well as the METEOSAT Infra Red Imagery. Figures 9.2a to 9.4a show the IR image, the 1000hPa gpm height field as well as the 500hPa gpm height field for 0000 UTC on 3 July 2001. On the IR image, the cold front is positioned west of the country at point A. The high level cloud near C locates the jet stream associated with the upper trough. By 1200 UTC the cold front cloud band had developed substantially (Fig 9.2c). The enhanced cumulus field at point B moved eastward. Figure 9.3c shows that the front had reached the South Western Cape and that the low-pressure system had deepened (cyclogenesis). The upper trough had moved eastward (Fig 9.4c) and the cloud band associated with it had caught up with the frontal cloud band. The vertical profile of omega (ω) for 1200Z (not shown) shows upward motion all the way to the upper troposphere with a minimum value of -2.4 Pa s^{-1} at 700hPa.

9.4.1.3 Cyclogenesis of the frontal system

This sequence of events indicates that the system was still developing as it moved over the South Western Cape. The reasons for the further development can be explained by using Pettersen's development process (Palmen, 1946). The temperature advection on 3 July 2001 was such that lower level warm air advection was maintained over the South Western Cape. Figure 9.5 depicts the temperature advection field for the 850- 700hPa layer at 0600Z on this day. The post frontal development behind the cold front happens in the cold air advection region behind the cold front below the upper thermal trough. Figure 9.5 shows an area of cold air advection behind the cold front at point B. At this point cold air advection at sea level was ahead of the upper trough. This will lead to the further development of the upper trough (Holton, 1992).

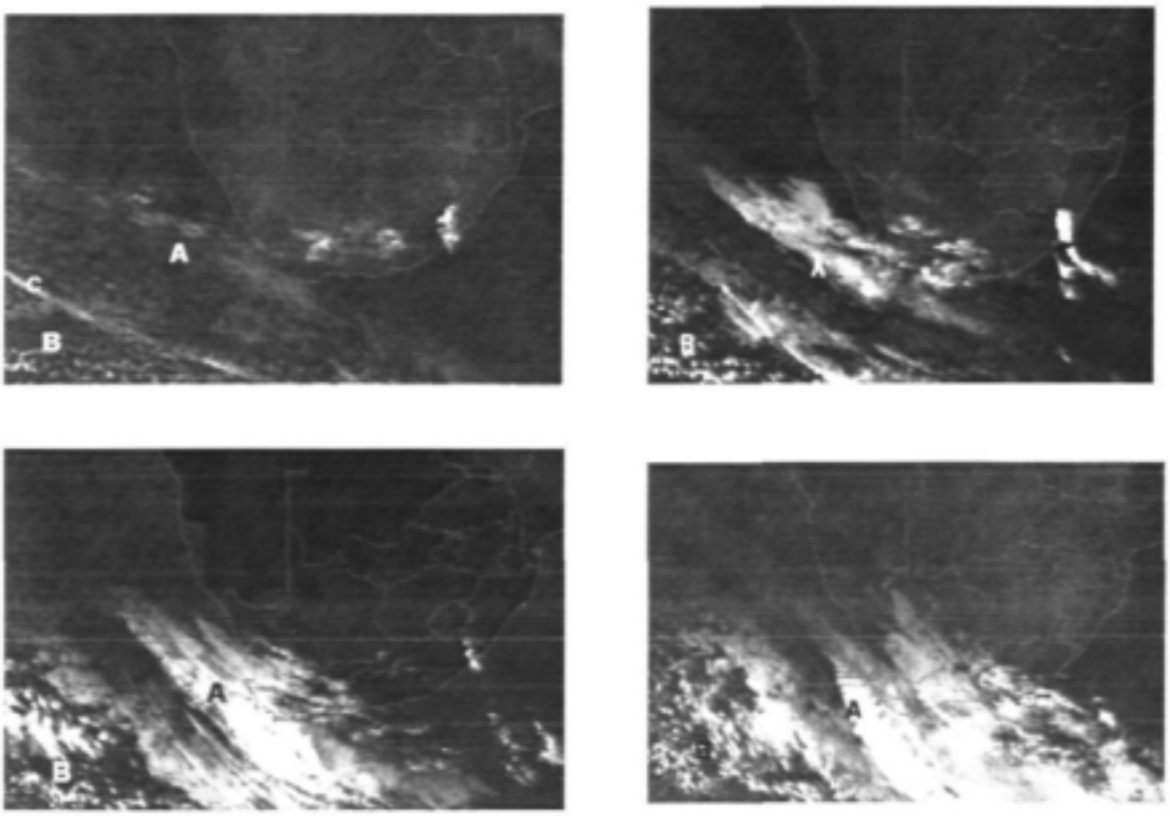

Figure 9.2a-d: Infra-red satellite image from a geostationary satellite on 3 July at 0000UTC, 0600UTC, 1200UTC and 1800UTC respectively. (Courtesy of EUMETSAT)

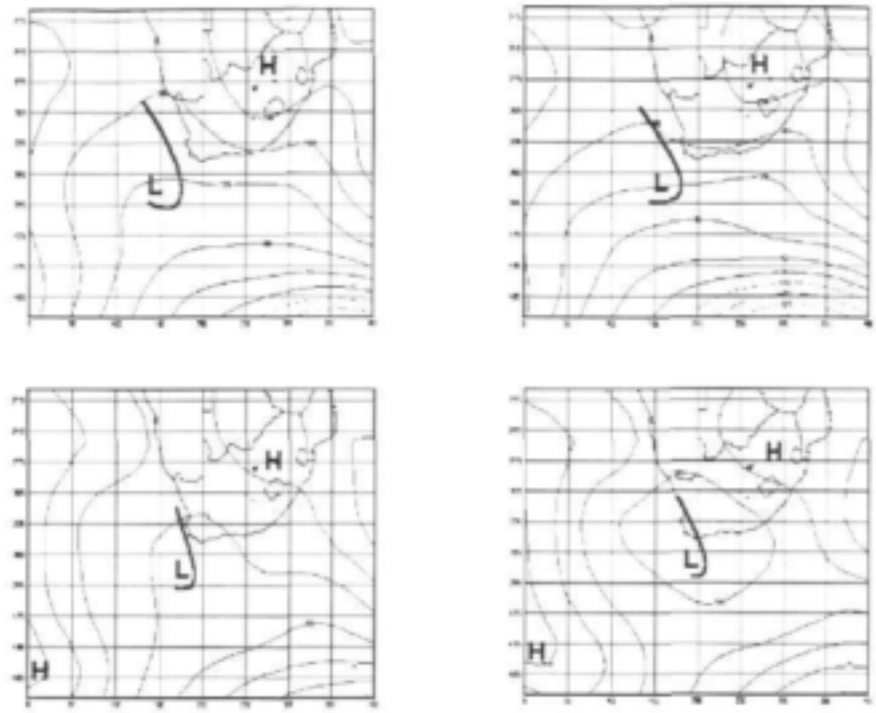

Figure 9.3a-d: 1000hPa geopotential heights on 3 July at 0000Z, 0600Z, 1200Z and 1800Z respectively

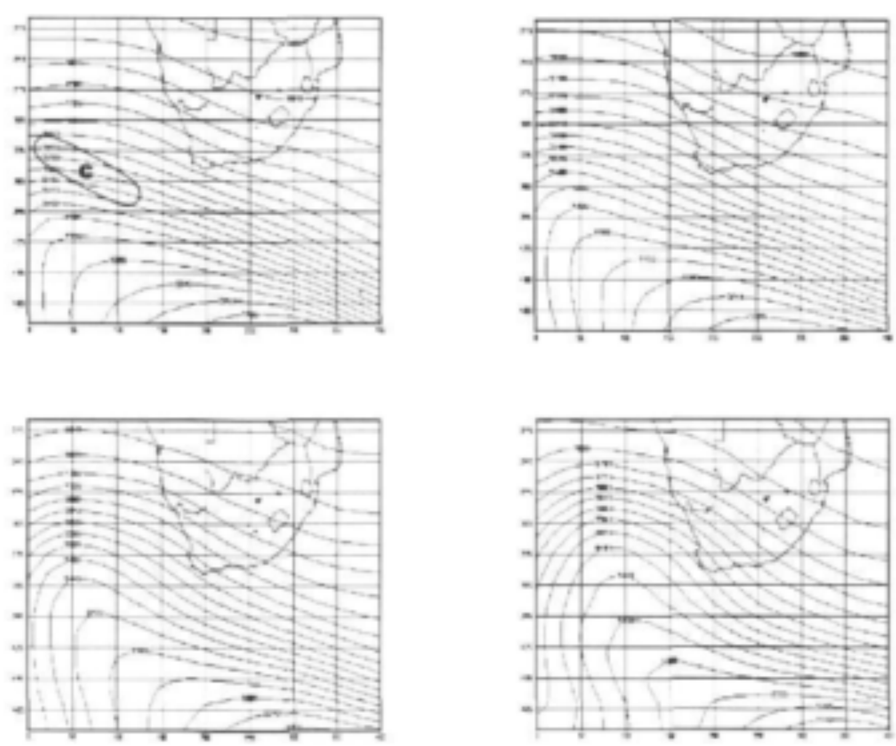

Figure 9.4a-d: 500hPa geopotential heights on the 3 July at 0000Z, 0600Z, 1200Z and 1800Z respectively.

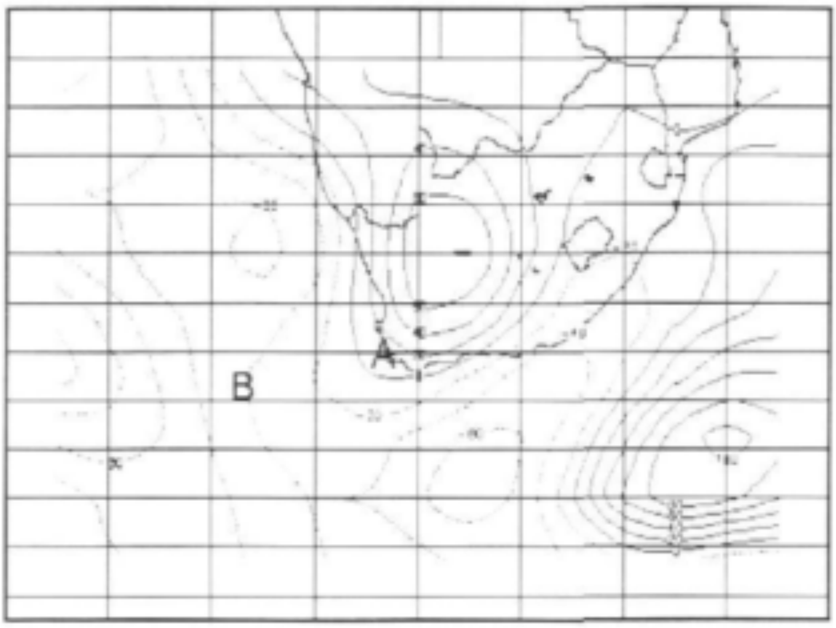

Figure 9.5: 700hPa - 850hPa temperature advection field at 0600Z on the 3rd July. Positive values indicate warm air advection.

9.4.2 Heavy rain and snow over the East Cape Province 15 to 21 July 2002

(Contribution by Mr. A Moatshe)

9.4.2.1 Introduction

During the week of 15 to 21 July 2002 the Eastern Cape interior experienced heavy snowfalls. Three hundred people including school children were trapped. Elliot was at the centre of the heavy snowfalls where about 3000 informal dwellings, 100 farmhouses and 50 shops were destroyed or damaged. Damage was estimated at R18 million excluding stock losses (SAPA, 2002). Significant and heavy rainfall also occurred during this time over the northern coast of KwaZulu-Natal and the adjacent interior.

9.4.2.2 Synoptic scale analysis

An intense cold front moved over the southern parts of the country between 15 and 17 July 2002. Following this front a strong southerly wind advected cold maritime air northward. A cut-off low (COL) was placed southeast of the country on the 16th. A new upper low started to redevelop over the southeastern interior of South Africa because of the strong cold air advection over these regions. By 17 July, this new COL had moved northwards and was situated over the central interior of South Africa. On the 19th the COL was situated over the central interior and have deepened since the 18th by 110gpm (Fig. 9.7a). A surface low-pressure system developed in the southern Mozambique Channel on the 19th (Fig. 9.6a). To the south of this low and over the entire South Africa the cold air continued to be advected over the country but now from the east. This cold air advection resulted in the maintenance of the COL over the central interior with a second upper low developing off the west coast of South Africa (Fig. 9.7b). On the 20th a strong surface on-shore flow prevailed over the east coast (Fig. 9.6b). The COL in the upper air contributed to copious rain and snowfall over the East Coast. Mandini, Mtunzini and Ulundi received 252mm, 239mm and 114mm of rainfall respectively on the 20th.

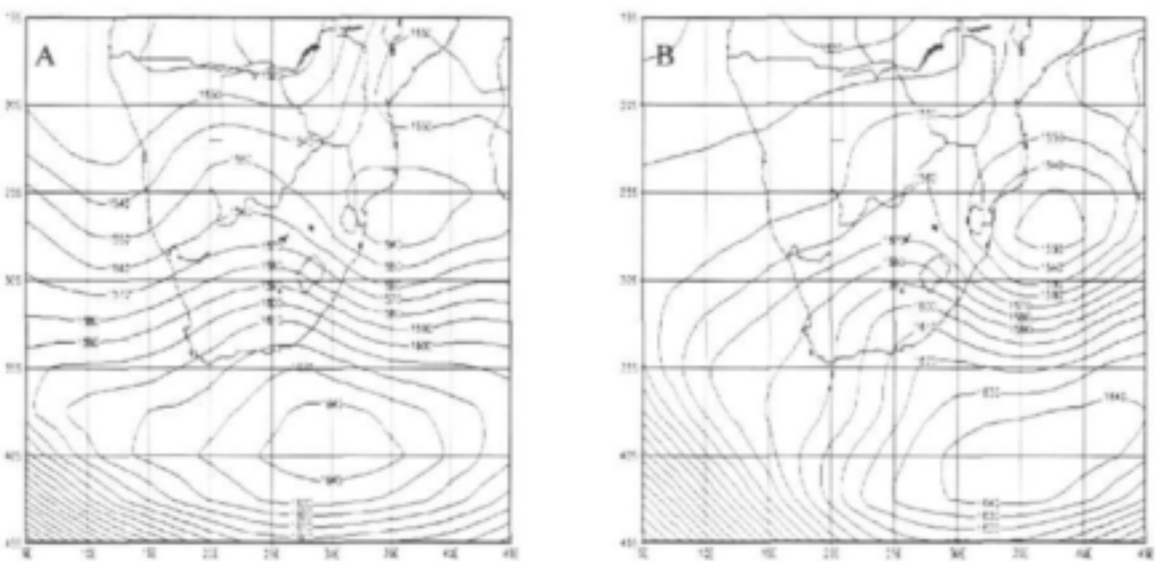

Figure 9.6: Geopotential heights at 850hPa on (A) 19 and (B) 20 July 2002

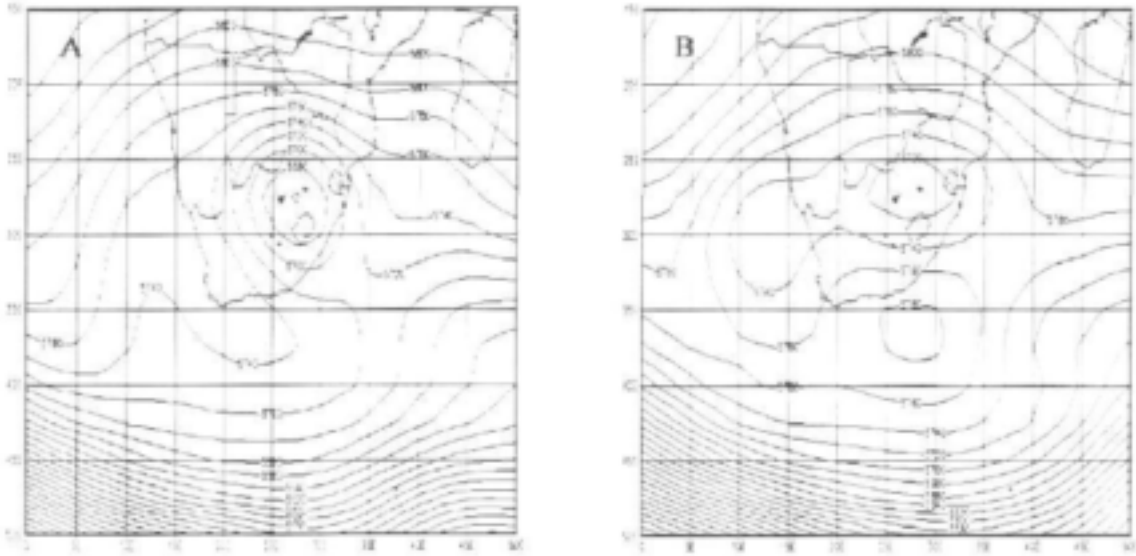

Figure 9.7: Geopotential heights at 850hPa on (A) 19 and (B) 20 July 2002

9.4.3 Localised Flooding over Gauteng in December 2002

(Contribution by Ms L Burger)

9.4.3.1 Introduction

During the last two weeks of December 2002, a persistent presence of tropical surface moisture, along with high levels of diurnal heating, caused the frequent development of thunderstorms over Gauteng. On the afternoon of the 27^{th} December two significant storms developed. The first storm wreaked havoc in the Vereeniging/Evaton area, while the second storm left the CBD of Klerksdorp flooded when 70mm of rain fell within 45 minutes. Huge losses were caused by the vast amount of hail that fell. Cleaning operations were hampered by another severe storm that hit the Klerksdorp/Stilfontein district on Saturday the 28^{th} (Rae, 2002).

The National Severe Storms Laboratory (NSSL) in the United States describes the severe convective storm as one which produces one or more of the following phenomena:

- a tornado
- strong wind gusts, exceeding 50 knots
- hail larger than 19 mm in diameter.

Rainfall from cumulonimbus clouds depends strongly on the surface moisture content. In a study conducted by Maddox (1979), it was found that flash flood events in the United States exhibited typical surface mixing ratios of 10 to 14g/kg (Cotton et al., 1989). Klemp et al.,

(1986) states that the convective storm type depends on the vertical shear (especially within the lowest 5-6 km), but thermodynamic conditions should also be taken into account.

9.4.3.2 Data and methodology

Eta model data for the 27th and 28th of December 2002 as well as gauge rainfall data were obtained from the South African Weather Service (SAWS). In order to compare the Eta model's precipitation forecast with the rain gauge data, difference maps were created with the aid of Idrisi Geographic Information System (GIS) software. In all instances the gauge rainfall was subtracted from the Eta precipitation forecast.

9.4.3.3 Eta and gauge rainfall comparison

The areas where the model under forecast rainfall are shown in figure 9.8. Klerksdorp is indicated with an arrow. On the 27th, the model under forecast rainfall by 48 mm (Fig. 9.8a), *while it forecast its maximum rainfall to the east of the actual event, over estimating by 24* mm (Fig. 9.8b). On the 28th, the model under forecast rainfall by 18 mm at Klerksdorp (Fig. 9.8c). Over the eastern escarpment the model over forecast rainfall on the 28th with 28 mm (figure 9.8d).

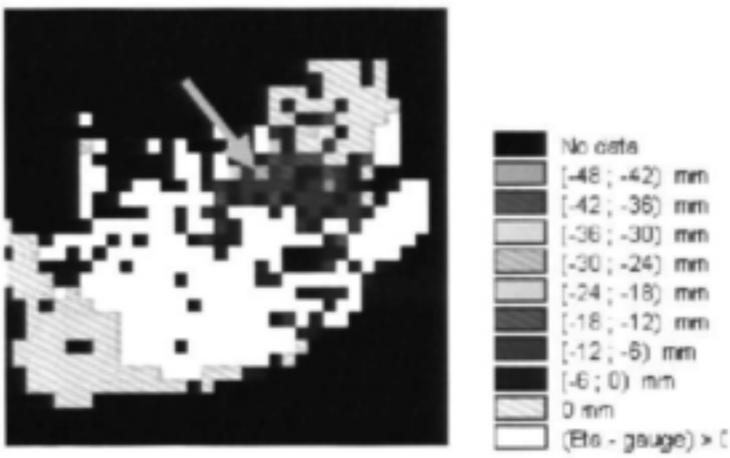

Figure 9.8(a): Eta rainfall minus gauge rainfall for the 27th of December 2002.

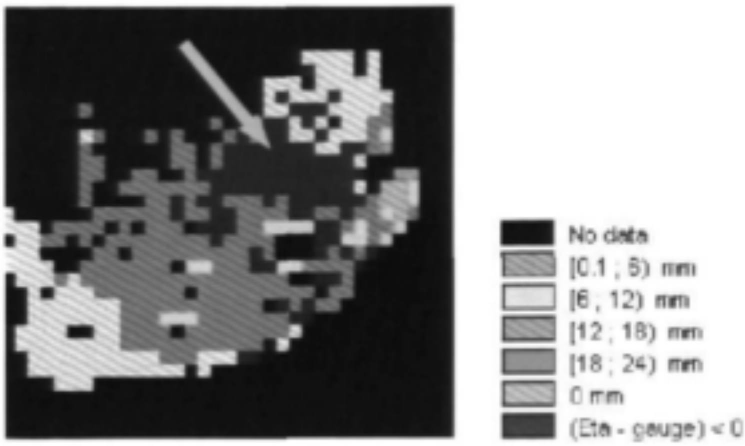

Figure 9.8(b): Eta rainfall minus gauge rainfall for the 27th of December 2002.

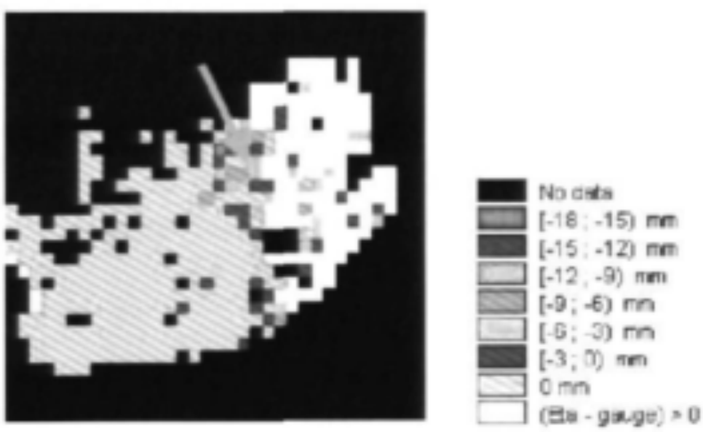

Figure 9.8(c): Eta rainfall minus gauge rainfall for the 28th of December 2002.

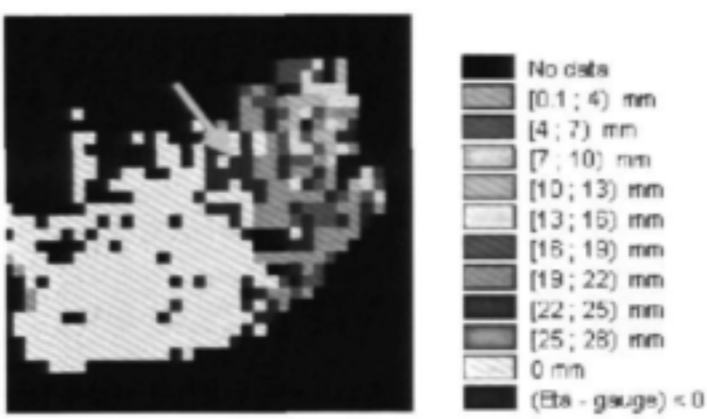

Figure 9.8(d): Eta rainfall minus gauge rainfall for the 28th of December 2002.

The surface pressure pattern on the 27th (Fig. 9.9a) shows the Indian Ocean high ridging in over the north-eastern parts of the country and Botswana, advecting moist air into the region where the thunderstorms developed. A surface trough extends from Namibia south-eastwards on the 27th and 28th (Fig. 9.9a and b). The vertical gpm height profile on the 28th shows the upper air trough leaning eastwards with height (Fig. 9.10a and b). Cumulonimbus clouds formed to the east of the upper air trough axis within the zone of moist surface air.

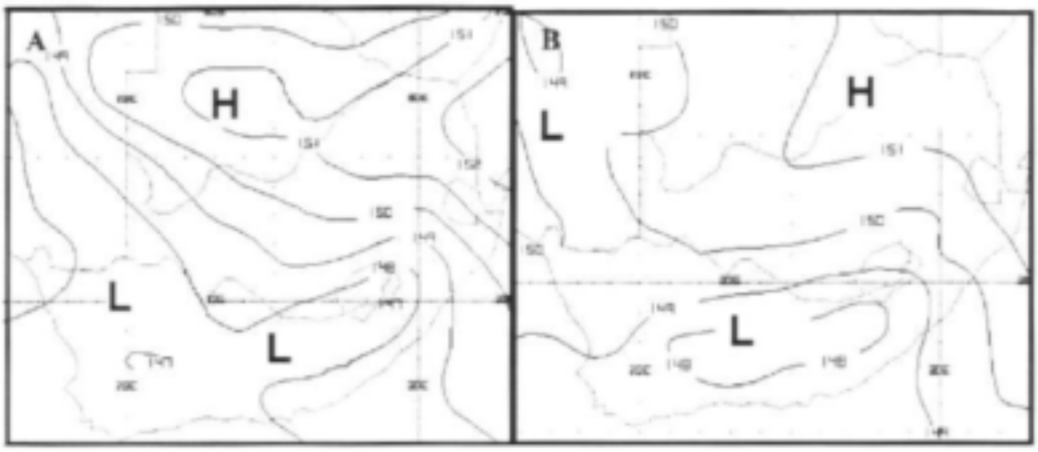

Figure 9.9: 850 hPa Geopotential heights for the 27th(A) and 28th (B) of December 2002 at 1200UTC.

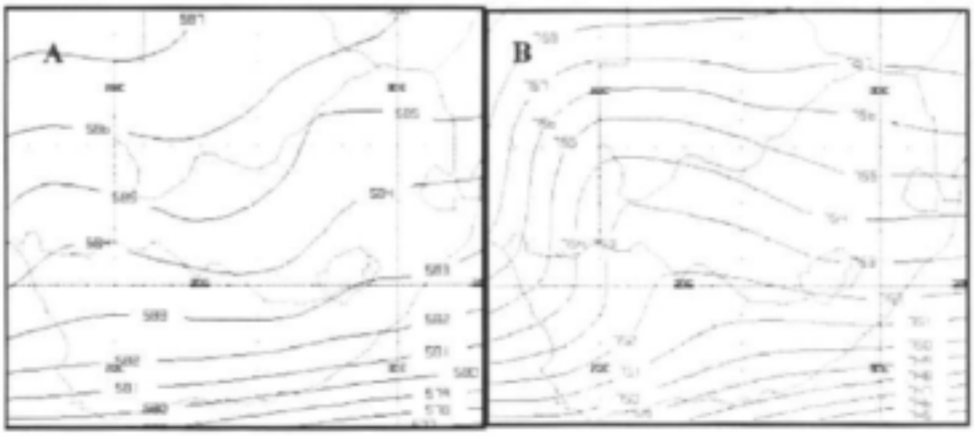

Figure 9.10: 500 hPa (A) and 400hPa (B) Geopotential heights for the 28th of December 2002 at 1200UTC.

Figure 9.11 depicts Eta model mixing ratio values at 850hPa for the 27th of December 2002 (1200UTC). Mixing ratio values on the 27th varied between 12g/kg and 15g/kg within the area where the thunderstorms developed. A surface thermal ridge axis was present to the west of the axis of maximum moisture on the 27th December 2002. On both days the airflow pattern as indicated by the Eta model showed inflow of low level (850 hPa) warm, moist air from the north east and a westerly upper level (400hPa) inflow of cool dry air over the parts of South Africa where the storms developed.

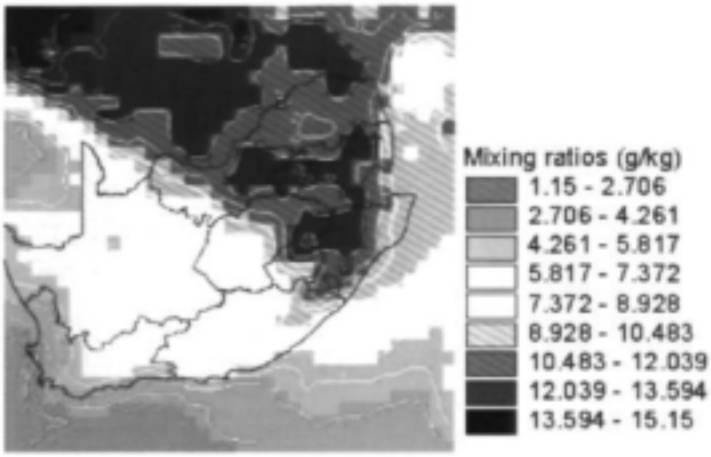

Figure 9.11: Eta model mixing ratios at 850 hPa on the 27th of December 2002 at 1200UTC.

9.4.3.4 Conclusions

The Eta model forecasted rainfall for the 27th and 28th of December 2002, but with maximum rainfall to the east of where the actual heavy falls occurred and also underestimated the amounts.

9.4.4 Severe Thunderstorm Environments over South Africa

(Contribution by Mr M Roux)

9.4.4.1 Introduction

South African severe thunderstorms and severe weather are notoriously difficult to predict and are often not observed because of an inadequate reporting network over the country. Brooks et al. (2003) identified important parameters for severe storm environments based on the United States of America (USA). NCEP re-analysis data were used to develop a three-year climatology of tordonadic environments. The central United States has 14 days per year with tornado conditions while South Africa has 3 days per year.

The parameters and dynamic variables Brooks et al. (2003) considers are:

a) The height of the mixed layer lifted condensation level (LCL) above ground level (AGL), (h_{LCL}),

b) The convective available potential energy $(CAPE)$,

c) The 2 – 4 km temperature lapse rate AGL (TLR),

d) The surface to 6km wind shear $(|Wdiff_6|)$

e) The surface to 1km wind shear $(|Wdiff_1|)$.

Brooks et al. (2003) also considers the most favorable time for the occurrence of tornadoes to be 1800UTC close to the time maximum temperatures occur, over the central USA

The aim of this research is to investigate whether the parameters identified by Brooks et al. (2003) existed for three known tornadic events over South Africa using NCEP re-analysis data provided by Dr. Brooks. The three events were:

- The Harrismith tornado on 15 November 1998.
- The Umtata tornado on 15 December 1998.
- The Mount Ayliff tornado on 18 January 1999.

A first objective was to determine if the data for 1200UTC would not give a better representation for South African tornadoes than 1800UTC. A second objective in this report is to investigate if Brooks et al. (2003) parameters and critical values need to be adjusted for the elevated terrain over South Africa.

9.4.4.2 Method

The NCEP data approximated the heights ASL for Harrismith, Umtata and Mount Ayliff at 1271m, 1347m and 786m respectively. The actual heights ASL for three areas are 1617m for Harrismith, 747m for Umtata and 975m for Mount Ayliff.

The height of the mixed layer LCL as well as the parcel and environmental temperatures were calculated for each of the three events at 1200UT and 1800UT. Following Brooks et al. (2003) entrainment was taken into consideration here.

The following procedures were carried out for each assent:

- Calculate the pressure of the LCL (Poolman, 1992)
- Calculate $CAPE$ (Holton, 1992 and Poolman, 1992)
- Calculate the 2-4 km AGL, temperature lapse rate
- Calculate the surface to 1km wind difference
- Calculate the surface to 6km wind difference

9.4.4.3 Discussion and results

The relationships between the parameters and dynamic variables considered by Brooks et al. (2003) were tested for the three South African tornadic events. The relationships were comprised of (a) $|Wdiff_6|$ against $CAPE$, (b) TLR for the three events and finally (c) $|Wdiff_1|$ against h_{LCL}.

$CAPE$ and $|Wdiff_6|$ for the three events at 1200UTC were plotted onto the diagram from Brooks et al. (2003). (Fig. 9.12). The black line shown in figure 9.12, which is termed a "best" discriminator line was obtained using linear discriminant analysis (Wilks (1995) cited in Brooks et al. 2003). This linear discriminant analysis was applied for all soundings associated with severe weather with $CAPE \geq 100J/kg$ and using $\log(CAPE)$ and $\log(|Wdiff_6|)$ as the input parameters (Brooks et al. 2003). From this analysis Brooks et al. (2003) concluded that soundings, which lie above this line, are more likely to be associated with significant severe thunderstorms. The Harrismith event fell just below the line with $CAPE = 333.89Jkg^{-1}$ and $|Wdiff_6| = 12.66ms^{-1}$, but still fitted well in comparison to the soundings over the USA, whereas the Umtata event fell above the line with $CAPE = 287.47Jkg^{-1}$ and $|Wdiff_6| = 47.35ms^{-1}$ fitting better with United States soundings. The Mount Ayliff event could not be compared to this line, since $CAPE < 100Jkg^{-1}$.

Figure 9.13 displays the Skew – T gram for Harrismith at 1200UT utilizing the NCEP data. The RAOB CAPE over Harrismith on 15 November 1998 at 1200UT was 269Jkg^{-1}. The LFC was at 580hPa and the LNB to at 260hPa. In figure 9.13 entrainment was taken into consideration, this resulted in the severe storm indicators not being very favorable. Table 9.1 indicates the significant difference in CAPE values when entrainment is not considered. It is clear from this table that when entrainment is not considered CAPE values associated with severe storms are achieved.

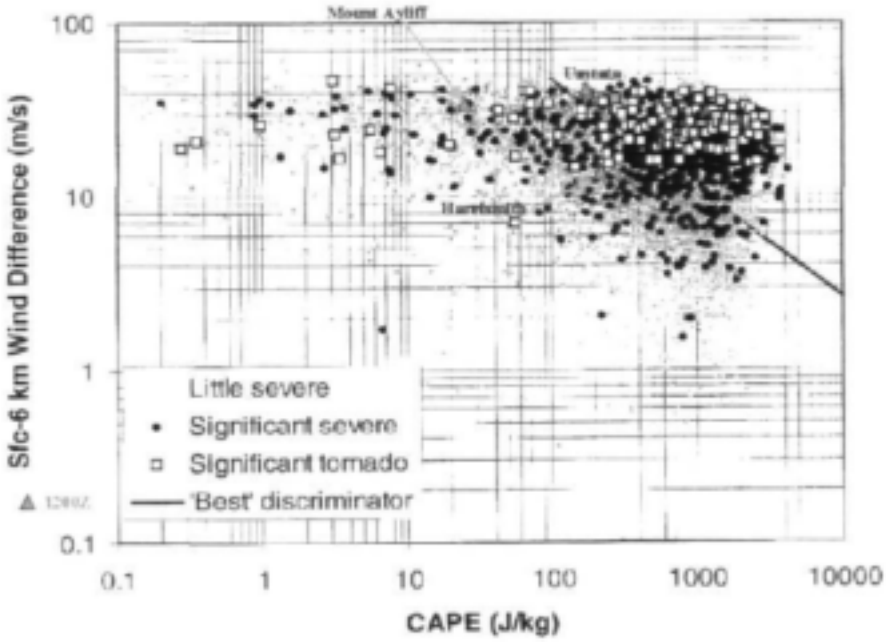

Figure 9.12: Magnitude of the vector wind difference between the surface and 6 km (ms^{-1}) and CAPE (Jkg^{-1}) for all reanalysis soundings associated with severe thunderstorms in the United States for the period 1997 – 1999. Soundings are segregated by weather type: non-significant severe weather (small grey dots), significant non-tornadic severe weather (large black dots) and significant tornadoes (open squares). The grey triangles represent the position of South African events at 1200UT in when comparing these same two variables.

Table 9.1: Comparison of calculated CAPE (Jkg^{-1}) with entrainment to RAOB CAPE without entrainment for all three events at 1200UT.

Event	$CAPE(Jkg^{-1})$ (With entrainment)	$RAOB\ CAPE(Jkg^{-1})$ (Without entrainment)
Harrismith	333.89	659.00
Umtata	287.47	2172.00
Mount Ayliff	28.17	2036.00

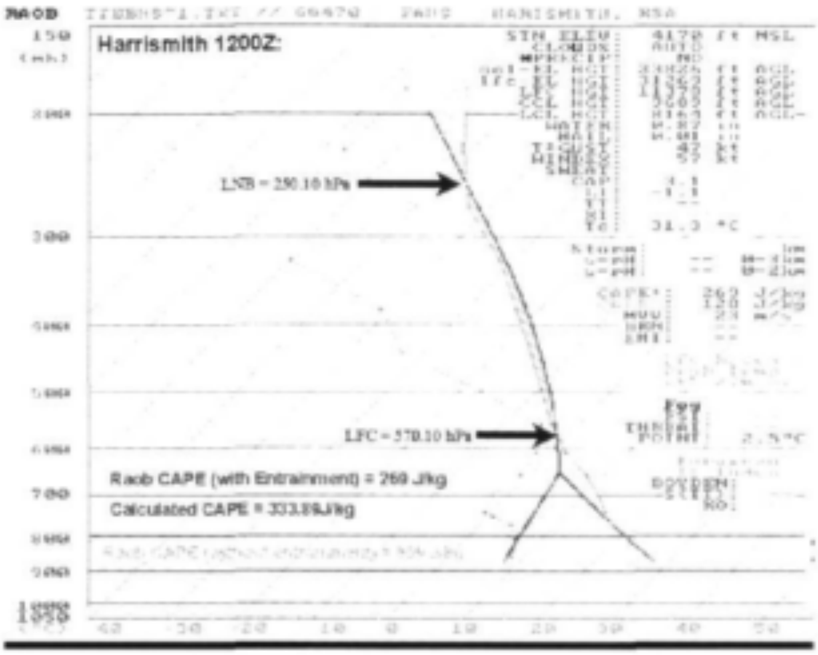

Figure 9.13: RAOB skew – T gram for Harrismith on 15 November 1998 at 1200UT.

Considering all the soundings performed over the USA between 1997 – 99, almost 78% of the significant severe soundings have $TLR \geq 6.50Kkm^{-1}$, whereas a mere 30% of the less severe soundings are that unstable (Brooks et al. 2003). Figure 9.14 illustrates this fact by way of displaying a cumulative distribution function of TLR for all significant severe thunderstorm soundings (black line) and other soundings (grey line) over the USA. The vertical line in figure 9.14 represents $TLR = 6.50Kkm^{-1}$. Soundings that lie to the right of this vertical line have $TLR > 6.50Kkm^{-1}$. For the three events over South Africa, $TLR > 6.50Kkm^{-1}$. (Table 9.2 and Figure 9.14).

The relationship between $|Wdiff_1|$ and h_{LCL} was considered for each of the events at both times and compared with the general trend set by the USA soundings (Fig. 9.15). The general idea behind figure 9.15 is that low LCL heights and strong shear are favourable for tornadic events. The three lines in Fig. 9.15 are discrimination planes with $|Wdiff_1|$, h_{LCL} and station elevation (m ASL) as the input parameters (Brooks et al. 2003). The values for h_{LCL} and $|Wdiff_1|$ for the three events at both 1200UTC and 1800UTC can be referred to in Table 9.1

Table 9.2: The values for the parameters and dynamic variables of interest calculated for the three South African events at both 1200UT and 1800UT

Variable	Harrismith 1200UT	Umtata 1200UT	Mount Ayliff 1200UT	Harrismith 1800UT	Umtata 1800UT	Mount Ayliff 1800UT
$R\ (gkg^{-1})$	7.55	9.32	10.48	8.46	9.04	10.50
$LCL\ pressure\ level$ $(hPa), (R = Rs)$	650.1	732.9	796.8	727.7	758	837.6
$h_{LCL}\ (m)$	2478.49	1338.06	1203.75	1545.32	1039.88	778.03
$CAPE\ (Jkg^{-1})$	333.89	287.47	28.17	0	1.63	0.88
$\|Wdiff_1\|\ (ms^{-1})$	19.58	20.73	16.06	10.98	16.31	5.77
$\|Wdiff_6\|\ (ms^{-1})$	12.66	47.35	40.09	31.40	39.98	67.90
$TLR\ (Kkm^{-1})$	7.9	7.00	7.33	7.61	6.30	7.17

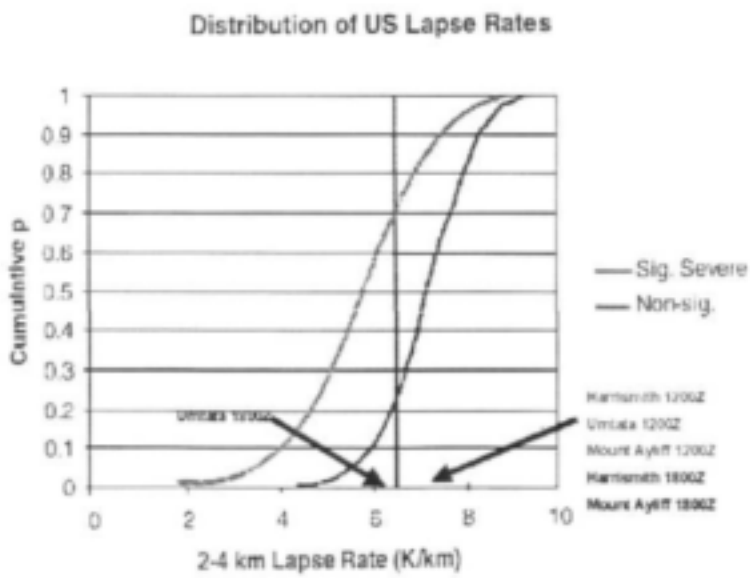

Figure 9.14: Cumulative distribution functions of the 2 – 4 km AGL temperature lapse rates (Kkm^{-1}) for all significant severe thunderstorm soundings (black line) and other soundings (grey line) for all 1997 – 1999 United States soundings. The lapse rate of 6.5 Kkm^{-1} indicated by vertical line. Arrows indicate which of the South African events at which times are above or below the 6.5 Kkm^{-1} temperature lapse rate.

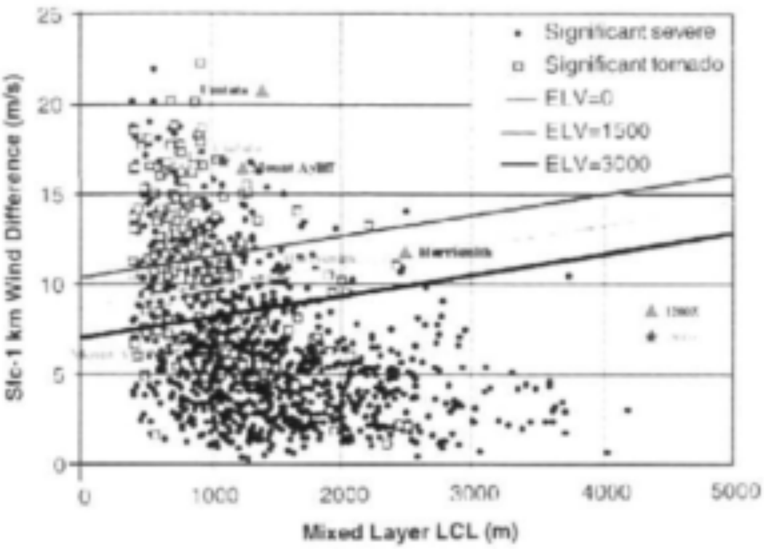

Figure 9.15: Magnitude of the vector wind difference between the surface and 1km (ms^{-1}) and height of mixed layer lifted condensation level (in m) for United States reanalysis soundings associated with significant severe thunderstorms, segregated by weather type: non – tornadic soundings and tornadic soundings (open squares). Thick black, thick grey and thin black lines are lines obtained from linear discriminant analysis associated with a station elevation of 0, 1500, 3000 metres respectively. The black triangles represent the position of the South African events at 1200UT when comparing the same two parameters. The grey stars represent the position of the South African events at 1800UT when comparing the same two parameters.

9.4.4.4 Conclusions

The 1200UTC results are a better representation for South Africa regarding the system devised by Brooks et al. (2003).

The parameters devised by Brooks et al. (2003) worked well over South Africa for two of the three events with large wind shear even though the $CAPE$ is small.

Based upon the three events, entrainment should not be used for identifying severe tornadic environments with the NCEP data over South Africa.

9.4.5 Widespread heavy rainfall in the Drakensberg mountains

(Contribution by Ms M Martin)

9.4.5.1 Introduction

The KwaZulu Natal Drakensberg Mountains play a major role in the rainfall distribution pattern of South Africa. The KwaZulu Natal Drakensberg Mountains extend from 28°30'S to 30°30'S and 28°30'E to 29°30'E (Fig 9.16). They vary in altitude from 1400m to 3000m above mean sea level. Forming part of the major escarpment of the country, this landform is to a large extent responsible for the position of the 1000mm annual rainfall isohyet. Summer thunderstorms provide the most significant contribution of rainfall to the Drakensberg escarpment (Tyson *et al*, 1976). This report investigates the rainfall in the area of the Drakensberg with reference to two COL systems. This happened on 13 June 2002 and 19 March 2003.

9.4.5.2 Data and Methods

Data used for this investigation included NCEP reanalysis data from the Climate Diagnostic Centre (www.cdc.noaa.gov). The variables considered included vorticity, divergence, vertical motion, geopotential heights and analysed on pressure levels from 850hPa to 300hPa. The vorticity was studied at 850, 500 and 200hPa. Vertical profiles of wind divergence and vertical velocity were extracted at grid close to the study area. They were at 27.5°S 30°E (A), 30°S 27.5°E (B) and 30°S 30°E (C). The daily rainfall data for 36 stations in the Drakensberg area were obtained from the SAWS. Rainfall data at five-minute temporal resolution from five automatic weather stations (AWS) were acquired from Mr Werner Nel. These data were used to isolate the time, which the rainfall fell on a particular day. Nel and Sumner (2005) discussed rainfall from several automatic weather stations in the Drakenburg area. Sentinal Peak is the highest point where rainfall is currently measured in South Africa (3 165m).

Two of Nel and Sumners' (2005) stations were Sentinel and Royal Natal. The SAWS also operates stations close to these locations. Comparing the data resulted in the SAWS rainfall data at these two stations not to be used, as there was a large discrepancy between the two data sets. There was also a poor correlation between these two SAWS stations and with the other rainfall stations.

Figure 9.16: Drakensberg Mountains study area. Stars indicate the position of the rainfall stations.

In this research, widespread heavy rainfall in the region is defined when at least five stations received rainfall greater than 30mm and 80% of all stations reported rainfall. There were 12 days on which widespread heavy rainfall occurred. (Table 9.3)

Table 9.3: Dates on which widespread heavy rainfall occurred in the Drakensberg.

24 January 2002	14 August 2002
29 January 2002	18 August 2002
30 January 2002	16 December 2002
31 January 2002	19 March 2003
30 May 2002	13 April 2003
13 June 2002	22 April 2003

9.4.5.3 Results and Discussion

a) 13 June 2002

The rainfall on the 13[th] of June began in the early afternoon and continued until the early hours of the 14[th]. The AWS data revealed that the rainfall was most intense between 23:00SAST and 01:00SAST. The highest rainfall total recorded on this day was 37mm at Bulwer. Eighty nine percent of the stations reported some rainfall and there were seven stations that recorded more than 30mm of rainfall in the 24 hr period.

At 850hPa a sharp trough was situated south of the country (Fig.9.17a). This trough extends to the southern interior at 500hPa where there was a closed circulation pattern (Fig 9.17b). The minimum gpm height at 500hPa was 5660gpm. The low pressure system was displaced to the towards the east at 300hPa with a minimum height of 9240gpm.

Convergence at 850hPa (Fig 9.17a) was evident over the eastern half of the country at the surface. Over the study area, values are around 100 $*10^{-6}$ s^{-1} but just north of that, values up to 150 $*10^{-6}$ s^{-1} were computed. Strong divergence dominated the western regions at 850hPa. At 400hPa (fig not shown) divergence values were small over the Drakensberg.

The minimum values of omega (maximum vertical motion) at A, B and C were -0.23, -0.38 and -0.3 $Pa.s^{-1}$ respectively. The strongest upward motion occurred at the 400hPa level at all three points. At 700hPa water vapour mixing ratio 6 g.kg^{-1} The precipitable water in the 850 to 300hPa layer over the study area was around 14 kg.m^{2}.

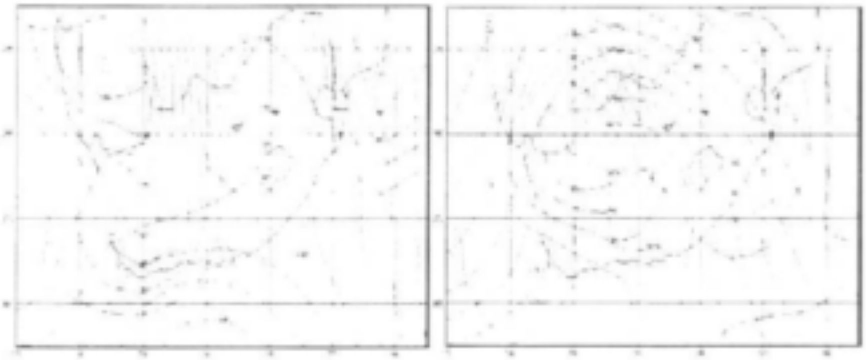

Figure 9.17: The 850hPa geopotential heights (dashed) and horizontal wind divergence (a) and at 500hPa (b) on the 13th of June 2002. Solid lines are divergence and dotted lines are convergence.

b) 19 March 2003

Precipitation started on the morning of the 19th of March and lasted for almost the entire 24-hr period. The maximum rainfall recorded was 79mm at Cobham. On this day 95% of the stations reported rainfall and 27 stations reported more than 30mm of rainfall in 24 hours. The most intense rainfall period was from 14:45 to 15:00 SAST.

In this instance an 850hPa high-pressure system was located southeast of the country causing a strong on-shore flow into the study area (Fig. 9.18a). At 700hPa (fig not shown) a closed low-pressure cell existed over the Northern Cape. The low intensified from the 700 to 500hPa levels (Fig 9.18b). The centre of the closed low at 500hPa was at 5800gpm.

On the 19th of March the Drakenberg region experienced convergence from 850hPa up to the 500hPa level. The magnitude of the convergence at the surface (Fig9.18a) was 100 $*10^{-6}$ s^{-1}. Divergence increased dramatically to almost 200 $*10^{-6}$ s^{-1} over the study area at 300hPa.

The 19th of March the minimum values vertical motion was -0.4, -0.45 and -0.38 Pa.s^{-1} at A, B and C respectively (figs not shown). The most significant features to note of the profiles for the day in March are the large magnitudes of vertical motion at the surface. At A, B and C, 850hPa vertical motion is at -0.25 Pa.s^{-1}.

Over the study area the mixing ratio was 11 g.kg^{-1} (at 850hPa) and precipitable water was 28 kg.m^{-2}. A value of greater than 20 kg.m^{-2} was identified as being associated with heavy rainfall from tropical weather systems (Dyson, 2000).

9.4.5.4 Comparison between the events

The 850hPa level indicates that the two systems did not show the same pressure distributions, with the day in March exhibiting the more common pattern leading up to COL development, being the ridge to the south of the country. The centre of the closed low in the June event was further east at 300hPa than the low at 300hPa in the March event. The entire system in the middle to upper troposphere on the 19th does not extend as far north as the system on the 13th (at the same levels). At 1800Z on the 13th of June, approximately the time of the rainfall, the low was not closed at 500hPa. The 19th of March example displayed a closed low at 1200Z from the 700hPa level to the upper troposphere.

Through most of the troposphere and up to 300 hPa negative vorticity indicated that the system in June had a more intense circulation than the one in March. At 200hPa however, the circulation intensity of the 19th of March is greater than on the 13th of June

In June, vertical profiles at point A and C showed a rapid increase of vertical motion with height in the surface to 400hPa layer whereas at point B there was a slow increase of vertical motion with height between the surface and 700hPa. The opposite situation occurred on the 19th of March were point B showed rapid increase in vertical motion with height up to 500hPa and A, and in particular C, remained almost constant with height from the surface to 700hPa.

Moisture amounts on the 19th of March 2003 were significantly greater than those on the 13th of June 2002. The moisture source on 13 June was from the north whereas the moisture was advected into the study area by south easterlies wind at 850hPa in March. There were also indications of a tropical influence in the situation on the 19th of March with high mixing ratio and precipitable water values.

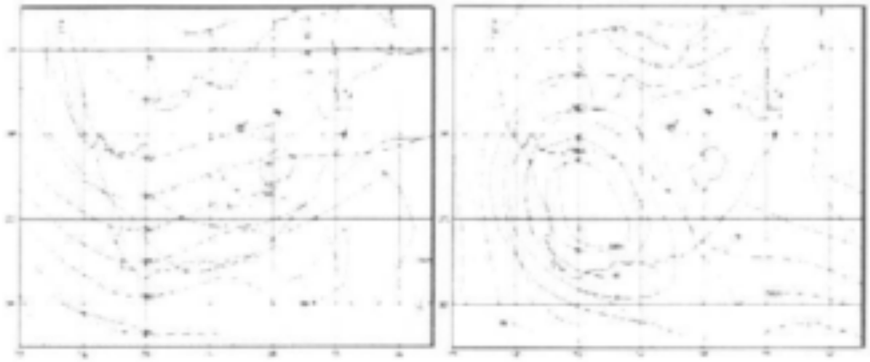

Figure 9.18: Same as figure 7.17 but on the 19th of March 2003.

9.4.5.5 Summary and conclusions

The results of the investigation into the various variables on both days are given in Table 9.4. These results show that classification of intensity needs to be consistent. Depending on whether rainfall amounts or circulation intensities are used as decided factors the category each system will fall under would be different.The surface onshore flow in March was responsible for the low level moisture advection. This was not the case for the June event.

The results achieved here are also contrary to what was stated by Tyson *et al.* (1976) in that in June, the winds from the north advected the moisture necessary for rain from the COL and not the typical south westerlies behind a cold front in winter.

With the tighter gradients, lower heights and greater negative vorticity values being evident on the June day, it is suggested that this system could be regarded as the more intense of the two systems. Based on the rainfall totals recorded from the two systems, the March event would normally be considered the more intense system. It could be argued that the lower precipitation amounts on 13 June 2002 were not an indication of a weaker system but rather that a moisture source was limited.

Table 9.4: Comparison of dynamic variables value's on the two study days

Variables	**13 June 2002**	**19 March 2003**
Maximum amount of rainfall	36.5mm	79mm
Geopotential heights	5660gpm at 500hPa 9240gpm at 300hPa	5800gpm at 500hPa 9510gpm at 300hPa
Orientation of trough axis	NW to SE north of	NW to SE
Orientation with height	SE	SE
Closed circulation	500 – 300hPa	700 – 300hPa
Average 500 – 300hPa temperatures	-33°C	-24°C
Vorticity	$3 * 10^{-5}$ s^{-1} at 850hPa $9 * 10^{-5}$ s^{-1} at 500hPa $9 * 10^{-5}$ s^{-1} at 200hPa	$2 * 10^{-5}$ s^{-1} at 850hPa $8 * 10^{-5}$ s^{-1} at 500hPa $10 * 10^{-5}$ s^{-1} at 200hPa
Divergence	Divergence above 400hPa and at 700hPa	Divergence above 400hPa and convergence at the top of the troposphere
Winds and mixing ratio (at 850hPa)	N to NE, 6 $g.kg^{-1}$	SE, 11 $g.kg^{-1}$

CHAPTER 10
REFERENCES

Alexander W.J.R. and Van Heerden J. (1991). Determination of the risk of widespread interruption of communications by floods. *Department of Transport Research Project* **RDAC 90/16.**

Betts A.K. (1986). A new convective adjustment scheme. Part I: Observational and theoretical basis. *Quart. J. Roy. Meteor. Soc.*, **112,** 677-691.

Betts A.K. and Miller M.J. (1986). A new convective adjustment scheme. Part II: Single column tests using GATE wave, BOMEX and arctic air-mass data sets. *Quart. J. Roy. Meteor. Soc.*, **112,** 693-709.

Brooks H.E. Lee J.W. and Craven J.P. (2003). The Spatial Distribution of Severe Thunderstorm and Tornado Environments from Global Reanalysis Data. *Atmospheric Research,* ***67-68**, July-September 2003,* 73-94p

Climate Diagnostics Centre (2003). The NCEP/NCAR Reanalysis Project.
www.cdc.noaa.gov/cdc/data.ncep.reanalysis.html

Conway E.D (1997). *An Introduction to Satellite interpretation,* Johns Hopkins University Press, Baltimore, 255pp.

Cotton N.W.R. and Anthes R.A. (1989). *Storm and Cloud Dynamics.* Academic Press, Inc, 883pp

Crimp S.J. van den Heever S.C. D'Abreton P.C. Tyson P.D. and Mason S.J. (1997). Mesoscale Modelling of Tropical-Temperate Troughs and Associated Systems over Southern Africa. *WRC Report* **595/1/97,** 395 pp.

De Coning E. Forbes G.S. and Poolman E.P. (1998). Heavy precipitation and flooding on 12-14 February 1996 over the summer rainfall regions of South Africa: Synoptic and Isentropic analyses. *Ntl. Wea. Dig.* **22** 25-36.

De Villiers M.P. (1992). The role of orographic forcing on heavy precipitation over Natal. *Unpublished M.Dip. Thesis*, Tech. of Pretoria, S. Afr.

Dyson L.L. (2000). A dynamical forecasting perspective on synoptic scale weather systems over southern Africa. *Unpublished M.Sc. Thesis*, Univ. of Pretoria, S. Afr.

Dyson L.L. and Van Heerden J. (2001). The heavy rainfall and floods over the northeastern interior of South Africa during February 2000. *S. Afr. J. Sci.* **97** 80-86p

Dyson L.L. and Van Heerden J. (2002). A Model for the Identification of Tropical Weather Systems over South Africa. *Water SA*, **28** *No. 3, 249-258p* .

Dyson L.L. Van Heerden J. and Marx H.G. (2002). Short-term weather forecasting techniques for heavy rainfall. *WRC Report: 1011/1/02*. 136 pp.

Dyson L.L. and Van Heerden J. (2005). A Tropical Heavy Rainfall Identification System. *Article accepted for publication. Weather and forecasting*

Deyzel I.T.H. Pegram G.G.S. Visser P.J.M. Dicks D. (2004). Spatial interpolation and mapping of Rainfall (Simar) Vol 2. Radar and satellite products. *WRC Report : 1152/1/04*

Estie K.E. (1981). The Laingsburg flood disaster of 25 January 1981. *S. Afr. Weath. Bur. News Lett.* 383, 19-32.

Geerts B. (1998). Satellite-based rainfall estimations.
www-das.uwyo.edu/~geerts/cwx/notes/chap10/satellite_rain.html

Harrison M.S.J. (1983). A generalised classification of South African summer rain-bearing synoptic systems. *J. Climatology* **4**, 547-560.

Harrison M.S.J. (1986). A synoptic climatology of South African rainfall variations. *Unpublished PhD Thesis*, University of Witwatersrand. 341 pp.

Hayward L.Q. and Van den Berg H.J.C. (1968). Die Port Elizabeth-Stortreens van 1 September 1968. *S. Afr. Weath. Service Newslett.* **234,** 157-169

Holton J.R. (1992). *An introduction to Dynamic Meteorology*. Academic Press, Inc. 511pp.

Hoskins B.J. and Bretherton F.P. (1972) Atmospheric frontogenesis models: Mathematical formulation and solution. *J. Atmos. Sci.* **29**, 11-37.

Huschke R.E. (1959). *Glossary of Meteorology*. Am. Meteorol. Soc. 638 pp.

Janjic' Z.I. (1984). Non-linear advection schemes and energy cascade on semi-staggered grids. *Mon. Wea. Rev.*, **112,** 1234-1245.

Janjic' Z.I. (1990). The step-mountain coordinate: Physical package. *Mon. Wea. Rev.*, **118,** 1429-1443.

Janjic' Z.I. (1994). The step-mountain eta coordinate model: Further developments of the convection, viscous sublayer, and turbulence closure schemes. *Mon. Wea. Rev.*, **122**, 927-945

Laurent H. Jobard I. and Toma A. (1997). Validation of satellite and ground based estimates of precipitation over the Sahel. *Atmospheric Research* **47-48** (1998) 651-670.

Karoly D.J. and Vincent D.G. (1998). Meteorology of the Southern Hemisphere. **27** N0. 49. *Am. Met. Soc.* 410 pp

Mesinger F. (1984). A Blocking technique for representation of mountains in atmospheric models. *Riv. Meteor. Aeronautica,* **44,** 195-202.

Mesinger F. Janjić Z. Ničković S. Gavrilov D. and Deaven D. (1988). The Step-mountain Coordinate: Model description and performance for cases of Alpine lee cyclogenesis and for a case of an Appalacian redevelopment. *Mntly. Wea. Review* **116** 1493-1518.

Michalakes J. (1997). MM90: A scalable parallel implementation of the Penn State /NCAR Mesoscale Model (MM5). *Parallel Computing* **23**. pp. 2173-2186

Murphy A.H. (1995). A coherent method of stratification within a general framework for verification. *Mon. Weather Rev.* **123** 1582-1588.

Murphy A.H. and Epstein E.S. (1967). Verification of probabilistic predictions: A brief review. *J. Appl. Meteorol.* **6** 748-755.

Murphy A.H. and Winkler R.L. (1984). Probability forecasting in meteorology. *J. Am. Stat. Assoc.* **79** 489-499.

Murphy A.H. and Winkler R.L. (1987). A general framework for forecast verification. *Mon. Weather Rev.* **115** 1330-1338.

Murphy A.H. Hsu W. Winkler R.L. and Wilks D.S. (1985). The use of probability in subjective quantitative precipitation forecasts: Some experimental results. *Mon. Weather Rev.* **113** 2075-2089.

Nel W and Sumner PD (2005). First rainfall data from the KZN Drakensburg escarpment edge (2002 and 2003). *Water SA,* ***31*** *No. 3, 399-402p*

Palmen E. (1946). Discussion of the problems concerning Forntal Analysis in the Free Atmosphere. *Mitt. Met. Institute. University of Helsinky.* **57.** 47pp

Pegram G.G.S. (2004). Spatial interpolation and mapping of rainfall (Simar) Vol 3: Data merging for rainfall map production. *WRC Report : 1153/1/04*

Poolman E.P. and Terblanche D. (1984). Tropiese siklone Demonia en Imboa. *S. Afr. Weath. Service News Lett.* **420,** 37-45

Preston-White R.A. and Tyson P.D. (1993). *The Atmosphere and Weather of Southern Africa.* Oxf. Univ. Press. 374 pp.

PRETORIA NEWS (2001).Floods And Flu Epidemic have Cape in the Doldrums. 23/7/2001. Pretoria

Rae K.J. (2002). Hail, late December 2002. www.weathersa.co.za

Sanders F. (1963). On subjective probability forecasting. *J. Appl. Meteorol.* **2** 191-201

SAPA . (2002). Farm Snow Losses Devastating.

SAWS. (2002). SIMAR Project. http://metsys.weathersa.co.za/simar-info.html

Schulze B.R. (1965). General Survey. Climate of South Africa. WB28. S. Afr. Weath. Bur., Private Bag X97, Pretoria 0001.

Stanski H.R. Wilson L.J. and Burrows W.R. (1989). Survey of common verification methods in meteorology. World Weather Watch Technical Report no.**8** *WMO/TD No.385.*

STAR (2001). Gauteng in line for cold Weekend, 5/7/2001, Johannesberg.

Strydom P.H. and Nel C. (1996). Die Weer van Julie 1996. *S. Afr. Weath. Service Newslett.* **568,** 22-26

Taljaard J.J. (1985). Cut-off lows in the South African region. *S. Afr. Wea. Bur. Technical Pap.* **14**, 153 pp. S. Afr. Weath. Bur., Private Bag X97, Pretoria, 0001

Taljaard J.J. (1995). Atmospheric circulation systems, synoptic Climatology and weather phenomena of South Africa. Part **4**: Surface pressure and wind phenomena in South Africa. *S. Afr. Wea. Bur. Technical Pap.* **30**, *42* pp. S. Afr. Weath. Bur., Private Bag X97, Pretoria, 0001

Tennant W.J. and van Heerden J. (1994). The influence of orography and local sea-surface temperature anomalies on the development of the 1987 Natal floods: a general circulation model study. *S. Afr. J. Sci.* **90**, 45-49.

Triegaardt D.O. Terblanche D.E., van Heerden J. and Laing M.V. (1988). The Natal floods of September 1987. *S. Afr. Weath. Bur. Tech. Paper* **19**, 62 pp. S. Afr. Weath. Bur., Private Bag X97, Pretoria 0001.

Triegaardt D.O. van Heerden J. and Steyn P.C.L. (1991). Anomalous precipitation and floods during February 1988. *S. Afr. Weath. Bur. Tech. Paper* **23**, 25 pp. S. Afr. Weath. Bur., Private Bag X97, Pretoria 0001.

Tyson P.D. Preston-Whyte R.A. & Schulze R.E. (1976). The Climate of the Drakensberg, *Natal Town and Regional Planning Reports*, The Natal Town and Regional Planning Commission, Pietermaritzburg, 78 pp.

Van Heerden J. and Hurry L. (1987). *South Africa's weather patterns*. Acacia. 95 pp

Wilks D.S. (1995). *Statistical Methods in the Atmospheric Sciences. An Introduction.* Academic Press, San Diego, 467pp.

Zhao Q. and Carr F.H. (1997). A prognostic cloud scheme for operational NWP models. *Mon. Wea. Rev.*, **125**, 1931-1953.

Other related WRC reports available:

Daily rainfall mapping over South Africa: Modelling

Pegram G; Sinclair S; Wesson S

At the beginning of 2003 the South African Weather Service (SAWS) website began to offer a set of detailed daily maps of the previous day's rainfall over the whole of RSA and some neighbouring territories. This product was the outcome of the SIMAR (Spatial Interpolation and Mapping of Rainfall) research programme. The regular publication of the maps allowed designers/researchers involved in SIMAR the opportunity of receiving feedback from users with a view to improvement of the product. This follow-up project (Daily Mapping of Rainfall over South Africa: Modelling) and its companion project (Daily Mapping of Rainfall over South Africa: Infrastructure and Capacity Building) together address the various infra-structural, capacity-building and computational issues need to ensure that the daily rainfall mapping programme of the SAWS is so improved that it meets user needs for high-resolution rainfall data in the best possible way.

In this modelling study, the following six areas of improvement of SIMAR were earmarked for research and all were successfully addressed.

1) Effective methods were developed to repair parts of radar images contaminated by reflectivity values which are not precipitation (e.g. ground clutter, anomalous propagation etc).

2) Precipitation estimates made aloft by radar were successfully extrapolated to ground level and confirmation obtained that the estimates are valid. One of the factors contributing to non-triviality of the extrapolation procedures is the occurrence of bright-band effects due to melting ice at certain levels in stratiform cloud systems. If not successfully addressed, bright band effects lead to gross errors in rainfall estimation.

3) A methodology was developed to use instantaneous images of moving rainfields, captured periodically by radar or satelites, to compute meaningful accumulations of rainfall over from 6 minutes to 24 hours and longer.

4) A new conditional merging algorithm was adopted as the optimal way of combining accumulated radar or satellite rainfields with rain gauge data

5) The methodology developed in SIMAR for rainfall estimation using METEOSAT-7 data was converted to make it appropriate for use with the higher precision data being obtained from MSG (METEOSAT 8).

6) The optimal method for forecasting rainfields into the near future (up to 2 hours ahead) was selected from three candidates which included three candidates, one being a newly developed method using 3-dimensional Empirical Mode Decomposition in combination with Adaptive Time Series Forecasting.

The techniques relating to these areas of improvement have been combined in a new Improved Rainfall Merging Algorithm for producing optimally estimated rainfields called IRMA.

Report Number: 1425/1/06 **ISBN No: 1 77005 400 6**

TO ORDER: Contact **Publications** - Telephone No: 012 330 0340
Fax Number: 012 331 2565
E-mail: publications@wrc.org.za

Water Research Commission
Private Bag X03, Gezina, 0031, South Africa
Tel: +27 12 330 0340, Fax: +27 12 331 2565
Web: http://www.wrc.org.za